Stress and translation : implication of 16S rRNA methylations in Escherichia coli and characterization of a toxin-antitoxin system of Sinorhizobium meliloti

Manon Thomet

THESE DE DOCTORAT DE

L'UNIVERSITE DE RENNES 1
COMUE UNIVERSITE BRETAGNE LOIRE

ECOLE DOCTORALE N° 605
Biologie Santé
Spécialité : Microbiologie, Virologie, Parasitologie

Par
Manon THOMET

Stress and translation: implication of 16S rRNA methylations in *Escherichia coli* and characterization of a toxin-antitoxin system of *Sinorhizobium meliloti*

Thèse présentée et soutenue à Rennes, le 30 novembre 2018
Unité de recherche : UMR 6290 – Groupe Ribosomes, Bactéries et Stress

Rapporteurs avant soutenance :

Axel Hartke	Professeur Université Caen
Olivier Namy	Directeur de Recherche – CNRS, UMR9198 Université Paris-Sud

Composition du Jury :

Président :	Brice Felden	Professeur Université Rennes 1 –Directeur de Recherche INSERM U1230
Examinateurs :	Axel Hartke	Professeur Université Caen
	Olivier Namy	Directeur de Recherche – CNRS, UMR9198 Université Paris-Sud
	Eliane Hajnsdorf	Directeur de Recherche – CNRS, UMR8261 Université Paris Diderot
Dir. de thèse :	Gwennola Ermel	Professeur Université Rennes 1
Co-dir. de thèse :	Isabella Moll	Professeur Université Vienne (Autriche)

Doing my PhD between two countries was not the easiest (for sure) but it gave me so much! I grew up (for sure), learned so much (for sure) and I met so many great people who helped me in one way or another. So, at the end of those amazing three years, I have a lot of persons to thank!

First of all, I would like to thank Gwennola and Isa for offering me this position, trusted me and supported me on this project. I learned so much during those three years thanks to you!

Merci à tous les membres du jury d'avoir accepté d'examiner ce travail.

Merci à Daddychou et Mamoune qui ne savent pas ce que c'est un ribosome (et encore je ne vous ai jamais parlé des méthylations de la petite sous-unité) malgré mes explications hasardeuses (oui parce qu'il y a deux sous-unités dans le ribosome) mais c'est même pas grave (oui parce que ça c'est à peine l'introduction…)! Vous avez retenu le mot ! Et merci pour votre soutient de près comme de loin ! Je vous aime.

Un grand et global merci à mon équipe rennaise ! Du bas : Lydie (pour toutes tes petites attention, ta bonne humeur et ton entrain), Marion (attention Marion, un frelon! Et merci pour ta relecture attentive), Marie-Christine, Renan, Sylvie, Annie, Fanny, Gwennolos et Carla, et du haut : Charlotte, Reynald, Manu, Sophie. Merci pour les repas, les conseils, le thé de 16h (une institution), les fous rires, les cafés, les discussions (pas forcément liées au labo), les blagues, le soutien, les jeux des dates et les horoscopes du journal… Travailler dans cette ambiance c'est pas toujours facile (surtout quand on est plus que quatre et que tout le monde est parti en vacances) mais c'est tellement agréable.

Merci à Carlos, mon professeur de microbiologie (oui ?), qui m'a passionnée pour la bactériologie et la génétique bactérienne (oui ?). Parce que oui, Carlos vos cours sont particuliers (oui ?) mais plus que des cours vous nous racontiez des histoires (oui ?) et moi ça m'a fasciné. Et merci à Carlos mon chef (non mais non…), qui a beaucoup discuté (non mais…), chipoté (mais non…), relu et corrigé ma thèse. Vos tics de langage m'amusent. Merci à Gwennola, pour avoir cru en moi surtout (même moi j'y crois pas), m'avoir supportée (littéralement), pour les longues heures de travail, pour la relecture et la réécriture et plein de choses quoi ! Merci merci merci !

A mon amie Sylvie, ma maman du labo, qui m'a vu surexcitée (souvent), démotivée (une ou deux fois), piquer des crises (régulièrement ? vraiment ?), pleurer (UNE fois ! UNE !), râler (juste une fois aussi non ?), fondre au soleil et geler de froid, avec qui j'ai manipé (pas assez), fait du yoga fitzen (pas assez non plus), rigolé et papoté (sûrement trop)

et chanté (tout le temps). Merci pour ton aide et ton soutien qui m'ont été plus que précieux ! Ta bonne humeur nous rend tous plus légers tu sais ? Tu es formidable !

Vielen Dank an meine Labor-KollegInnen! To the cool kids from the lab hehehe! Katie, you're great, thanks for practical help (yeah I should definitely begin with that you're amazing), your Viennese sense of humor (haha). Heather thank you so much for not speaking German (so that I'm not the only one haha!), for working next to me (you can be very funny but I guess we shared that), for your scientific advices too, for your good mood, for helping us with our poor English vocabulary, and you're the best post-doc in the lab right?! Liebe Nick, danke! Nick, you are the best. There is not much I can add. Thanks for being always cheerful, funny, helpful, nice… you are the best. You are my cutie. So guys, thanks for sharing coffee, lunch, cocktails, gossips and much more!

Merci à Denis pour ces belles aventures en mer, ça a été un énorme bol d'air frais et salvateur à chaque fois ! Naviguer avec toi c'est fun, instructif et on les fume tous en plus !

Bien sûr un grand grand merci à tous mes copains qui savent à quel point je tiens à eux, j'espère !

To the Gang. To my little Stevie, baby Julian, Jon and Rol, crazy Anja, Finnie, the Flo, Aimee and little Iana. Gangsters, you made my Viennese life so sweet and funny. Thanks for everything, the parties, the coffees, the dinners, the movies, Vienna, Prague, Moscow… We shared so much and I love you guys. Stevie, you are such a lovely friend, so kind and funny, I enjoyed all that time we spent together. And we've got the groove! Juls, babe, you and your swimming lessons hin hin hin. Roli thanks for your kindness, I loved so much those girly breaks to enjoy a coffee, a glass of wine and gossiping about everybody else! Joni, you are crazy. Finn, I definitely miss your weird sense of humor, the weird movies we watched together, your weird smoothies and all those moments we shared… Thank you for being here when I needed you. Little Iana, little Iana, so many things to say. It was so nice to do all this stuff with you (damn, you are so active, too much stuff), running (you made me run… unbelievable), exercising (this yoga/climbing/fitness/push-up thing of yours…), going to the cinema, skiing, hiking, being crazy, eating, drinking, living together (watching you during your sleep hehehe)… You are a wonderful friend, thank you so much for all you've done for me, for all those memories and for the black-outs too.

A mes supertops copines Clairouille et Yo ! Toujours là quand il faut les meufs ! Même busy in London ou gone to the Meeting Island ! Franchement vous êtes au top et je suis bien contente de vous avoir, on se calle un apéro un de ces quatre ? Et comme on dit en polonais, gotchétchatché !

Merci à mes copains Minus et Laurette, d'être venus me voir à Vienne et de m'avoir toujours dignement accueillie chez vous ! Et puis à Youni aussi parce qu'on a plus ou moins fait le bout de chemin ensemble et ton canapé m'a recueillie régulièrement (merci canapé).

A Charlotte. Parce que mon chaton, on en a parcouru des choses ensemble, tu as vu où on en est ? J'ai l'impression d'avoir réussi plein de choses grâce à toi et avec toi. Mes révisions déjà, parce que j'en aurai pas été capable toute seule (non mais ces trucs débiles qu'on a dû retenir… souviens toi l'éco ou pire la sécurité microbienne…), le projet tut (hahaha ce projet ! Que des bons souvenirs au final qui l'eut cru ?), les stages, la thèse… Non mais la thèse ! L'éclate totale quoi. Donc merci d'avoir subi mon sale caractère depuis 6 ans, à la cité U, en cours, dans notre appart, au labo, à Fougères, à Vienne, à Porspo, en mer, en voiture, sur terre, à vélo… Heureusement, tu as bu rouge plus d'une fois et jamais seule ! Hehehe, boum bébé !

Merci à Dear Prudence, une belle chanson mais surtout le plus beau des bateaux ! Et à Mycose le chat. Et à ma famille aussi, allez. Merci à tous les machins et machines que j'ai croisées sans retenir leur nom parce que je suis nulle en nom (et que ça me fait rire).

Et bien sûr un immense merci à Charly. Je ne pourrais jamais te remercier assez pour tout ce que tu as fait (enfin, on va attendre que tu finisses ta thèse). Merci de rester, d'être si patient, gentil, tendre, compréhensif, généreux, attentioné… tu es le meilleur quoi. Merci pour ces longues heures à m'écouter chouiner, merci de m'avoir remotivée quand il fallait, merci de m'avoir écoutée et conseillée et merci pour tout quoi ! Merci, je t'aime. Je t'aime je t'aime.

INDEX

LIST OF ABBREVIATIONS

30SIC: 30S initiation complex
70SIC: 70S initiation complex
aaRS: aminoacyl-tRNA synthetase
Amp: ampicillin
cAMP: cyclic adenosine monophosphate
anti-SD: anti-Shine-Dalgarno
CAT: chloramphenicol acetyl transferase
Cm: chloramphenicol
CSP: cold shock proteins
DNA: deoxyribonucleic acid
EF: elongation factor
EF-G: Elongation factor G
EF-Tu : elongation factor thermo unstable
HSP: Heat Shock protein
IF: initiation factor
Kan: kanamycin
LB: Luria Bertani, lysogenic broth
DC: Decoding centre
GDP: Guanosine diphosphate
GFP: green fluorescent protein
GTP: Guanosine triphosphate
lmRNA: leaderless messenger RNA
mRNA: messenger RNA
ORF: Open reading factor
Ori: origin of replication
PCR: polymerase chain reaction
PheRS: Phenylalanine-tRNA synthetase
PTC: Peptidyl transferase centre
RBS: ribosome-biding site
Rmf: ribosome modulation factor
ROS: Reactive oxygen species
RF: release factor
$_{GFP}$RLU: GFP relative fluorescence units
$_{mC}$RLU: mCherry relative fluorescence units
RNA: ribonucleic acid
RNase: ribonuclease
RRF: ribosome recycling factor
rRNA: ribosomal RNA
rsm: ribosomal small subunit methyltransferase
SAM: S-adenosyl-L-methionine
SD: Shine-Dalgarno
TA: Toxin-Antitoxin
tRNA: transfer RNA
Tet: Tetracyclin
tmRNA: transfer messenger RNA
UTR: untranslated region

I. Introduction

1. General introduction

Bacteria are organisms able to live in a wide range of environments. The conditions they face are constantly changing in terms of resource availability, competition, abiotic factors... therefore bacteria have to adjust quickly and precisely their metabolism. Such adjustments must be fast and mainly depend on transcriptional and translational regulation. Hence, to adapt to environmental changes, gene expression must remain functional despite stresses.

Bacteria have developed specific regulations to cope with stressful conditions involving all steps of gene expression. Multiple mechanisms affecting transcription, translation and post-translational modifications are known, involving regulatory proteins, regulatory RNAs and enzymes altering proteins.

The ribosome performs protein synthesis and is a highly conserved machinery. Translation involves many factors and is tightly regulated. Mechanisms regulating translation mainly consist of aborting or favouring it using regulatory RNAs, riboswitches, proteins… During stress response, they act to adjust protein synthesis in order to redirect the metabolism. Thus translation is a key process and must remain efficient despite the conditions. We aim to study how the ribosome itself could modulate its activity. This machinery is known to bear modifications in its ribosomal RNAs. These modifications are conserved among species and even among the three kingdoms for some, suggesting a crucial role. Nevertheless, their physiological function and the regulation of the modification enzymes remain mainly uncharacterized, particularly during stress adaptation. In this work, we aimed to study the importance of some rRNA methylations in stress adaptation and translation fidelity during stress.

2. The ribosome and the translation process in *Escherichia coli*

Gene expression can be described as the processes leading to production of gene functional supports (which can be either proteins or non-coding RNA). It is composed of transcription of one gene into a messenger RNA (mRNA) subsequently translated into a protein. The translation process is realized by a complex cellular machinery called the ribosome.

2.1. The bacterial ribosome

Bacterial ribosomes have a sedimentation coefficient of 70 Svedberg (S). This machinery is a ribonucleoprotein complex, composed of two-third RNA and one third protein (Deutscher, 2009). It is asymmetrical and made up of two sub-units: a large one (50S) and a smaller one (30S) (Figure 1). The large sub-unit contains 33 proteins (L1-L36) and two ribosomal RNAs (rRNAs), 23S (2904 nt) and 5S (120 nt). The 30S subunit is composed of 21 proteins (S1-S21) and one RNA, the 16S rRNA (1542 nt). The two subunits assemble during translation initiation to form the 70S particle.

Interestingly, the catalytic activity of the ribosome is due to the RNA components, hence the ribosome is a ribozyme. In addition, the two subunits hold different activities. The small subunit is responsible for binding the mRNA and decoding the 3-letter code it is bearing while the 50S subunit is capable of forming peptide bond between the nascent peptide and the incoming amino acid. Those two reactions are performed by the ribosome together with aminoacyl transfer RNAs (tRNAs). tRNAs are charged with the correct amino acid by specific aminoacyl-tRNA synthetases (aaRSs). Those charged tRNAs can be considered as substrates for the ribosome and provide it with amino acids. There are three sites for tRNA binding on the ribosome: the A-site where aminoacyl-tRNA binds and is decoded, the P-site holds the tRNA carrying the growing nascent polypeptide chain and the E-site for the exit of the uncharged tRNA (Figure 1).

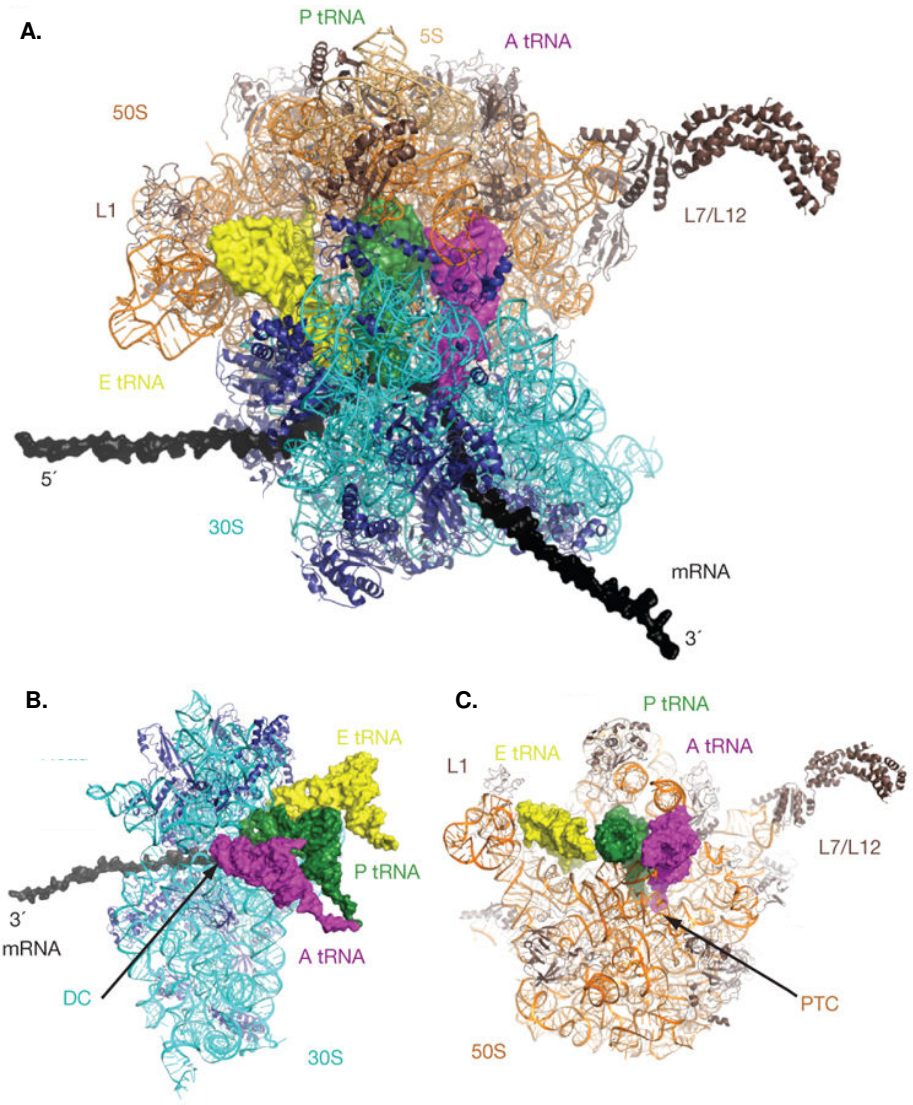

Figure 1: The bacterial ribosome and its subunits. A: the 70S ribosome with an mRNA (in black) and tRNAs in A-, P- and E- site. B: the 30S subunit and C: the 50S subunit, tRNAs are also pictured to indicate the position of the sites (adapted from Schmeing and Ramakrishnan, 2009)

16S, 23S and 5S rRNAs are synthesized in a single transcript. This precursor RNA has to undergo nucleolytic processing by several RNases to produce the three mature rRNAs. Their maturation is concomitant with transcription, folding of secondary structures and binding of ribosomal proteins (Shajani *et al.*, 2011). Moreover, during their maturation, rRNAs are chemically modified at several specific positions. Different types of post-transcriptional modifications can be found such as base and ribose methylations or isomerization of uridines into pseudouridines and will be discussed in another chapter.

2.2. The translation process in bacteria

The bacterial translation can be divided into four main steps: initiation, elongation, termination and recycling (Figure 2).

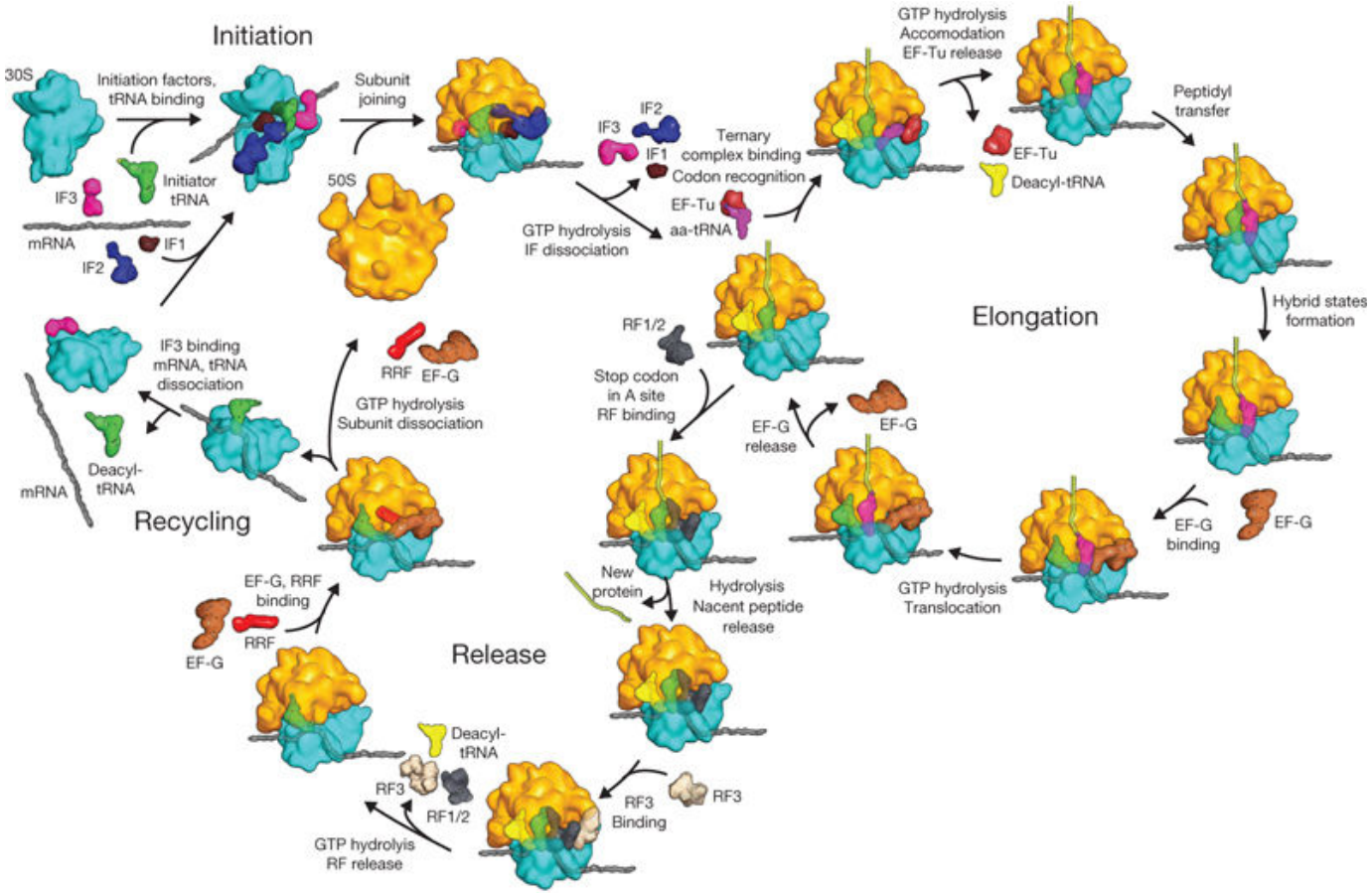

Figure 2: Overview of the translation process in *Escherichia coli.* The four main steps (initiation, elongation, termination and recycling) are represented (from Schmeing and Ramakrishnan, 2009).

a. Initiation

To initiate translation, the 30S subunit needs to recruit several actors such as the three initiation factors (IF), the mRNA, the initiator tRNA fMet-tRNA^{fMet} and the large subunit (Figure 2). Indeed, translation initiation starts with the formation of the 30S initiation complex (30SIC) in which the mRNA start codon and the anticodon of the initiator tRNA are correctly positioned in the P-site. Subsequently, the large subunit is recruited to form the 70S initiation complex (70SIC) which is able to perform peptide bond formation and then elongation (Gualerzi and Pon, 2015).

Canonical mRNAs carry two characteristic features: a start codon on which translation specifically begins and a ribosome biding site (RBS) to recruit the small subunit. The most frequent initiation codon is AUG although several other triplets can be used. Indeed, in *E. coli*, AUG coding for methionine is used as a start codon in 82% mRNAs, the valine codon GUG in 13.8% and the leucine codon UUG in 4.35% (Hecht *et al.*, 2017). The other important region of the mRNA, the RBS, is characterized by the Shine-Dalgarno (SD) sequence, localized in the 5' untranslated region (UTR), about five to nine nucleotides upstream of the start codon (Ringquist *et al.*, 1992). As this region is partially complementary to the anti-SD located at the 3' end of the 16S rRNA (Shine and Dalgarno, 1974), the interaction between SD and anti-SD recruits the ribosome to the RBS. However, there are mRNAs, called leaderless mRNAs (lmRNAs), which completely lack the 5' UTR. They start directly with a start codon and do not have any SD sequence, but can still be translated (Udagawa *et al.*, 2004). The existence of such mRNAs underlines the fact that the SD sequence is not necessary for translation initiation. Although they seem to be largely spread (Srivastava *et al.*, 2016; Zheng *et al.*, 2011), only a few are naturally present in *E. coli* (for example lambda repressor *cI* (Balakin *et al.*, 1992)).

Concerning canonical mRNAs, the initiation factors (IF 1 to 3) allow for correct positioning of fMet-tRNA^{fMet} over the start codon within the P-site leading to the formation of the 30SIC. IF3 binds the small subunit in the E-site and prevents binding of the 50S subunit. The mRNA is recruited thanks to the interactions between SD and anti-SD and the start codon is positioned in the P-site. IF1 binds to the empty A site to prevent binding of aminoacyl tRNA. Then IF2*GTP interacts with the 30S subunit and helps positioning fMet-tRNA^{fMet} in the P site. Decoding of the start codon occurs in the P-site where IF3 discriminates for the correct codon-anticodon interaction (Grigoriadou *et al.*, 2007). Then, the 50S subunit joins, helped by IF2*GTP, and upon GTP hydrolysis the three IFs are released: the 70S initiation complex is formed (Caban *et al.*, 2017).

Yamamoto *et al.* described another mechanism for translation initiation that they called "70S scanning initiation" in which the 70S ribosome does not dissociate at

the end of a translation cycle and directly re-enters a new one (Yamamoto *et al.*, 2016). Here, the three initiation factors and the initiator tRNA bind the 70S ribosome and allow it for scanning the mRNA in order to find the start codon and the SD sequence. IF1 would inhibit binding of aminoacyl tRNA and EF-Tu, thus permitting the 70S to continue scanning. Eventually, the ribosome would find the start codon and the initiation factors would dissociate to form the 70SIC.

Translation initiation of leaderless mRNAs differs from canonical mRNAs. As leaderless mRNAs do not bear SD sequence, their binding to the 30S subunit strongly depends on IF2 and fMet-tRNA^{fMet} (Grill *et al.*, 2001) but is inhibited by IF3 (Grill *et al.*, 2001; Tedin *et al.*, 1999). Moreover, 5' phosphorylated AUG stabilizes their association with the small subunit as well as the formation of 70SIC (Giliberti *et al.*, 2012). Other studies also showed that lmRNAs translation can be initiated directly with 70S monomers (Moll *et al.*, 2004; O'Donnell and Janssen, 2002). In that case, lmRNA binding depends on recognition of their AUG start codon by ribosomes and this interaction is stabilized by fMet-tRNA^{fMet} (Brock *et al.*, 2008).

b. Elongation

Once the 70SIC is formed, the ribosome is ready to enter the elongation cycle. During this step, new amino acids are added to the nascent peptide chain. The ribosome contains the initiator tRNA in the P-site and the A-site is empty. Thus, with the help of several elongation factors (EF), it needs to recruit the second aminoacyl tRNA, decode it, add the second amino acid to the nascent chain and translocates all tRNA to free the A-site in order to re-enter a new cycle (Figure 2).

First, EF-Tu*GTP, bound to an aminoacyl tRNA in a ternary complex, is recruited in the A-site. There, within the decoding centre, the correct aminoacyl tRNA in accordance with the mRNA codon is selected. This process is termed decoding and leads to codon-anticodon interaction between mRNA and tRNA (Demeshkina *et al.*, 2012; Ogle *et al.*, 2001). This interaction induces conformational rearrangements which have several consequences (Rodnina *et al.*, 1995): it results in GTP hydrolysis and dissociation of EF-Tu*GDP from the ribosome (Villa *et al.*, 2009) followed by

accommodation of the aminoacyl tRNA in the peptidyl transferase centre (PTC) (Valle *et al.*, 2003).

The first peptide bond is then synthesized between fMet and the second amino acid. This peptidyl transferase reaction consists in a nucleophilic attack of the ester carbon of the peptidyl-tRNA (here, fMet-tRNA^{fMet}) by the amino group of aminoacyl tRNA (Lang *et al.*, 2008). As a consequence, the nascent peptide chain is transferred to the tRNA in the A-site.

Subsequently, the ribosome needs to move A- and P-site tRNAs to the P-site and E-site respectively. This translocation process has to be synchronized with the mRNA that shifts by exactly one codon in order to maintain the open reading frame. Errors or programmed frameshifts can occur at this stage leading to lecture of an overlapping codon thus changing the reading frame.

Following peptide bond formation, tRNAs in A and P sites move spontaneously: their position on the 30S subunit is not changed (A and P sites) while their 3' extremities are moved to the P and E sites of the large subunit respectively. These hybrid tRNA states lead to a movement of ratchet of the small subunit. Subsequently, the elongation factor EF-G associated with GTP binds the ribosome. GTP hydrolysis triggers mRNA and tRNAs movement relative to the 30S subunit (Rodnina *et al.*, 1997). It also induces a movement of reverse ratchet and as a result the ribosome is in its canonical form. The A-site is now empty for the next tRNA to be recruited and the ribosome is ready for the next round of elongation.

c. Termination and recycling

The elongation cycle continues until the ribosome reaches a stop codon, the signal of the end of the coding sequence. Termination and recycling steps result in the release of the neo-synthesized protein and in dissociation of the 30S and 50S subunits. Consequently, after recycling, the ribosome is able to initiate another round of translation.

There are three stop codons: UAA, UAG, and UGA which are not recognized by any tRNA but by a class I release factor (RF) RF1 or RF2. RF1 recognizes UAA and UAG while RF2 recognizes UAA and UGA (Scolnick *et al.*, 1968). Their specifity relies on a “tripeptide anticodon”: PXT in RF1 and SPF in RF2 (Ito *et al.*, 2000). Both release factors also have a conserved GGQ motif which plays a role in peptide hydrolysis.

When a stop codon reaches the empty A-site, RF1 or RF2 binds the ribosome resulting in conformational rearrangements of the ribosome. Those changes allow for interactions between RF1/2 peptidic anticodon and the stop codon in the decoding centre and also lead to positioning of the GGQ motif in the PTC (Laurberg *et al.*, 2008; Weixlbaumer *et al.*, 2008). Release of the polypeptide chain is triggered by RF1/2 nucleophilic attack of the ester bond between the peptide and the P-site tRNA (Jin *et al.*, 2010).

The class II release factor RF3 permits dissociation of RF1 or RF2. This factor is a GTPase and can bind either GDP or GTP with an equivalent affinity (Koutmou *et al.*, 2014). The complex ribosome-tRNA-RF1/2 recruits RF3 associated with GDP. Subsequently, GDP is exchanged for GTP resulting in conformational changes of the ribosome (Gao *et al.*, 2007). It induces destabilization of RF1/2 binding and their release. GTP is then hydrolysed by RF3 leading to its dissociation from the ribosome.

After RF3 release, a deacylated tRNA is in the P-site and the mRNA is still associated with the ribosome. Thus, to initiate another round of translation, the two subunits of the ribosome have to be recycled. This step is realized by the ribosome recycling factor (RRF) together with EF-G*GTP. First, RRF is recruited in the A-site, then EF-G*GTP binds the complex and GTP hydrolysis promotes the dissociation of the two subunits (Zhang *et al.*, 2015). Finally, IF3 binds the complex 30 S-mRNA-tRNA and promotes their release. Thus, the small subunit is ready for a new round of initiation (Schmeing and Ramakrishnan, 2009).

Other studies tend to show that 70S splitting induced by RRF and EF-G is not necessary for translation initiation (Orelle *et al.*, 2015; Qin *et al.*, 2016; Yamamoto *et*

al., 2016). Indeed, ribosomes bearing covalently linked subunits, which cannot be split, can perform translation *in vitro. E. coli* cells are able to grow with such ribosomes although they are less active than wild type ribosomes (Orelle *et al.*, 2015). Qin *et al.*, (2016) showed that neither *in vitro* nor *in vivo* translation of a second cistron of a bicistronic mRNA requires RRF activity. As 70S scanning was described as highly dependent on fMet-tRNA availability, they propose that when the initiator tRNA is not available then RRF-dependant recycling takes place.

d. Ribosomal errors

Aforesaid, during translation, the ribosome discriminates against correct and incorrect aminoacyl tRNAs. This discrimination is due to the exclusion of incorrect tRNAs by the fact that ribosome control the stabilities of the codon-anticodon complexes and increase the rate of GTP hydrolysis. Many residues of the 16S rRNA are involved in the stability of the interaction of anticodon stem-loop fragments of tRNA and the codon triplets in the decoding site: adenines A1493 and 1492 in helix 44 of 16S rRNA, G518 and G530 in helix 18 of 16S rRNA, G1054 from helix 34 and ribosomal protein S12 (Ogle *et al.*, 2001). Such mechanism prevents misincorporations of amino acid within the nascent chain. Missense errors can also be caused by mistakes in aminoacylation of tRNAs. Taken together, misincorporations are considered to happen with a rate of one mistake per 10^4 codons in *E. coli* (Kurland, 1992; Reynolds *et al.*, 2010). The ribosome is susceptible to make other types of errors such as stop-codon read-through or frameshifting. They are thought to happen with rates of 10^{-2} and 10^{-5} respectively (Evans *et al.*, 2018).

Frameshifting is more costly for the cell than misincorporations. Once the ribosome changed reading frame, there is no way to re-establish it leading to translation of an erroneous and truncated protein which has to be degraded afterwards. However, in some specific cases, frameshifting can be used to regulate translation. In such cases, the rate of frameshifting is much higher (50 to 80% (Chen *et al.*, 2017; Tsuchihashi and Brown, 1992)) and uses signals to drive the ribosome to change frame. In *E. coli*, two genes use programmed frameshifting to regulate their translation: *prfB* and *dnaX*.

dnaX codes for two different products: gamma γ and tau τ subunits of DNA polymerase III (Blinkowa and Walker, 1990; Flower and McHenry, 1990; Tsuchihashi and Kornberg, 1990). The coding sequence of the τ subunit is in the canonical coding frame (0 frame) and the protein produced out of it contains 643 amino acids. A programmed -1 frameshift event (the reading frame is changed by one nucleotide in the 5' direction of the mRNA) is required to express the γ subunit (431 amino acids). It causes early termination of translation due to the presence of a stop codon downstream the slippery sequence. Consequently the γ subunit lacks the last two domains of τ subunit.

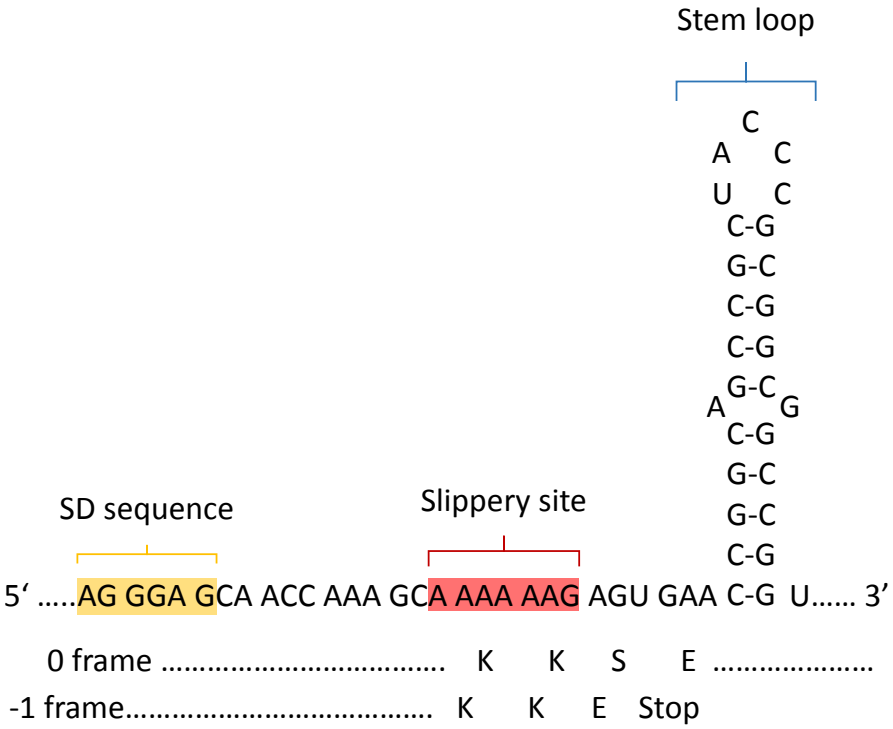

Figure 3: Signals of *dnaX* programmed frameshifting. The sequence of dnaX mRNA is represented with the SD-like sequence in the yellow box, the slippery sequence in the red box and the stem loop. The protein sequence in the canonical frame (0 frame) is indicated below as well as the sequence in the -1 frame following frameshifting (adapted from Caliskan *et al.*, 2015).

Three elements are essential for *dnaX* programmed frameshift: an internal SD-like sequence, a slippery site and a stem-loop (Figure 3) (Dunkle and Dunham, 2015). Frameshifting happens on the slippery site of which the in-frame sequence is A.AAA.AAG, decoded by two Lys tRNAs (Tsuchihashi and Brown, 1992). Codon-anticodon interactions at this site are unstable, and can lead to dissociation of the

first tRNALys (decoding AAA) that reassociates with the overlapping -1 codon (A.AA). The stem loop is located downstream of this site and slows down translation leading the ribosome to pause on the slippery sequence (Larsen *et al.*, 1997). It is also thought to obstruct tRNAs translocation. The internal SD-like sequence positioned upstream of the slippery site enhances frameshifting (Larsen *et al.*, 1994), probably by inhibiting translocation as well (Chen *et al.*, 2014).

prfB encodes release factor 2 (RF2) and, in order to produce active RF2, a +1 programmed frameshifting is required (the ribosome bypasses one nucleotide in the 3' direction of the mRNA). There are two signals driving the ribosome to change frame on *prfB* mRNA: an SD-like sequence and the slippery site CUU.UGA bearing an UGA stop codon (Donly *et al.*, 1990) (Figure 4).

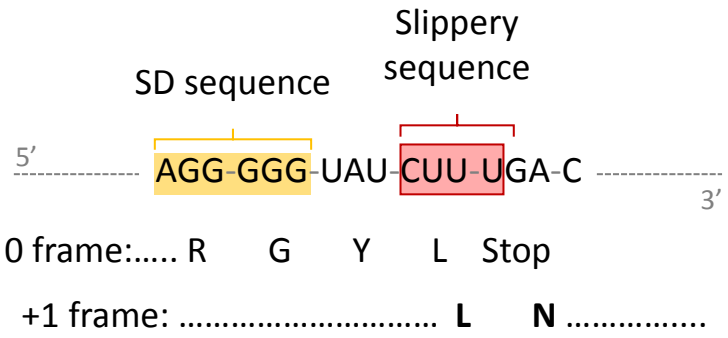

Figure 4: *prfB* signals driving +1 programmed frameshifting. The sequence of prfB mRNA is represented with the SD-like sequence in the yellow box and the slippery sequence in the red box. The protein sequence in the canonical frame (0 frame) is indicated below as well as the sequence in the +1 frame following frameshifting (adapted from Farabaugh, 1996).

The UGA stop codon is in frame and can be recognized by RF2 which therefore autoregulates its expression (Adamski *et al.*, 1993). Indeed, when RF2 is abundant enough, it recognizes the UGA codon and translation stops. However, when the levels of RF2 are low, the ribosome pauses at the UGA codon. Interactions between codon-anticodon in the decoding centre are perturbed and a rearrangement can occur leading the peptidyl-tRNA decoding CUU to read the UU.U overlapping codon (Liao *et al.*, 2008). The SD-like sequence, positioned upstream of the slippery site,

interacts with the anti-SD of the ribosome and drives its repositioning in the +1 frame (Dinman, 2012).

2.3. Impact of stresses on the translational machinery

Environmental variations can induce damages to biological macromolecules, such as ribosomes, thus compromising their functions. These environmental changes could impact directly the two principal functions of the ribosome governed by rRNAs (decoding and peptide bond formation) as well as functions that are controlled directly by ribosomal proteins. Oxidative, osmotic, heat and cold stresses induce transcriptional responses with dedicated regulations and/or translational responses that can be due to ribosome-associated factors, toxin actions or direct and indirect variations at the ribosome level.

a. Oxidative stress induces mistranslation and translational arrest

Oxidative stress may be defined as a disruption of the balance between free radicals (reactive oxygen species, ROSs) and antioxidant defences. Different studies have shown that ROSs could decrease translational fidelity. Indeed, ROSs can oxidize amino acids leading to the addition of a hydroxyl group, for example. Those damaged amino acids can be erroneously charged on tRNAs by aminoacyl-tRNA synthetases (aaRSs) and then incorporated into proteins. Usually, aaRSs have the ability to edit misacylated tRNAs with modified amino acids such as homocysteine, norleucine, α-aminobutyrate and *meta*-tyrosine (*m*-Tyr).

For instance, *m*-Tyr can be charged on $tRNA^{Phe}$ but PheRS is able to edit this misacylated tRNA and thus prevents its incorporation into proteins (Bullwinkle *et al.*, 2014). Under oxidative stress, *m*-Tyr accumulates in *E. coli* cells and PheRS editing activity becomes essential for survival. However, Bullwinkle *et al.*, 2014 showed that *m*-Tyr can escape PheRS editing in such conditions and that incorporation of *m*-Tyr into proteins is toxic for *E. coli*. They assumed that this residue is a target of ROSs and induces oxidation of proteins when cells are submitted to oxidative stress. Thus, incorporation of *m*-Tyr in the oxidized proteome is a threat to translational integrity.

In the same way, the translational fidelity has been shown to be reduced because of ROSs damages on the editing activity of threonyl-tRNA synthetase (Ling and Söll, 2010). This phenomenon of misacylation of tRNAs has been also observed

in eukaryotic cells where the level of Met-misacylated tRNAs increased up to tenfold upon exposure to oxidative stress (Netzer *et al.*, 2009).

Elongation factor G (EF-G) can also be impaired by oxidative stress. This key protein in elongation of translation is strongly oxidized when *E. coli* cells are treated with H_2O_2 (Tamarit *et al.*, 1998) and in a *sod*-mutant strain (Dukan and Nyström, 1999). The oxidation of EF-G results in the formation of a disulphide bond between two Cys residues (Cys114 and Cys 266) and inhibits its activity (Nagano *et al.*, 2012) leading to a translational arrest. Nagano *et al.*, 2015 have shown that oxidation of EF-G suppresses the hydrolysis of GTP and does not allow dissociation of EF-G from the ribosome resulting in a defect in EF-G turnover.

The effect of ROSs on the translational fidelity seems to be essentially caused by incorporation of altered amino acids. Some authors argue that incorporation of non-proteinogenic amino acids would give aberrant peptides that are prone to oxidative modification and would be part of the resistance mechanism to oxidative stress. Increasing misincorporation of Met residues into proteins could protect them against ROS-mediated damages (Netzer *et al.*, 2009). Mistranslation could then be beneficial under oxidative stress conditions. Fan *et al.*, 2015 also observed that an *rpsD* variant (I199N), harbouring higher levels of UAG read-through, has a better survival to H_2O_2 challenge than the wild type strain.

b. Variations of translation under osmotic stress

The so-called osmotic stress corresponds to differences between external and internal osmolality. In most studies, hyperosmotic stresses are realized by increasing concentrations of salts such as NaCl in the medium. The consequence of such stress is an instantaneous exit of water to equilibrate internal and external osmotic pressure inducing plasmolysis. The cell adaptation to this condition consists in turgor pressure recovery via accumulation within the cell of high levels of potassium glutamate and compatible solutes by neosynthesis of trehalose or by active uptake if those solutes are present in the medium (glycine betaine, ectoine…) (Wood *et al.*, 2001). Potassium glutamate accumulation is transient (roughly 15 min) and induces an increase of ionic strength, followed by the accumulation of organic osmolytes called

compatible solutes because they are neutral for cell metabolism. Briefly, the genetic response of the cell corresponds to an upregulation of genes (*proV*, *proP*, *proX*, *proW*, *otsA*…) encoding enzymes related to trehalose synthesis and active transporters of osmoprotective solutes (Weber *et al.*, 2006; Wood *et al.*, 2001). Ionic strength and compatible solutes exert a strong influence on translation *in vitro*: salts reduce translation efficiency while compatible solutes increased it (Brigotti *et al.*, 2003).

In vivo analysis of elevated hyperosmotic stresses, generated by different NaCl concentrations (0.1 M to 0.6 M) in minimal medium, showed that the translational elongation rate decreased by 50% but could be compensated by an increase of the ribosome content compared to the effect of nutrient starvation. The explanation for this slowdown of the elongation rate could be the reduced binding rate of tRNA ternary complexes (aminoacyl-tRNA/EF-Tu/GTP) (Dai *et al.*, 2018). A new approach consisting of comparative analysis of transcriptome and ribosome profiling allowed Bartholomäus *et al.*, (2016) to observe a correlated increase of transcription and translation of osmoprotective genes despite a global reduction of transcripts. Moreover, the transitionally up-regulated genes under osmotic stress correspond to genes encoding amino acid synthesis and iron transport even if those genes are in polycistronic mRNAs. Analysis of ribosome-protected fragments showed that ribosomes accumulate upstream of the start codon near the SD sequence of the translated genes.

In response to variations of external osmolality, the expression of translation factors and ribosome associated proteins is also affected. The initiation factor 2 (IF-2) accumulated significantly within the first 10 minutes after the application of the stress (Weber *et al.*, 2006). This raising would be linked with the transitory arrest of translation during plasmolysis. Another protein, RsgA, which facilitates the maturation of the small subunit decreases under salt stress. The absence of this protein conferred a better salt resistance to *E. coli* cells and a shortened lag phase after the application of salt stress. Deletion of RsgA permitted the suppression of impaired maturation occurring under salt stress in wild type cells (Hase *et al.*, 2009). Thus, when cells are submitted to salt variations, the maturation of ribosomes would be independent of RsgA which is indispensable in isotonic environments. The same

phenomenon of shortened lag phase after the application of osmotic stress has been observed in cells carrying deletions of genes encoding ribosomal maturation factors (RimM, RbfA), rRNA modification enzyme (RlmE that catalyses the 2'-O-methylation of ribose at the position U2552 of the 23S rRNA) or ribosomal protein S6 (RpsF)(Hase *et al.*, 2013).

Moreover, osmotic stress induces an increase of expression of another ribosome-associated protein, Rmf (ribosome modulation factor) which transforms active 70S ribosomes to dimeric forms. This higher expression is associated with a decrease in translational activity, in either *E. coli* or *Pseudomonas aeruginosa* cells (Aspedon *et al.*, 2006; Bartholomäus *et al.*, 2016).

c. Variations of translation under temperature changes

In response to sudden temperature elevation, bacteria have evolved a transient induction of a group of heat shock genes encoding heat shock proteins. This heat shock also causes accumulation of unfolded proteins and aggregation of proteins. Thus, the response is a ubiquitous strategy to allow, on the one hand, removal of denaturated proteins and in the other hand correct folding of neosynthetized proteins and low-damaged proteins.

Concerning the effects of sudden rise of temperature on ribosomes, several phenomena are involved. Erroneous dissociation of translating ribosome can occur resulting in a 50S subunit carrying a tRNA still attached to the nascent polypeptide chain (Jiang *et al.*, 2009). Hydrolysis of the peptidyl-tRNA is carried out by a small heat shock protein HslR (Hsp15). This protein HslR may interact with helix 84 of the 23S rRNA and peptidyl-tRNA to allow translocation. Such interaction allows optimized hydrolysis by termination release factor RF2. HslR would also participate to the rescue of the ribosome through a concerted action with ArfB (Giudice and Gillet, 2013).

Another protein has been shown to interact with the 30S subunit when cells are submitted to heat stress, BipA protein (deLivron and Robinson, 2008). BipA is a ribosome-dependant GTPase which is also involved in the assembly of the large subunit at low temperatures. Moreover, BipA is essential for the assembly of the

ribosome in a mutant lacking RluC (23S rRNA pseudouridine$^{955/2504/2580}$ synthase) (Choudhury and Flower, 2015).

Another aspect concerns the role of a chaperone protein such as DnaK which could be considered as a factor involved in ribosome assembly. At elevated temperatures, *E. coli dnaK* mutants show defective ribosome assembly and accumulation of 21S particles (precursors to mature 30S subunits) and 32S and 45S particles (precursors of mature 50S subunits) (Al Refaii and Alix, 2009; El Hage and Alix, 2004). René and Alix observed that the late steps of ribosome assembly are also arrested in wild type strain after a temperature rise. They explained that the mis-folded and degraded proteins resulting from this temperature rise would monopolize the chaperones and DnaK-dependent late stages in ribosome assembly would be restrained (René and Alix, 2011).

In a recent study using ribosome profiling, Zhang *et al.*, (2018) have noticed that some genes are up-regulated at the transcriptional level while others are regulated at the translational level. They also observed that this translational regulation is independent of the position of the ORF in a polycistronic mRNA. In this study, it has been noticed that the translational level of *infA* (coding for translation initiation factor IF1) was reduced by half during heat stress. Other genes were more translated under such conditions namely RstA, GadX, PheM, SdhC, and RelB. The increase of such proteins is related to response to acidic conditions, electron transfer and cleavage of mRNA in the site A of the ribosome. Moreover, upon heat shock, the ribosome-protected fragments are more numerous around the starting region of a coding sequence suggesting that ribosomes may pause in this region.

Regarding cold stress, when cells from a culture in exponential phase are submitted to reduced temperature (37°C to 10°C), cell growth stops during 6 hours and is correlated with a significant decrease of protein synthesis (Jones *et al.*, 1987). In a recent publication, Zhang *et al.*, 2018 have analysed quantitatively and temporally the translational ability during this acclimation phase. A 50-fold decrease in protein synthesis rate was observed 3 minutes after the cold shock and about a total 200-fold decrease was obvious after 30 minutes. After this 6 hours incubation,

translation resumes with a 3.5-fold increase in protein synthesis rate. Using ribosome profiling, Zhang *et al.*, 2017 showed that the initiation of translation is compromised which is in agreement with the findings of Gualerzi *et al.*, 2011. *In vitro* experiments showed that translation variations could be due to either cis- or trans-acting elements. The *cis*-acting elements correspond mainly to the mRNA conformation that could result in exposure of the SD sequence and the presence of an AU-rich S1 binding region. The *trans*-acting elements gather essentially the cold shock protein (CSP) such as CspA and initiation factors such as IF1, IF2 and IF3. After a cold shock, during the acclimation phase, these factors show an increased synthesis and the ratio IFs/ribosome rises (2 to 3-fold after 2 to 4 hours of cold shock) (Gualerzi *et al.*, 2011). Zhang *et al.*, 2018 also reported that CSPs involved in the modulation of the mRNA structure have high fold change: from 500- to 18,5-fold increase. This increase concerns CspB, CspG, CspH, CspF, CspI and CspA. Concerning CspA, it is quite abundant in unstressed cells as well: about 50-fold higher to CspG, 125-fold for CspB and around 750-fold higher for all other Csps. In this publication, it could be mentioned that RNaseR, which is required for mRNA degradation, shows a 14,35-fold change. The increased synthesis of Csps is to be related to the fact that Csps control mRNA structure and participate in the modulation of the translation efficiency that is necessary to cope with cold stress and to maintain an efficient translation also at normal temperature.

Cold shock also affects tRNAs maturation which could thus have an impact on translation. Indeed, during cold adaptation, the fidelity of tRNA nucleotidyl-transferases (enzymes adding the CCA triplet at tRNAs 3' end) decreases (Ernst *et al.*, 2018).

3. Ribosomal RNA methyltransferases

As previously mentioned, rRNAs can be post-transcriptionally modified during their biosynthesis. There are three major types of modifications in rRNAs: uridine can be converted into pseudouridine, riboses can be methylated on their 2' hydroxyl groups and nucleotide bases can be methylated at different positions (Figure 5). Specific enzymes are required to catalyse those modifications, namely pseudouridine synthases and methyltransferases. Methyltransferases need a methyl donor in order to transfer the methyl group to its target while pseudouridine synthases catalyse the isomerization of the target. Almost all methyltransferases use S-adenosyl-L-methionine (SAM) as donor.

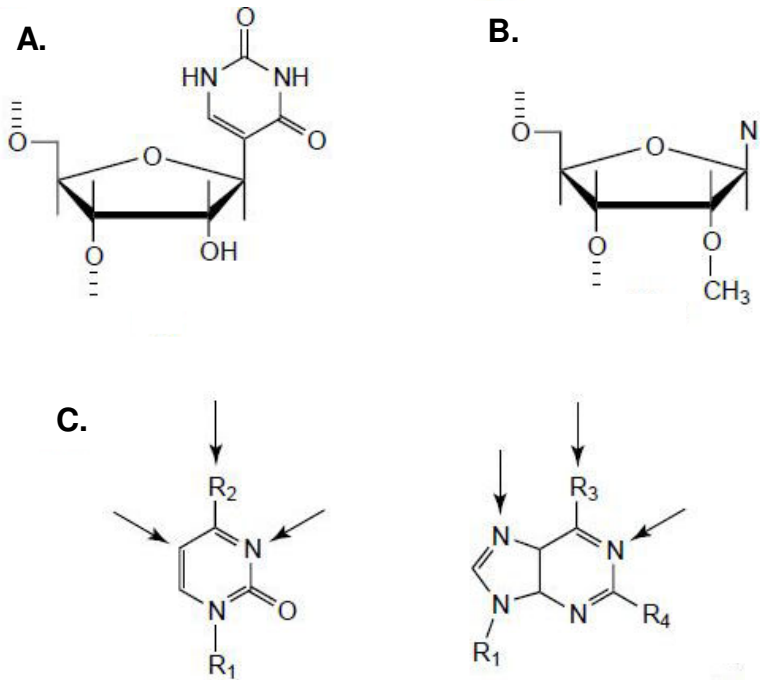

Figure 5: rRNA modifications and their possible localizations in base or ribose: A. pseudouridine, B. ribose methylation and C. base methylation; arrows indicate the positions that can be methylated (adapted from Decatur and Fournier, 2002).

Table 1: Overview of rRNA modifications (pseudouridines, ribose methylations and base methylation) in different organisms (from Sergiev *et al.*, 2011).

	Human	Yeast	*E. coli*
Pseudouridines	91	44	10
Ribose methylations	105	54	4
Base methylations	10	10	19

Interestingly, the number of rRNA modifications is correlated with the complexity of a given organism (Table 1). Indeed, while human ribosomes contain more than two hundred modifications, *Escherichia coli* ribosomes exhibit less than forty. Moreover, ratios of those modifications are completely different. For instance, there is a majority of base methylations in *E. coli* rRNAs and a minority of ribose methylations while it is the opposite in human and yeast, which also contain proportionally more pseudouridines.

This observation can be explained by the different machineries. In fact, *E. coli* uses site-specific methyltransferases and pseudouridine synthases meaning that one enzyme will modify one (or two) nucleotides. As a consequence, deletion of one enzyme leads to the absence of the related modification. This modification mechanism would be too costly in eukaryotes regarding the number of modified nucleotides within their rRNA. Consequently, they use instead “guided” enzymes that consist in ribonucleoproteic complexes containing a core methyltransferase or pseudouridine synthase associated with a specific small RNA. The latter is complementary to the target thus it is a “guide” that confers the specificity of the enzyme (Decatur and Fournier, 2002). This modification mechanism allows eukaryotes to have a limited number of ribose methyltransferases or pseudouridine synthases. Nevertheless, they still use site-specific methyltransferases for base methylation (Motorin and Helm, 2011).

Modifications of ribose and bases may confer new and different chemical properties to rRNA molecules. Pseudouridines share with uridines the ability to form Watson-Crick interactions with adenosines but have an additional hydrogen donor at position 5 (N-H as depicted in Figure 5) where uridines exhibit a C-H at this position. As a result, pseudouridines may form new hydrogen bonds and they are also known to form stacking interactions, both could contribute in rRNA structure and stability (Hamma and Ferré-D’Amaré, 2006). Concerning 2’-O-methylation of the ribose, the methyl group replaces a hydroxyl group which is a potential hydrogen bond donor. The methyl group is also bulkier than hydrogen. Consequently 2’-O-methylation can be involved in hydrophobic contacts in one hand and can introduce steric effects within rRNA structure in the other hand. Bases can be modified at different positions,

even simultaneously (bimethylated nucleotides for instance). As well as 2'-O-methylations, they are involved in hydrophobic contact and steric effect. In addition some dimethylated nucleotides can prevent Watson-Crick pairing (Helm, 2006).

3.1. Modifications in *Escherichia coli* rRNAs

The 70S ribosome of *E. coli* contains 36 modified nucleosides (listed in Table 2). They are all clustered in the active sites of the ribosome: decoding centre, peptidyl transferase centre, subunit bridges and exit tunnel (Figure 6). This localization tends to underline their functional relevance during translation.

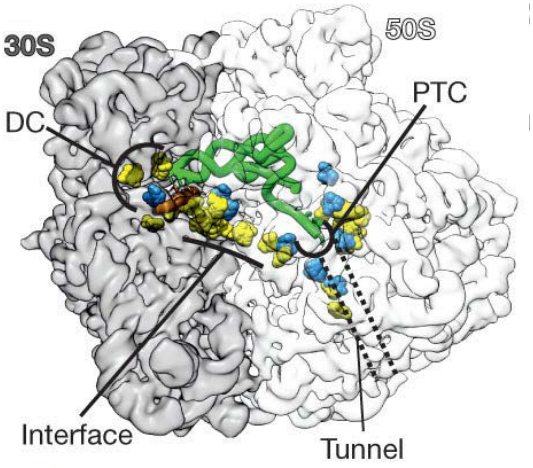

Figure 6: *E. coli* 70S ribosome and localization of rRNA modifications. The initiator fMet-tRNAfMet is depicted in green in the P-site. DC: deconding centre, PTC: peptidyl transferase centre (adapted from Fischer *et al.*, 2015).

So far, there are eleven modifications identified within *E. coli* 16S rRNA: 10 methylations and one pseudouridylation (Table 2 and Figure 6). Among them, there are six methylated residues within the decoding centre (m^2G966, m^5C967, m^4Cm1402, m^3U1498, $m^6{}_2$A1519 and $m^6{}_2$A1518) (Figure 7). Recent structural studies pointed out their relevance in *E. coli* and *Thermus thermophilus* ribosomes (Fischer *et al.*, 2015; Polikanov *et al.*, 2015). Indeed, they are in contact with the mRNA or the t-RNA and thus could regulate their interactions with the 16S rRNA (Figure 7).

Table 2: Modified nucleosides in *E. coli* rRNAs and their associated enzymes

Modified nucleoside in the 16S rRNA	Modification enzyme	Modified nucleoside in the 23S rRNA	Modification enzyme
		m^1G745	RlmAI
$\Psi516$	RsuA	$\Psi746$	RluA
m^7G527	RsmG	m^5U747	RlmC
m^2G966	RsmD	$\Psi955$	RluC
m^5C967	RsmB	m^6A1618	RlmF
m^2G1207	RsmC	m^2G1835	RlmG
$m^4Cm1402$	RsmH, RsmI	$\Psi1911$	RluD
m^5C1407	RsmF	$m^3\Psi1915$	RluD, RlmH
m^3U1498	RsmE	$\Psi1917$	RluD
m^2G1516	RsmJ	m^5U1939	RlmD
$m^6{}_2A1518$	RsmA (KsgA)	m^5C1962	RlmI
$m^6{}_2A1519$	RsmA (KsgA)	m^6A2030	RlmJ
		m^7G2069	RlmKL
		Gm2251	RlmB
		m^2G2445	RlmKL
		hU2449	
		$\Psi2457$	RluE
		Cm2498	RlmM
		oh^5C2501	RlhA
		m^2A2503	RlmN
		$\Psi2504$	RluC
		Um2552	RlmE
		$\Psi2580$	RluC
		$\Psi2604$	RluF
		$\Psi2605$	RluB

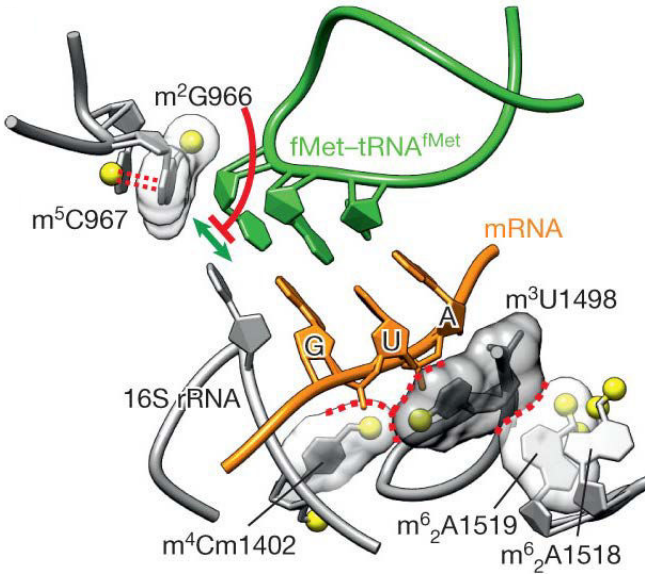

Figure 7: *E. coli* decoding centre. Methylations clustered within the decoding centre are depicted in yellow, mRNA in orange and initiator fMet-tRNAfMet in green. Methylations form hydrophobic contacts (red dashed lines) (adapted from Fischer *et al.*, 2015).

As depicted in Figure 7, methylation at position G966 may interact with the initiator fMet-tRNA^{fMet} restricting its mobility. The correct orientation of m^{2}G966 allowing for such role is due to base stacking interactions caused by the methyl group of m^{5}C967.

The base modifications m^{4}Cm1402, m^{3}U1498, m$^6{}_2$A1519 and m$^6{}_2$A1518 form together a network of hydrophobic interactions which could stabilize the binding of the mRNA to the P-site. m^{4}Cm1402 and m^{3}U1498 are in contact with the mRNA codon held in the P-site and their orientation is maintained by the dimethylated m$^6{}_2$A1519 and m$^6{}_2$A1518.

In conclusion, rRNA modifications seem to be of particular relevance. Their positions within the functional regions of the ribosome tend to highlight their probable role in the translation process. However, taken one by one, none of them is necessary neither for cell survival nor translation (Sergiev *et al.*, 2011). Moreover, the 16S rRNA can be *in vitro* transcribed, thus lacking modifications, and can be recruited for *in vitro* translation although such ribosomes are less efficient than wild type ones (Fritz *et al.*, 2015; Jewett *et al.*, 2013; Krzyzosiak *et al.*, 1987).

No functional and physiological roles have been attributed yet to those modifications. Nevertheless, structural studies tend to answer this question. Indeed, according to the high-resolution structure, methylations of the decoding centre could play an important role in initiation of translation or during decoding. Here, we will describe the different modifications located within the decoding centre and their associated methyltransferases.

a. RsmA modifies $m^6{}_2A1518$ and $m^6{}_2A1519$

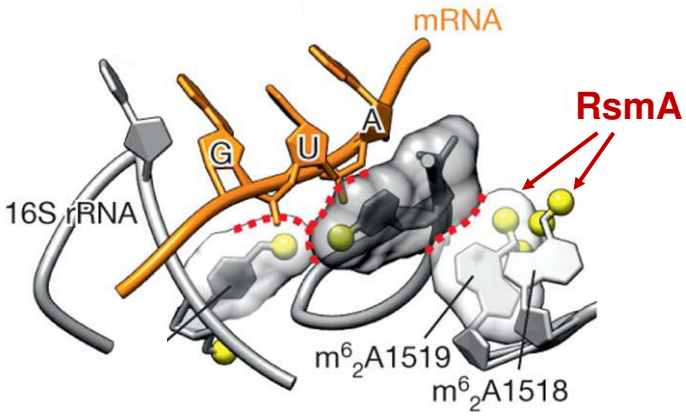

Figure 8: RsmA dimethylates the two nucleotides $m^6{}_2A1518$ and $m^6{}_2A1519$ in the decoding centre (adapted from Fischer *et al.*, 2015)

RsmA modifies two adjacent nucleotides located close to the 16S rRNA 3' end in helix 45: A1518 and A1519 (Figure 8). The modification catalysed by RsmA actually consists in dimethylation of $m^6{}_2A1518$ and $m^6{}_2A1519$ (Poldermans *et al.*, 1979). Interestingly, those dimethylations are highly conserved among bacteria, archaea and eukaryotes (O'Farrell *et al.*, 2006). Moreover, the enzyme family is also conserved. In fact, RsmA ortholog Dim1p from *Saccharomyces cerevisiae* can methylate *E.coli* 16S rRNA *in vivo* (Lafontaine *et al.*, 1994).

This conservation probably explains why this enzyme and its mode of action have been extensively studied compared to other rRNA methyltransferases. RsmA modifies the rRNA at a late step of biogenesis but before 30S subunit is fully matured. Indeed, *in vitro* studies showed that it requires ribosomal proteins S6, S8, S11, S15, and S18 but S21 and IF3 are inhibitory (Thammana and Held, 1974) furthermore it does not act on either naked 16S rRNA or the active 30S subunit (Desai and Rife, 2006). It was suggested that methylation triggers the release of

RsmA (Connolly *et al.*, 2008) which is consistent with the fact that its affinity is lower for the methylated rRNA (Poldermans *et al.*, 1979). It was shown that in a *rsmA*-mutant strain there is an accumulation of 16S rRNA precursors while overexpression of the enzyme leads to accumulation of free 30S subunits (Connolly *et al.*, 2008). Connolly *et al.* suggested that RsmA could play an important role in maturation of the 30S subunit in a translational active form.

Other structural studies investigated further this hypothesis. Crystal structure of unmethylated ribosomes from *Thermus thermophilus* has been determined and suggests that the dimethylations added by RsmA participate in the correct formation of helices 44 and 45 (Demirci *et al.*, 2010). Thus they would allow proper packing of the decoding centre and their lack would perturb A- and P-sites structure. Thereafter the cryo-electron microscopy structure of RsmA bound to an inactive 30S subunit has been solved (Boehringer *et al.*, 2012). RsmA would prevent binding of 50S thus 70S formation and permit final rRNA processing and conformation. Those structural studies concluded that RsmA could act as a checkpoint in ribosome assembly: the enzyme would bind a late but inactive rRNA precursor and the dimethylations would allow a correct packing of the rRNA and its final processing, thus RsmA would prevent immature 30S subunit to enter initiation of translation.

However, neither the enzyme nor the modifications are essential. In fact, early studies detected that some strains naturally lack the dimethylations making them resistant to the antibiotic kasugamycin (Helser *et al.*, 1972). Compared to a wild type strain, absence of those modifications does not have any effect in growth at 37°C, however, it induces a cold hypersensitivity (Connolly *et al.*, 2008). Although canonical translation is similar to the wild type, the mutant strain also exhibits a higher level of translation with non-AUG initiation codons (O'Connor *et al.*, 1997) and an increased level of stop codon read-through and frameshifting (van Buul *et al.*, 1984).

Das *et al.*, (2008) investigated on discrimination of the initiator $tRNA^{fMet}$, which possesses three consecutive G-C base pairs in the anticodon loop. This characteristic feature seems to be essential for translation initiation and is highly conserved. They built a plasmid coding for $tRNA^{fMet}$ with an AUC anticodon that permits specific initiation of a chloramphenicol acetyl transferase (CAT) gene harbouring an UAG as initiation codon. The three G-C pairs of this initiator tRNA were changed with the pairs found in the anticodon loop of elongator $tRNA^{Met}$. Such

mutant tRNA^{fMet} is deficient in initiating translation in a wild type strain. They observed that the mutant strain Δ*rsmA* is able to translate the *cat* gene using this mutant initiator tRNA^{fMet}. Consequently, dimethylations $m^6{}_2A1518$ and $m^6{}_2A1519$ seems to play a role in accuracy of translation initiation. Moreover, they found that a mutation in *folD* gene enables translation initiation of the *cat* reporter gene with the mutant tRNA^{fMet}. This *folD* mutation also leads to reduced levels of SAM (the methyl donor of rRNA methyltransferases) resulting in lower levels of rRNA methylations.

b. Modifcations added by RsmB and RsmD modulate interactions with tRNA

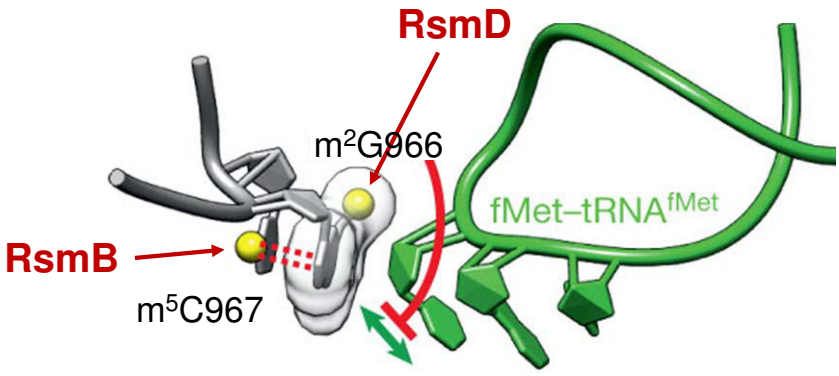

Figure 9: RsmB modifies m^5C967 and RsmD methylates m^2G966 in the decoding centre (adapted from Fischer *et al.*, 2015).

RsmB is responsible of the modification of m^5C967 (Tscherne *et al.*, 1999) and the adjacent G966 is also methylated by the methyltransferase RsmD at the N2 position of the guanosine (Lesnyak *et al.*, 2007) (Figure 9). Those two enzymes are highly specific for their respective nucleotide position in 16S rRNA and display mutually exclusive specificities (Weitzmann *et al.*, 1991). Indeed, RsmB is the only 16S rRNA methyltransferase to act *in vitro* on naked 16S rRNA and binding of ribosomal proteins S7 and S19 inhibits its methyltransferase activity (Gu *et al.*, 1999; Weitzmann *et al.*, 1991). On the other hand, RsmD uses the assembled 30S ribosomal subunit as preferential substrate *in vitro* (Lesnyak *et al.*, 2007; Sergeeva *et al.*, 2012). Thus, while RsmB could also be considered as a checkpoint in ribosome assembly, RsmD has to act on the 30S subunit prior to translation. Structural data suggest that they could play a role in tRNA binding (Fischer *et al.*, 2015) and their involvement in initiation of translation or accuracy have been investigated.

Translation with non-AUG initiation codon has been studied for the mutant strains Δ*rsmB*, Δ*rsmD* and the double mutant Δ*rsmBD* (Arora *et al.*, 2013a). For most codons, translation in wild type and mutant strains was similar but was higher with AUU codons (about half more in Δ*rsmB* and twice more in Δ*rsmD* and Δ*rsmBD*). Moreover Burakosky *et al.* also implicated the modifications m^5C967 and m^2G966 in binding of initiator $tRNA^{fMet}$. Indeed, it seems that ribosomes lacking both methylations are deficient in the formation of the 30S IC *in vitro* due to increased fMet-$tRNA^{fMet}$ dissociation (Burakovsky *et al.*, 2012). Methylations m^5C967 and m^2G966 seems to have different effects on spontaneous frameshifting. In Δ*rsmB* mutant strain, neither +1 nor -1 frameshifting was affected compared to a wild type strain while both increased in Δ*rsmD* (Arora *et al.*, 2013b).

Absence of RsmB and RsmD has a slight effect on growth, indeed doubling time in Δ*rsmB,* Δ*rsmD* and Δ*rsmBD* is slightly higher than in the wild type. The double mutant Δ*rsmBD* was shown to be cold sensitive and could not compete with the wild type, when grown together (Burakovsky *et al.*, 2012).

c. RsmE methylates m^3U1498 which contact the mRNA

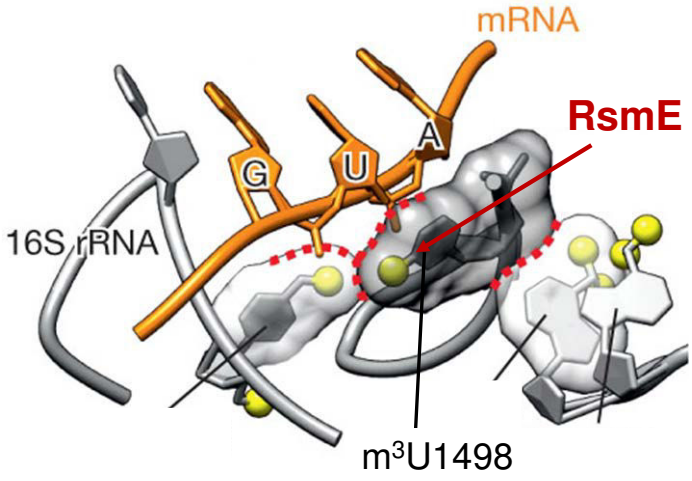

Figure 10: RsmE modifies nucleotide m^3U1498 in the decoding centre (adapted from Fischer *et al.*, 2015).

RsmE is responsible of the methylation of m^3U1498, located on the top of helix 44 (Basturea *et al.*, 2006) (Figure 10). The enzyme was first characterized in 2006 and although it shares structural features of the SPOUT family, it defines a new family of RNA methyltransferases and has its own specific motifs (Basturea *et al.*,

2006; Zhang *et al.*, 2012). It methylates preferentially the assembled 30S ribosomal subunit (or a late and highly structured assembly intermediate) (Basturea and Deutscher, 2007).

Compared to a wild type strain, *rsmE* mutant does not have any difference in growth but, interestingly, is less competitive when both strains are cultured together (Basturea *et al.*, 2006). The methylation m^3U1498 also seems to play a role in initiator tRNA selection: in the *folD* genetic background (with a reduced level of SAM), Δ*rsmE* mutant strain exhibited higher translation of an orthogonal CAT gene using its specific orthogonal initiator tRNA (Das *et al.*, 2008).

d. Base methylation m4Cm1402 catalysed by RsmH interacts with the mRNA

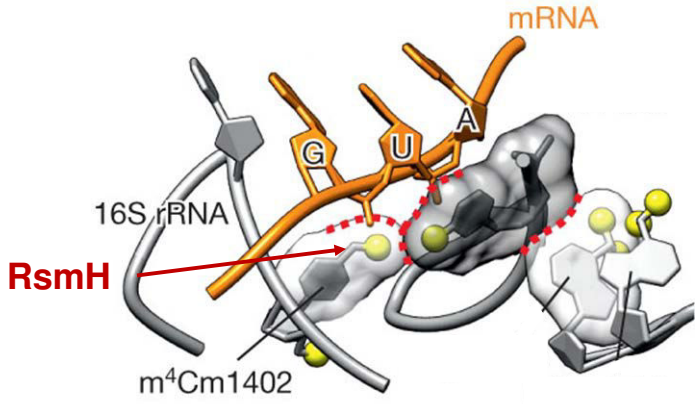

Figure 11: RsmH methylates the base of nucleotide C1402 in the decoding centre (adapted from Fischer *et al.*, 2015).

The nucleotide at position C1402 undergoes two different modifications: an N^4-methylation catalysed by RsmH and a 2'-O-methylation added by RsmI (Figure 11). Both enzymes use the 30S subunit as preferential substrate (Kimura and Suzuki, 2010). The modification catalysed by RsmH is part of a network of interaction within the decoding centre while the ribose methylation is more buried inside the 30S subunit (Figure 11) (Fischer *et al.*, 2015). Thus, regarding our interest for the decoding centre in particular, we will focus on the base methylation added by RsmH.

Kimura and Suzuki (2010) studied several translational features (non AUG initiation, stop codon read-through, ORF maintenance) on wild type and Δ*rsmH* mutant strains. Interestingly, Δ*rsmH* mutant exhibited a decrease in stop codon read-through and in +1 frameshift while -1 frameshift and AUU initiation increased. The

mutant strain also showed a slight increase of its doubling time in LB medium compared to the wild type.

3.2. Variations in expression of rRNA modification genes during stress

This part focuses on data relative to the variations of the expression of methyltransferases RsmA, RsmB, RsmD, RsmE and RsmH under stressful conditions such as oxidative, osmotic and changes in temperature. Different studies showed that, after the application of stresses, expression of these methyltransferases varied at the level of either transcription or translation. Thus, under stresses, the pool of ribosomes could vary, at least for methylation of 16S rRNA nucleotides positioned in the decoding centre.

a. Variations of expressions of methyltransferases under oxidative stress

Analysis of data from Jozefczuk *et al.*, 2010 shows that RsmA has a 3-fold decreased rate of transcripts under oxidative stress mediated by addition of hydrogen peroxide. In this study, RsmD has a 2-fold increased rate of transcripts which is in accordance with the results of Bojanovič *et al.*, 2017 who analysed the global transcriptional responses to oxidative stress in *Pseudomonas putida*. The expression of the other methyltransferases (RsmB, RsmE and RsmH) does not change during hydrogen peroxide challenge.

b. Variations of expressions of methyltransferases under osmotic stress

About osmotic shift, there was no variation in transcription of the methyltransferases of interest according to either Gunasekera *et al.*, (2008) or Shabala *et al.*, (2009). Study on the uropathogenic *E. coli* CFT073 strain in minimal medium with 0,3 M NaCl cultured at 30°C show that only *rsmD* and *rsmE* transcriptions were slightly downregulated (about 2-3 fold change) whereas the transcriptions of *rsmA*, *rsmB* and *rsmH* did not change (Withman *et al.*, 2013). In *Pseudomonas putida*, after addition of 0,5M of NaCl in minimal medium, transcription of *rsmH* varies slightly (Bojanovič *et al.*, 2017).

c. Variations of expressions of methyltransferases under temperature changes

During heat stress, transcription of *rsmA* decreases with a 5-fold rate after 10 minutes of temperature rising from 30°C to 45°C (Jozefczuk *et al.*, 2010; Zhao *et al.*, 2005). This transcription decrease is also correlated to a significant fold change of the enzyme production using ribosome profiling (Zhang *et al.*, 2017). Concerning the methyltransferase RsmB, Jozefzuck *et al.* (2010) have also shown that the transcription has a 5-fold decreased rate which correlates with a decrease in the production of this methyltransferase (Zhang *et al.*, 2017). The two methyltransferases RsmD and RsmE do not present any change either using transcriptomic data or ribosome profiling analysis (Jozefczuk *et al.*, 2010; Zhang *et al.*, 2017). However, the data concerning the methyltransferase RsmH are relatively discordant: Jozefzuck *et al.*, 2010 found a 3-fold increase in terms of transcription and Zhang *et al.*, 2017 did not reveal any noticeable change using ribosome profiling analysis.

The cold stress does not seem to affect the expression of methyltransferases. The analysis of data from Jozefzuck *et al.* (2010) allow to notice a 2-fold decreased rate of transcription of *rsmE*, but no significant variation in protein abundance was detected after cold change (Zhang *et al.*, 2018).

4. Toxin-Antitoxin modules and stress

Toxin-antitoxin (TA) modules are small genetic elements that are frequently found in plasmids and prophages where they are involved in post-segregational killing. Therefore, they were first considered as addiction modules. They are also abundant in bacterial genomes, they belong to the pool of genetic elements that are frequently transferred horizontally (Harms *et al.*, 2018).

Typically, TA systems encode a stable toxic protein and a labile antitoxin on an operon (Page and Peti, 2016). During favourable growth conditions, the antitoxin counteracts the deleterious effect of the toxin and represses transcription of the operon. Hence, degradation of the antitoxin results in the relief of the autoregulation and leads to production of the toxin (Harms *et al.*, 2018).

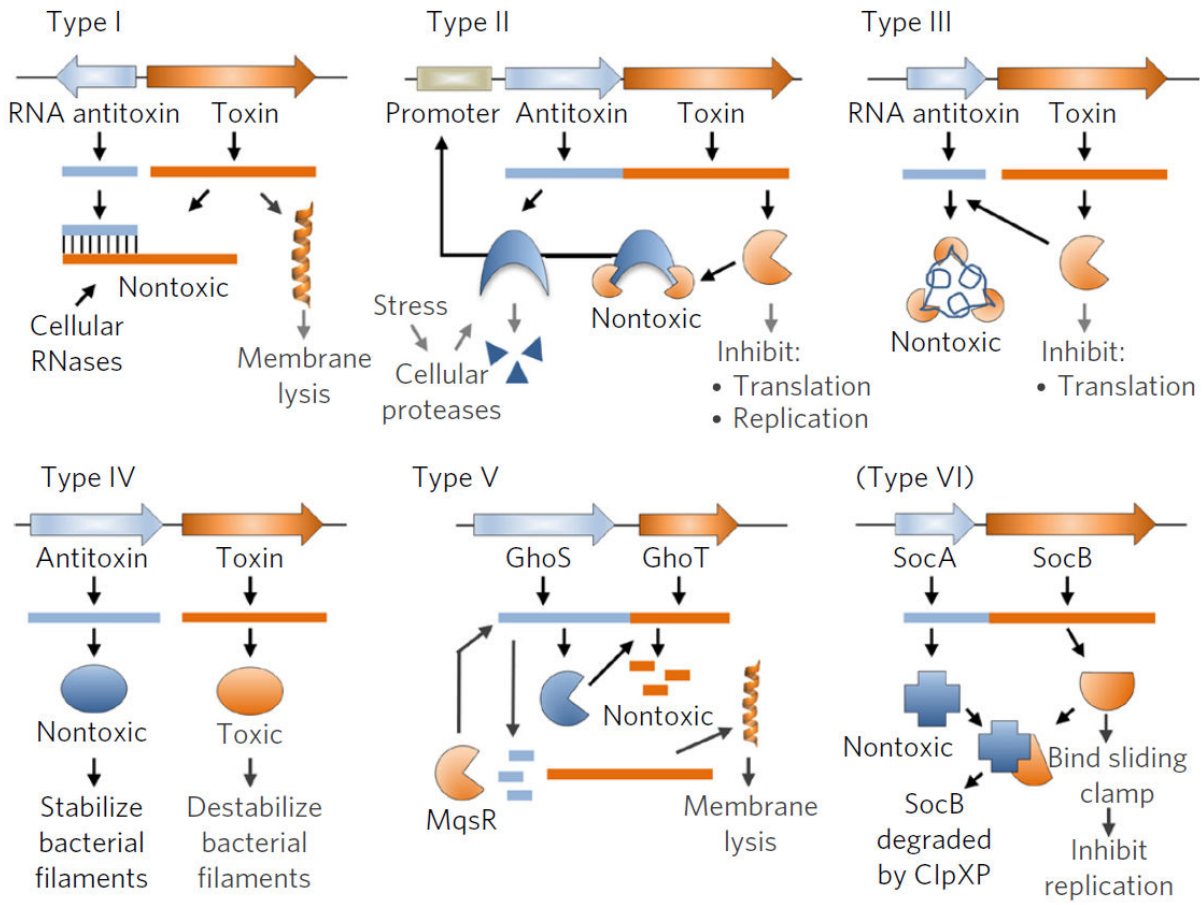

Figure 12: Different types of toxin antitoxin modules and their targets. Toxins are depicted in orange, antitoxins in blue (Page and Peti, 2016).

Different types of toxin-antitoxin modules have been defined regarding the nature of the antitoxin and its mode of action on the associated toxin (Figure 12). In types I and III, antitoxins are RNA molecules controlling toxins by inhibition of translation or direct binding respectively. Type II antitoxins are proteins that bind and inhibit their targeted toxin protein. In type IV, both components are proteins as well but inhibition of toxins by antitoxins is indirect, the antitoxin prevents action of the toxin by stabilizing its cellular targets (Harms *et al.*, 2018). More recently, types V and VI were described and each family contains a single occurrence, so far. Type V GhoS/GhoT with antitoxin GhoS is an antisense with endoribonuclease activity cleaves ghoT toxin mRNA (Wang *et al.*, 2012). Type VI, SocA/SocB, consists of antitoxin presenting toxin to ClpXP for proteolysis (Aakre *et al.*, 2013).

Their role in bacterial physiology is mainly considered as related to stress adaptation and metabolism management (Buts *et al.*, 2005). Transcriptional regulation of TA modules is integrated into cellular signalling pathways, allowing a direct connection between stress perception and toxin activation. This includes transcriptional control of the operon by stress as described for SOS inducible TA by LexA repressor, or CRP and Sxy for *hicAB* operon in *E. coli* (Turnbull and Gerdes, 2017) but also antitoxin stability affected by ppGpp and proteases whose amounts increased under stress (Muthuramalingam *et al.*, 2016).

Toxins have a wide variety of actions, either direct or indirect (Figure 13): they can inhibit DNA replication, destabilize cell wall and inhibit protein synthesis by interacting with the ribosome or as endoribonucleases degrading bulk mRNAs (Harms *et al.*, 2018). The main known mechanisms concern endonucleolytic cleavage as performed by RelE, MazF, HicA and SymE, action on tRNA (HipA, VapC, TacT, AtaT), direct action on the ribosome (RatA, VapC) or EF-Tu (Doc) and synthesis of antisense RNA which promotes mRNA cleavage (Darfeuille *et al.*, 2007; Harms *et al.*, 2018). Among the thirteen type II TA systems of *E. coli*, the RNases are well represented: seven belonging to the RelE family toxin, two fitting in the MazF/Kid family and one encoding a toxin from HicA family.

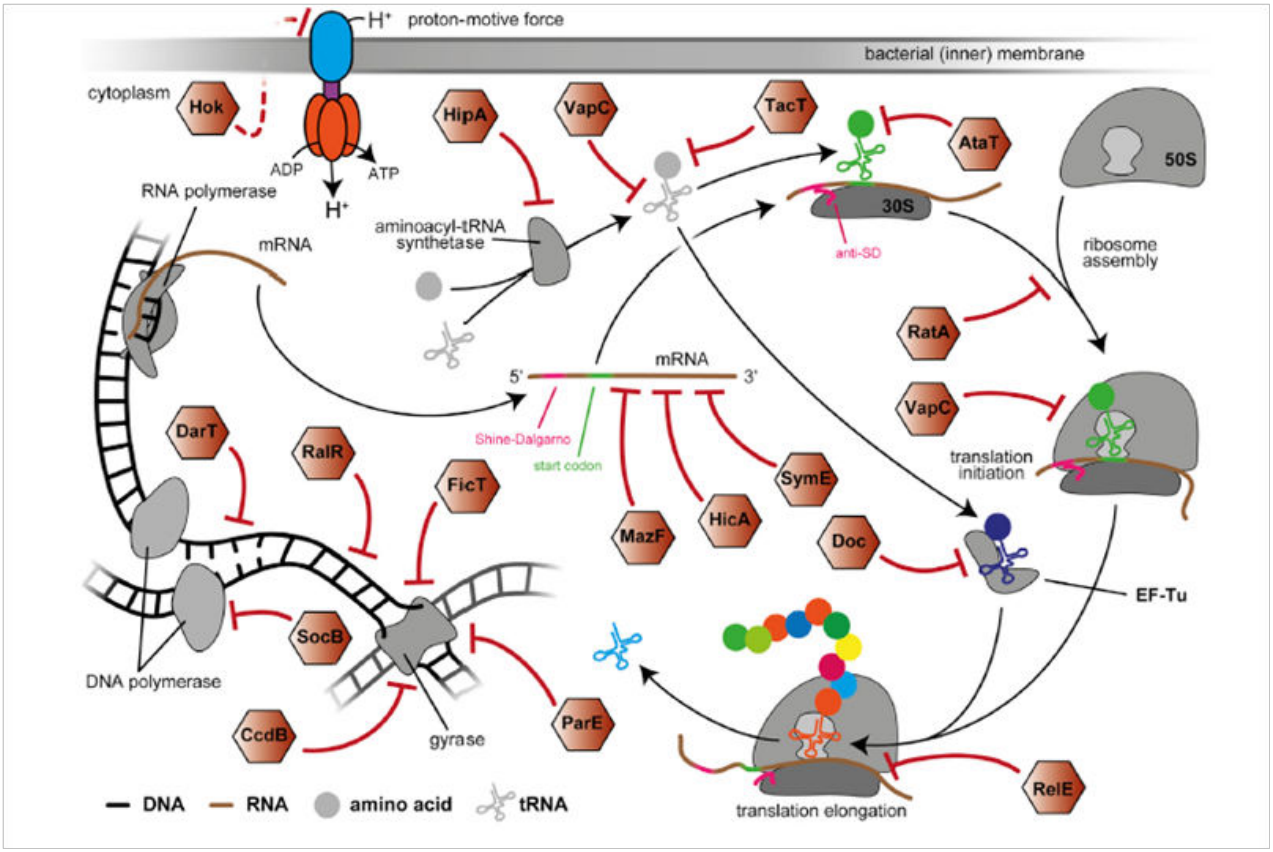

Figure 13: Actions and cellular targets of toxins (Harms *et al.*, 2018).

Toxins belonging to the MazF/Kid family have been well described and are considered as ribosome-independent mRNA endonucleases. They target sequences (three to seven nucleotides), and contribute to mainly abolish translation and generate specific mRNAs such as leaderless mRNAs and specialized ribosomes.

mazEF is a type II toxin-antitoxin system encoding a labile antitoxin (MazE) which can bind to the stable toxin (MazF) preventing its lethal action. *mazEF* expression is negatively auto-regulated, since the fixation of either MazE or MazE-MazF complex prevents transcription of these genes (Marianovsky *et al.*, 2001). The expression of *mazE* and *mazF* is also regulated by environmental stress. Upon stress, the production of MazE is stopped and the antitoxin is degraded by ClpPX (Aizenman *et al.*, 1996). This permits MazF to exert its toxic function as endoribonuclease that specifically cleaves single-stranded RNAs at ACA-sites (Zhang *et al.*, 2003). As a result, during stress conditions MazF rapidly degrades bulk mRNA resulting in a severe inhibition of protein synthesis (Culviner and Laub, 2018).

It was observed that about 10% proteins were still produced after *mazF* induction (Amitai *et al.*, 2009). That means that not all mRNAs are completely

degraded by MazF. Distinct mRNAs are cleaved at ACA-sites just upstream of the translational start-codon, removing the 5' untranslated region (UTR) containing the SD sequence, leading to production of leaderless mRNAs. Moreover, MazF is also able to cleave the 16S rRNA in the context of the ribosome, upstream of the position 1500, thus removing the last 43 nucleotides from its 3'-end. This leads to the loss of the anti-SD sequence (Vesper *et al.*, 2011). The ribosomes harbouring the truncated 16S rRNA (70SΔ43) are unable to initiate translation of canonical mRNA (which still contain the 5'UTR including the SD sequence) due to the absence of the SD/anti-SD interaction. However, lmRNAs are selectively translated by 70SΔ43, the so-called "stress ribosomes" (Vesper *et al.*, 2011).

Another type II TA system, the *hic* AB system is broadly found in bacteria, where HicA RNase toxin and HicB the antitoxin. Mutation in *hicB* was shown to suppress SigmaE lethality (Jørgensen *et al.*, 2009). HicA activity results in a bacteriostatic effect. The induction of HicA inhibits translation and induces cleavage of mRNAs and also of transfer-messenger RNA (tmRNA) (Jørgensen *et al.*, 2009) which is involved in the rescue of stalled ribosomes (Giudice and Gillet, 2013). When examining the regulation of this TA system, Winter *et al.*, (2018) have shown that the interactions between the toxin HicA and the antitoxin HicB are quite complex and modulate the binding to the operator sites of the operon *hic AB*. Moreover, Winter *et al.* (2018) have demonstrated that the binding sites of HicB overlap the predicted -10 and CRP-binding sequences. This fact highlights the connection between the induction of HicA and metabolic changes.

II. Aims and relevance

A major challenge is to apprehend the regulation of protein synthesis in bacteria dividing in a permissive optimal environment and bacteria facing harmful conditions due to temperature, osmotic, oxidative and other changes.

Numerous previous studies explored either transcriptomic or proteomic variations induced by such changes and, more recently, translatomic differences using the new method of ribosome profiling. However, transcript levels are sparsely correlated to protein abundance (Guimaraes *et al.*, 2014). When Lu *et al.*, (2007) examined, in *E. coli*, the differences of protein levels in correlation with transcripts, they stated that 47% of the protein abundance could be explained by the mRNA levels. Therefore, 53 % of the protein content would originate from post-transcriptional regulation which includes regulatory RNA-mediated, riboswitches, so-called translational regulations including the regulations directly due to the ribosomal variations that we could name ribosomal regulation.

This ribosomal regulation has to be connected to the concept of ribosome heterogeneity that emerges during the last years in prokaryotes (Byrgazov *et al.*, 2013; Sauert *et al.*, 2015) and in eukaryotes (reviewed in Genuth and Barna, 2018). Such regulation could have important implications in bacterial antibiotic resistance and in some human ribosomopathies associated with variations of either eukaryotic or mitochondrial ribosomes. Thus, some evidence shown there are functional selective ribosomal subpopulations with modifications in either rRNA or r-proteins content and composition. Of course, other ribosomal associated factors are involved, directly or indirectly (modified or altered factors), in modulation of the translation activity and in stress response.

One element could have its importance in ribosome heterogeneity: the modifications added post-transcriptionnally, such as nucleobases modifications. Modifications of the 16S rRNA occur on either naked 16S rRNA (with a link with the ribosome biogenesis) or on 30S particles (with a link with translation activity and stability). In this work, we focused on methylations clustered in the decoding centre, catalysed by the methyltransferases RsmA, RsmB, RsmD, RsmE and RsmH. Analysis of expressions (from transcriptome and translatome data) of those methyltransferases indicates that variations occur in immediate response and

adaptation to stresses. Globally, the transcription and the translation of these methyltransferases are affected with a tendency to decrease upon stresses such as temperature, oxidative and osmotic changes. In this context, we aim to understand the implications of the methylations of the decoding centre in protein synthesis. We studied their effects on canonical and non-canonical translation with a focus on leaderless mRNAs translation and frameshifting, when cells are in either favourable or stressful conditions.

Another great impact during stresses is the implication of toxin-antitoxin (TA) modules with the delivery of toxins from their counteracting antitoxins. Among these TA modules, one well-known system, MazEF is involved in the modulation of the translation in response to stressful conditions. MazF toxin could produce specialized ribosomes (without the anti-SD) and leaderless mRNAs. The impact of such toxins, *i.e.* endoribonucleases, would have to be analysed on translation. The main difficulty to analyse endoribonucleases effects is that induction of such toxins promotes, generally, growth arrest. In this way, a strategy would be to use a heterologous system (HicAB of *Sinorhizobium meliloti*) with an inducible expression in order to produce truncated mRNAs in *E. coli* and evaluate *trans*-translation in the future.

In this context, this work is composed of two parts: one part focusing on the effects of methyltransferases targeting the decoding centre and the second part aiming the characterization of the TA module HicAB of *Sinorhizobium meliloti*.

III. Chapter I: Implication of 16S rRNA methyltransferases in translation in *Escherichia coli*

1. Introduction

In all organisms, every type of RNA molecules (mRNAs, tRNAs, tmRNA and rRNAs) are post-transcriptionally modified. The *Escherichia coli* 70S ribosome contains 36 modified nucleotides of particular relevance. They are all located in the functional centres of the ribosome (decoding centre, interface of the subunits, peptidyl transferase centre and exit tunnel) and are very conserved, underlying their potential importance. Although the biological function of these modified bases is still unclear. Therefore we investigated their possible role during stress response. We specifically focused on the six 16S rRNA methylations that are located in the decoding centre at positions 966, 967, 1402, 1498, 1518 and 1519. We aimed to evaluate their implication in translation.

2. Materials and methods

2.1. Bacterial strains

The bacterial strains used in this study are listed in Table 3. The strains were grown at 37 °C in Luria Bertani (LB) (Miller, 1972) or in the minimal media M9 (supplemented with 20 mM glucose or L-arabinose) and 12 g/L of agar for solid media. Antibiotics were added as needed at the following concentrations: 100 µg/mL of ampicillin (Amp), 30 µg/mL of chloramphenicol (Cm), 25 µg/mL of kanamycin (Kan), 10 µg/mL tetracycline (Tet).

Table 3: Bacterial strains used in this study.

Strains	Genotype	Reference
MG1655	F-, λ-, *ilvG- rfb*-50 *rph*-1	Blattner *et al.*, 1997
STL14025	F-, lacZ4823, mhpC281::Tn10, λ-, *rph*-1	Seier *et al.*, 2011
BW25113	Δ(*araD-araB*)567, *ΔlacZ4787*(::rrnB-3), λ-, *rph*-1, Δ(*rhaD-rhaB*)568, *hsdR514*	Baba *et al.*, 2006
JW0050-3	BW25113 *ksgA733::kan*	Baba *et al.*, 2006
JW3250-2	BW25113 *rsmB725::kan*	Baba *et al.*, 2006
JW3430-4	BW25113 *rsmD720::kan*	Baba *et al.*, 2006
JW2913-1	BW25113 *rsmE721::kan*	Baba *et al.*, 2006
JW0080-1	BW25113 *rsmH788::kan*	Baba *et al.*, 2006
MG6006	MG1655 (F-, λ-, *ilvG- rfb*-50 *rph*-1, *rpsB*-HIS6, *rpsT*-STREP)	Laboratory collection
MG6416	6006 *lacZ4823, mhpC281::Tn10*	This study
ΔrsmA::kan	MG1655 *ksgA733::kan*	This study
ΔrsmB::kan	MG1655 *rsmB725::kan*	This study
ΔrsmD::kan	MG1655 *rsmD720::kan*	This study
ΔrsmE::kan	MG1655 *rsmE721::kan*	This study
ΔrsmH::kan	MG1655 *rsmH788::kan*	This study
ΔrsmA 6417	6416 *ΔrsmA*	This study
ΔrsmB 6418	6416 *ΔrsmB*	This study
ΔrsmD 6419	6416 *ΔrsmD*	This study
ΔrsmE 6420	6416 *ΔrsmE*	This study
ΔrsmA	MG1655 *ΔrsmA*	This study
ΔrsmB	MG1655 *ΔrsmB*	This study
ΔrsmD	MG1655 *ΔrsmD*	This study
ΔrsmE	MG1655 *ΔrsmE*	This study
ΔrsmH	MG1655 *ΔrsmH*	This study

2.2. Plasmids and oligonucleotides

Plasmids, oligonucleotides and gene fragments used in this study are listed in Table 4, 5 and 6 respectively.

Table 4: Plasmids used in this study.

Plasmids	Characteristics	Reference
pBAD24	Ori pBR322, *araC*, P_{BAD} , *bla*	(Guzman *et al.*, 1995)
pKD46	oriR101 w/repA101ts, *araC,* Para , *bla,* λ(γ,β,exo)	Datensko and Wanner (2000)
pCP20	FLP+λ ci857+ λ pR rep101Ts, *bla, cat*	(Cherepanov and Wackernagel, 1995)
pBAD24Nde+1	pBAD24 with *NdeI* site at transcriptional start of Para	This study
pmut3	Ori ColE1, PtacII , *gfpmut3*	Laboratory collection
pmut3+1	pmut3 *gfpmut3*:T16	This study
pmut3-1	pmut3 *gfpmut3*ΔA15	This study
pF38lacZSD	pBAD24Nde+1 lacZ with SD	This study
pF45lacZLL	pBAD24Nde+1 lacZ without 5' UTR	This study
pB01	Ori pBR322, *bla*, PtacII , *mcherry*, *gfpmut3*	This study
pB11dnaX	pB01 with *dnaX::gfpmut3*	This study
pB14prfB	pB01 with *prfB::gfpmut3*	This study
pB18gfp+1	pB01 with *gfpmut3*:T16	This study
pB19gfp-1	pB01 with *gfpmut3*ΔA15	This study

Table 5: Oligonucleotides used in this study.

Oligonucleotide	Targeted region	Sequence
BADNdeD	Transcription start site of pBAD24	GATCCTACCTGACGCTTTTTATCGCAACTCTCTACTGTTTCTCC ATATGCGTTTTTTTGGG
BADNdeR	Transcription start site of pBAD24	CTAGCCCAAAAAAACGCATATGGAGAAACAGTAGAGAGTTG CGATAAAAAGCGTCAGGTAG
lacZNdeF	lacZ	TGAGATCTGAGGAGCTAGcatATGCTGACTCTG
lacZSDEcoF	lacZ	CATGGCATGGATGAatTCTACAAATAATG
lacZSmaR	lacZ	CTCAAAGGTTACCCCgGgTGGGGCAC
mut3EcoF	gfp	aatgaattcAAAATGAGTAAAGGAGA
mut3XhoR	gfp	tatctcgagTTATTTGTATAGTTCAT
mut3SacF	gfp	caagagctcAGTAAAGGAGA
prfBEcoF	prfB	AAGgaattcATCatgTTTGAAATTAATCC
prfBSacR	prfB	aaagagctcCTGCAGATACCCCCTAA
rsmA F	rsmA	CCGATGTCGGCAGTTTTATT
rsmA R	rsmA	CAGATTGCGTATGGTTACGG
rsmB F	rsmB	GAACCTGCTCTCGTTACAACCT
rsmB R	rsmB	CCGTTGGTATCGACAACAGTAA
rsmD F	rsmD	TATGTGTTATCTGGCGGATTGA
rsmD R	rsmD	CAGAGCATTAACAAACGACCAA
rsmE F	rsmE	CGCGAAAGAGCTAACCTACACT
rsmE R	rsmE	GCCGAGCTTGATCATTATTCTT
rsmH F	rsmH	GATATCGACGCAGAGCAGTT
rsmH R	rsmH	AAATCGCAAAAGATCGTCAC
gfp0_F	gfp0 for *in vitro* translation	GCGAATTAATACGACTCACTATAGGGCTTAAGTATAAGGAG GAAAAAATATGAGTAAAGGAGAAGAACTTTTCACT

gfp-1_F	gfp-1 for *in vitro* translation	GCGAATTAATACGACTCACTATAGGGCTTAAGTATAAGGAG GAAAAAATATGAGTAAAGGAGAGAACTTTTCACT
gfp+1_F	gfp+1 for *in vitro* translation	GCGAATTAATACGACTCACTATAGGGCTTAAGTATAAGGAG GAAAAAATATGAGTAAAGGAGAATGAACTTTTCAC
gfp_R	gfp for *in vitro* translation	AAACCCCTCCGTTTAGAGAGGGGTTATGCTAGttaTTTGTATA GTTCATCCATGCCATG

Table 6: Genes synthesized used in this study.

Name	Sequence
mCherry	ttattatatcgatTTGACAATTAATCATCGGCTCGTATAATGTGTGGATTTCAGGAGCTAAGGAAgcta gcATGGTGAGCAAGGGCGAGGAGGATAACATGGCCATCATCAAGGAGTTCATGCGCTTCAAGG TGCACATGGAGGGCTCCGTGAACGGCCACGAGTTCGAGATCGAGGGtGAGGGtGAGGGCCGtC CaTACGAGGGCACCCAGACCGCCAAGCTGAAGGTGACCAAGGGTGGCCCCCTGCCCTTCGCCT GGGACATCCTGTCCCCTCAGTTCATGTACGGCTCCAAGGCCTACGTGAAGCACCCCGCCGACAT CCCCGACTACTTGAAGCTGTCCTTCCCCGAGGGCTTCAAGTGGGAGCGCGTGATGAACTTCGA GGACGGCGGCGTGGTGACCGTGACCCAGGACTCCTCCCTGCAGGACGGCGAGTTCATCTACAA GGTGAAGCTGCGCGGCACCAACTTCCCCTCCGACGGCCCCGTAATGCAGAAGAAGACCATGGG CTGGGAGGCCTCCTCCGAGCGGATGTACCCCGAGGACGGCGCCCTGAAGGGCGAGATCAAGC AGAGGCTGAAGCTGAAGGACGGCGGCCACTACGACGCTGAGGTCAAGACCACCTACAAGGCC AAGAAGCCCGTGCAGCTGCCCGGCGCCTACAACGTCAACATCAAGTTGGACATCACCTCCCACA ACGAGGACTACACCATCGTGGAACAGTACGAACGCGCCGAGGGCCGCCACTCCACCGGCGGC ATGGACGAGCTGTACAAGTAATAGGTTCTGTTctagaAAGTAACTGAACCCAAAGTCGTTAGTG ACGCTTACCTCTTAAGAGGTCACTGACCAAGgaattcattATGGAGCTCtttctcgagttatttaagctttatt at
mut3:T16	GGATCCTCTAGATTTAAGAAGGAGATATACATATGAGTAAAGGAGAATGAACTTTTCACTGGA GTTGTCCCAATTCTTGTTGAATTAGATGGTGATGTTAATGGGCACAAATTTTCTGTCAGTGGAG AGGGTGAAGGTGATGCAACATACGGAAAACTTACCCTTAAATTTATTTGCACTACTGGAAAACT ACCTGTTCCATGGCCC
mut3ΔA15	GGATCCTCTAGATTTAAGAAGGAGATATACATATGAGTAAAGGAGAGAACTTTTCACTGGAGT TGTCCCAATTCTTGTTGAATTAGATGGTGATGTTAATGGGCACAAATTTTCTGTCAGTGGAGAG GGTGAAGGTGATGCAACATACGGAAAACTTACCCTTAAATTTATTTGCACTACTGGAAAACTAC CTGTTCCATGGCCC
dnaX insert	gaattcATCATGAGTTATCAGGTCTTAGCCCGAAAATGGCGCCGCGTGCAGGGAGCAACCAAAG CAAAAAAGAGcGAACCGGCAGCCGCTACCCGCGCGCGGCCGGTGAATTGATAgagct

2.3. Competitive growth and stress adaptation

Cultures of the different strains MG6416, *ΔrsmA*::kan, *ΔrsmB*::kan, *ΔrsmD*::kan, *ΔrsmE*::kan and *ΔrsmH*::kan were conducted at 30°C in M9 minimal medium supplemented with glucose (Glc) (20 mM) (M9-Glc). Using overnight precultures in M9-Glc, 10 mL cultures were inoculated at an initial optical density at 600 nm (OD_{600}) of 0.05 for single cultures or 0.025 for co-cultures. When the single or co-cultures reached OD_{600} of 0.5, they were ten-fold serial diluted in M9 and 10 µL of

each dilution were plated on M9-Glc agar plates. In the case of single cultures, the dilutions were spotted on (i) three M9-Glc agar plates which were incubated at 30°C or 43°C for 24h and 16°C for 48h; (ii) one M9-Glc agar medium containing plumbagin (0.2 mM); and (iii) one M9-Glc agar medium containing NaCl (0.5 M); the last two plates were incubated at 30°C for 24h. In the case of co-cultures, the dilutions were spotted on the same kind M9-Glc agar plates that above, except one set of plates was supplemented with tetracycline (10 µg/mL) for the selection of MG6416 and another set of plates was supplemented with kanamycine (25 µg/mL) to select the mutant strain: *ΔrsmA*::kan, *ΔrsmB*::kan, *ΔrsmD*::kan, *ΔrsmE*::kan and *ΔrsmH*::kan

2.4. Plasmid construction

a. Construction of lacZ vectors

pBAD24Nde+1 is a plasmid derivative of pBAD24. This plasmid was built by annealing oligonucleotides BADNdeD and BADNdeR together and introducing the double stranded fragment between *Bam*HI and *Nhe*I restriction sites in pBAD24. The resulting construction (pBAD24Nde+1) contains a unique *Nde*I restriction site (CATATG) of which the second A (from ATG) is located at the transcription start site of pBAD24.

lacZ coding sequence (from ATG to stop codon) was amplified by PCR from MG1655 genomic DNA using lacZNdeF and lacZSmaR primers. The PCR product bears lacZ coding sequence with *Nde*I restriction site located at the initiation codon and *Sma*I restriction site immediately after the stop codon. The PCR fragment was digested with *Nde*I and *Sma*I and introduced into pBAD24Nde+1, resulting in pF45lacZLL.

lacZ open reading frame was amplified using primers lacZEcoF and lacZSmaR. The resulting fragment was introduced between *Eco*RI and *Sma*I sites in pBAD24Nde+1 resulting in pF38lacZSD.

b. Construction of pB01

pB01 plasmid is a derivative of pBAD24 vector. A DNA fragment harbouring P_{tacII}, mcherry sequence and restriction sites (Table 6) was synthesized and inserted in pBAD24 between *Cla*I and *Hind*III sites resulting in loss of araC, P_{BAD}, and multiple

cloning site. Subsequently, *gfp* coding sequence was amplified from pmut3 using primers mut3SacF and mut3XhoR, the fragment was digested using *Sac*I and *Xho*I and inserted between corresponding sites to obtain pB01.

c. Construction of pB18gfp+1 and pB19gfp-1

To modify *gfp* sequence by addition or deletion of one nucleotide, synthetic gene fragments mut3:T16 and mut3ΔA15 were synthesized. They correspond to the beginning of *gfp* sequence with insertion of one T at position 16 for *mut*3:T16 fragment or deletion of an A at position 15 for *mut*3ΔA15 fragment. The two fragments were cleaved with *Xba*I and *Nco*I enzymes and inserted between the corresponding sites of pmut3 plasmid resulting in pmut3+1 and pmut3-1 plasmids.

To build pB18gfp+1 and pB19gfp-1 plasmids, *gfp* sequence was amplified from plasmids pmut3+1 and pmut3-1 using primers mut3EcoF and mut3XhoR and the fragments were cleaved with *Eco*RI and *Xho*I enzymes. They were then introduced in pB01 between the corresponding sites to substitute *gfp*.

d. Construction pB11dnaX and pB14prfB

dnaX frameshift signals were synthesized as synthetic gene fragment (dnaX insert, Table 6). *prfB* sequence was amplified from MG1655 genomic DNA using primer prfBEcoF and prfBSacR. The two products were digested by *Eco*RI and *Sac*I and then inserted between the corresponding sites in pB01 resulting in pB11dnaX and pB14prfB plasmids.

2.5. Generation of *rsm* mutant strains

All *rsm* mutant strains were obtained using the method described by (Datsenko and Wanner, 2000). The genes of interest were amplified by PCR from their corresponding strains derivative of BW25113 (JW0050-3, JW3250-2, JW3430-4, JW2913-1 and JW0080-1) each containing one *rsm* gene fused to a kanamycin cassette (Baba *et al.*, 2006). Oligonucleotides specific of each locus were used (Table 5). The targeted strains (in which the mutation had to be transferred, namely MG1655 or 6416), were transformed with plasmid pKD46. The latter leads to the expression of the λRed homologous recombination system by addition of arabinose,

confers resistance to ampicillin and is thermosensitive thus is lost at 37 °C. To produce the recombination system, strains bearing pKD46 were grown in LB containing ampicillin and 20 mM L-Arabinose at 30°C until they reached OD_{600} of 0.6. Subsequently, cells were prepared for transformation of the DNA of interest (*rsm* gene fused with kanamycin cassette). They were harvested by cold centrifugation and washed twice with ice-cold sterile water. Cells were resuspended in 10% glycerol in order to obtain an OD_{600} of approximately 100 uDO. 100 µL of cells were mixed with 30 to 50 ng of the PCR product of interest. Electroporation was performed using Gene PulserII (Biorad) with parameters: 2.5 V, 25 µF, 5ms. Cells were resuspended in SOC medium (Hanahan, 1983) and incubated at 37°C for two hours. They were then plated on LB Kanamycin plates and incubated at 42°C overnight to lose pKD46 and select for recombinants. Colonies resistant to kanamycin and sensitive to ampicillin were selected and insertion of the cassette was checked by PCR using primers specific to regions flanking the genes of interest.

2.6. P1 transduction

To obtain *lacZ* mutant strains (6416 and derivatives) for subsequent use in β-galactosidase assays, the mutations *lacZ4823, mhpC281::Tn10* were transferred from the donor strain STL14025 to 6006 by P1 transduction (Miller, 1972). Transposon Tn10 bears a tetracycline resistance gene permitting selection of transductants using this antibiotic, *lacZ* and *mhpC* genes being close enough. To produce the phage lysate containing the mutation to transduce, the donor strain STL14025 was infected with P1cml. This phage caries a chloramphenicol resistance gene and repressor of the lytic cycle is thermosensitive thus production of phages is inducible at 42°C. The cells were cultured in LB supplemented with 2 mM $CaCl_2$ and 10 mM $MgSO_4$ at 37°C until they reached an OD_{600} of 0.3. Then, P1 phages were added and the culture was transferred to 42°C at a high agitation for 45 min to permit lysis of bacteria and production of phages. After lysis, 1 ml of the lysate was withdrawn and centrifuged to eliminate cell debris. Supernatant was transferred in a sterile microtube and 10 µL of CHCl3 was added. In parallel, the recipient cells (6006) were grown in LB at 37°C until OD_{600} = 1, then 2 mM $CaCl_2$ and 10 mM $MgSO_4$ were added. Aliquots of 500 µL were taken from the culture and put in contact with 50 or 100 µL of phage lysate for one hour at room temperature without shaking

to permit infection. Then, cells were harvested, washed with LB medium and plated on LB tetracycline plates to select for transductants. Tetracycline resistant colonies were isolated several times on LB Tetracycline plates to eliminate residual phages. Candidates were checked for loss of β-galactosidase activity on LB Tetracycline IPTG (isopropyl β-D-1-thiogalactopyranoside) plates.

2.7. β-Galactosidase assays

The strains derivative of 6416 (namely, MG6416, Δ*rsmA* 6417, Δ*rsmB* 6418, Δ*rsmD* 6419 and Δ*rsmE* 6420) containing plasmid pF38 or pF45 were grown overnight in M9 minimal medium complemented by Glucose and Ampicillin at 30°C, shaking. The overnight cultures were used to inoculate 50 mL of M9 Glucose Ampicillin at a starting optical density at 600 nm (OD_{600}) of 0.1. Cells were cultured at 30 °C, shaking, until they reached OD_{600} = 0.5. Then, cells were washed with M9 to get rid of the culture medium and resuspended in 800µL M9. 200 µL of cells were transferred in four different media corresponding to different stresses and containing L-Arabinose for induction of *lacZ* transcription (M9 L-Ara NaCl, M9 L-Ara H_2O_2, M9 L-Ara 16°C and M9 L-Ara 42 °C) at OD_{600} of approximately 0.3 for each. Those cultures were grown for an hour and a half at 30°C (or 16°C or 42°C if indicated). Subsequently, cells were pelleted and frozen prior to add 500 µL Sodium Phosphate Buffer (60 mM Na_2HPO_4, 40 mM NaH_2PO_4, pH=7). Cell walls were disrupted by adding 30 µL CHCl3 and 30 µL 0.1% SDS and vortexing for 15 sec. β-galactosidase activity was assessed at 30°C as following: 20 µL of cells were added to 180 µL of Z Buffer (60 mM Na_2HPO_4, 40 mM NaH_2PO_4, 10 mM KCl, 0.1 mM $MgSO_4$, 50 mM β-mercaptoethanol, pH 7.4) supplemented with 4 mg/mL ONPG (orthonitrophenyl-β-galactoside). Reactions were stopped by adding 100 µL 1M Na_2CO_3. Product intensity was measured at 420 nm and cell debris at 550 nm. The β-galactosidase activity was calculated in Miller Units (Miller, 1972) with the formula 1000 x (OD_{420}-1.75xOD_{550}) x total reaction volume (mL) / t (min) x OD_{600} x culture volume (mL).

2.8. Fluorescence assays

MG1655 wild type strain and isogenic mutant strains (Δ*rsmA*, Δ*rsmB*, Δ*rsmD,* Δ*rsmE* and Δ*rsmH*) were transformed with plasmids pB01, pB11dnaX, pB14prfB,

pB18gfp+1 or pB19gfp-1. The strains carrying those plasmids were grown overnight in M9 minimal medium supplemented with Glucose and Ampicillin at 37°C, shaking. Overnight cultures were used to inoculate 5 mL of M9 with Glucose and Ampicillin. When they reached OD_{600} = 0.5, five aliquots of 200 µL of cells were taken and stressed (0.3 M NaCl, 10 mM H_2O_2, 45°C or 16°C) or not. They were incubated in 96-well plates for 30 min at 37°C (or 16°C or 42°C if indicated). Subsequently fluorescence of GFP and mCherry was measured using Synergy H1 microplate reader (BioTek) with wavelengths of excitation 485 nm and 585 nm and of emission 515 nm and 612 nm respectively. As mCherry was used as internal control, ratios of fluorescence intensity of GFP over fluorescence intensity of mCherry (GFP/mCherry) were calculated.

2.9. In vitro translation assays

a. Ribosome purification

The ribosomes from MG1655 and mutant strains Δ*rsmA*, Δ*rsmB*, Δ*rsmD,* Δ*rsmE* and Δ*rsmH* were purified. Overnight cultures of the strains in M9 Glu were used to inoculate at 1% 2L of fresh M9 Glu. When the cultures reached OD_{600}=1, cells were harvested by centrifugation 8000 rpm, 10 min, 4°C and washed in Buffer A (20 mM Tris HCl pH 7.5, 0.1 M NH_4Cl, 3 mM β-Mercaptoethanol, 1 mM PMSF, 10 mM $MgCl_2$) (rotor JA-14, Beckman-Coulter). Dried pellets were frozen at -80°C overnight. Subsequently, pellets were resuspended in 3 mL of Buffer A and cells were lysed with a French Press cell (1250 PSI). Lysates were centrifuged at 13000 rpm, 40 min, 4°C (JA-17 rotor, Beckman-Coulter) and supernatants were loaded on 20-50% sucrose density gradients. Ultracentrifugation of the gradients was performed at 23000 rpm for 18h at 4°C in a SW28 rotor (Beckman-Coulter). Then, gradients were separated into fractions of 1 mL and their absorbance at 260 nm (A260) was monitored. Fractions corresponding to the 70S ribosomes were mixed together and diluted twice in Buffer A prior to another ultracentrifugation at 55000 rpm, 1h30, 4°C in a Ti70.1 rotor (Beckman-Coulter). Pellets were washed with Buffer A to remove sucrose and resuspended in 100 µL of Buffer A. Ribosomes were purified from three different cultures for each strain.

b. DNA matrix for in vitro translation

Three different PCR products were produced using the Q5 Taq polymerase (NewEngland Biolabs). Those products correspond to the T7 promoter (for *in vitro* transcription) and *gfp* in frame or in the second or third frame of translation, thus they were named gfp0, gfp+1 and gfp-1 respectively. The different amplifications were performed on pB01, pB18gfp+1 or pB19gfp-1 using primers gfp0_F and gfp_R, gfp+1_F and gfp_R; gfp-1_F and gfp_R respectively. Size of the PCR products was analysed on 1% agarose gel electrophoresis and were then purified using PCR Purification Kit (Qiagen).

c. In vitro transcription and translation

The ribosomes obtained from the different strains (MG1655 and *rsm* mutant strains) were tested for *in vitro* translation. For this purpose, the purified PCR products (gfp0, gfp+1 and gfp-1) were used as DNA matrix for *in vitro* transcription/translation using the PURExpress ∆ribosome kit (New England Biolabs). Reactions were set according to the manufacturer's protocol (10 µl Solution A; 3 µl Factor Mix; 30 pmol Ribosomes; 250 ng Template DNA; Nuclease-free H_2O up to 25 µL) and were incubated at 37°C for 3 h. GFP fluorescence was measured using the LS 45 Fluorescence Spectrometer (Perkin Elmer) with excitation at 485 nm and emission at 510 nm.

3. Results

To investigate the role of 16S rRNA methylations in translation, different genetic tools have been engineered. We specially focused on modifications located within the decoding centre. Thus, we first developed *E. coli* strains lacking one methyltransferase responsible for modification at this site. Then, we built several plasmids to study translation of canonical and leaderless mRNAs or frameshifting. The genetic tools we used in this study are presented in the first section of this chapter.

Then, data we obtained for every mutant strain are shown. We chose to analyse the results with a focus on each strain, before to discuss them globally. Data obtained with *ΔrsmE* mutant are presented first because this strain exhibited more phenotypic defects. Then results obtained using the mutant strains *ΔrsmB, ΔrsmD, ΔrsmA* and *ΔrsmH* are analysed.

3.1. Genetic tools

Since methylations seem to modulate interactions within the decoding centre, we aimed to study translation by ribosomes lacking those modifications. To study the effects of each of those methylations, we built isogenic mutants of the *E. coli* MG1655 strain, which are deleted for a single *rsm* gene: *ΔrsmA*, *ΔrsmB, ΔrsmD, ΔrsmE* and *ΔrsmH.* To do so, we used BW25113 strains from the Keio collection (Baba *et al.*, 2006) in which the coding sequence of each non-essential gene was replaced by a kanamycin cassette flanked by FRT sites. We amplified each region of interest: *ksgA733::kan, rsmB725::kan, rsmD720::kan, rsmE721::kan, rsmH788::kan* from mutant strains built by Baba *et al.* (2006). Then the PCR products were transferred in MG1655 using the method of one-step inactivation developed by Datsenko and Wanner (2000). Kanamycin resistance genes were then eliminated in the MG1655 mutants.

a. Investigations on canonical and leaderless translation

To investigate the role of those methyl groups during canonical translation, we constructed a plasmid (named pF38lacZSD) carrying a *lacZ* reporter. We inserted *lacZ* coding sequence in pBAD24 vector (Figure 14.A). Transcription of *lacZ* is under

control of arabinose promoter and can be induced by addition of arabinose in the medium. The mRNA produced carries the vector SD sequence (AGGAGG) upstream of the start codon. Translation of *lacZ* mRNA leads to production of β-Galactosidase whose activity can be easily assessed. *lacZ* is a robust reporter, which is not post-translationally regulated. Thus, β-Galactosidase activity directly reflects of translational efficiency.

We also hypothesized that lack of one methylation of the decoding centre could facilitate translation of leaderless mRNAs. To test this hypothesis, we built a leaderless *lacZ* reporter in pBAD24 vector, pF45lacZLL (Figure 14.B). To do so, we inserted *lacZ* coding sequence directly at the transcription start site of the vector. Thus, the transcript starts with AUG initiation codon and completely lacks 5' UTR. Consequently, β-Galactosidase produced from pF45lacZLL reflects the ability of the ribosomes to efficiently translate leaderless mRNA.

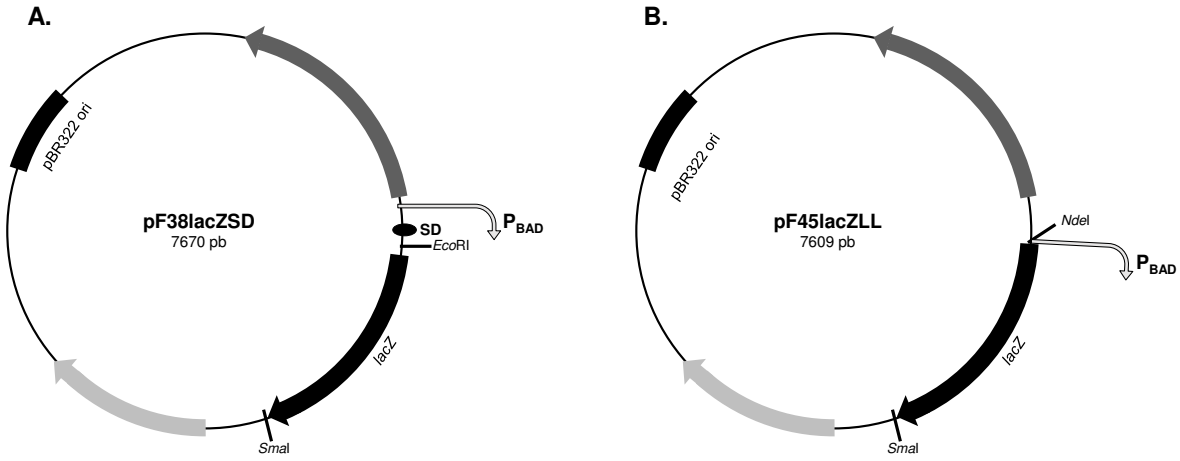

Figure 14: Schematic representation of plasmids pF38lacZSD (A) and pF45lacZLL (B) used for translation of canonical and leaderless mRNAs. pBR322 ori: origin of replication. *bla*: ampicillin resistance gene. P_{BAD}: arabinose promoter (inducible with L-arabinose). *lacZ*: β-galactosidase coding sequence. SD: Shine-Dalgarno sequence. *araC*: coding sequence for AraC – regulatory protein of arabinose operon.

To assess β-Galactosidase activity, we constructed strains carrying a *lacZ* chromosomal mutation (MG6416 (wild type), *ΔrsmA* 6417, *ΔrsmB* 6418, *ΔrsmD* 6419

and *ΔrsmE* 6420). This mutation was transferred from the strain STL14025 (harbouring a stop codon in *lacZ*) to MG1655 and *rsm* isogenic mutants by P1 transduction.

pF38lacZSD and pF45lacZLL were transformed in MG6416, and cells containing either plasmid were grown in M9 minimal medium and induced for 1h30 using L-arabinose. Subsequently, β-Galactosidase assays were performed. MG6416 containing pF38lacZSD had an activity of 5172+/-780 Miller units and of 133+/-35 Miller units when transformed with pF45lacZLL. When cells were not induced (cultured in M9 glucose), their activity was 74.7+/-21 with pF38lacZSD and 0.3+/-0.6 with pF45lacZLL. Consequently, even though translation of leaderless *lacZ* mRNA was about 40 times less efficient than that of canonical *lacZ,* it is significant when compared to non-induced cultures containing pF45lacZLL.

b. Study of maintenance of the reading frame

We also aimed to study how methylations would help in maintaining codon-anti-codon interactions in the decoding centre during the elongation step. To address this question we studied frameshifting in MG1655 and isogenic mutants (*ΔrsmA*, *ΔrsmB, ΔrsmD, ΔrsmE* and *ΔrsmH*). We developed a dual fluorescent reporter system which encodes green fluorescent protein (GFP) and mCherry (Figure 15). Excitation and emission properties of those proteins are very different and allow for a simultaneous detection. Thus, fluorescence is detected directly in the bacterial growing culture.

All constructions were built from pB01 which harbours a wild type GFP and so was used as control construction (Figure 15.A).

Genes coding for mCherry and GFP are co-transcribed using a single constitutive promoter (PtacII) to minimize variations in their transcription (Figure 15). They have the same SD sequence (AAGGAA), six nucleotides upstream of their AUG initiation codon. mCherry coding sequence and GFP SD sequence are separated by a 80 nt spacer so that translation initiation of both proteins can be independent. Translation of mCherry reflects canonical translation. Subsequently, we used GFP as a reporter for programmed or spontaneous frameshift events.

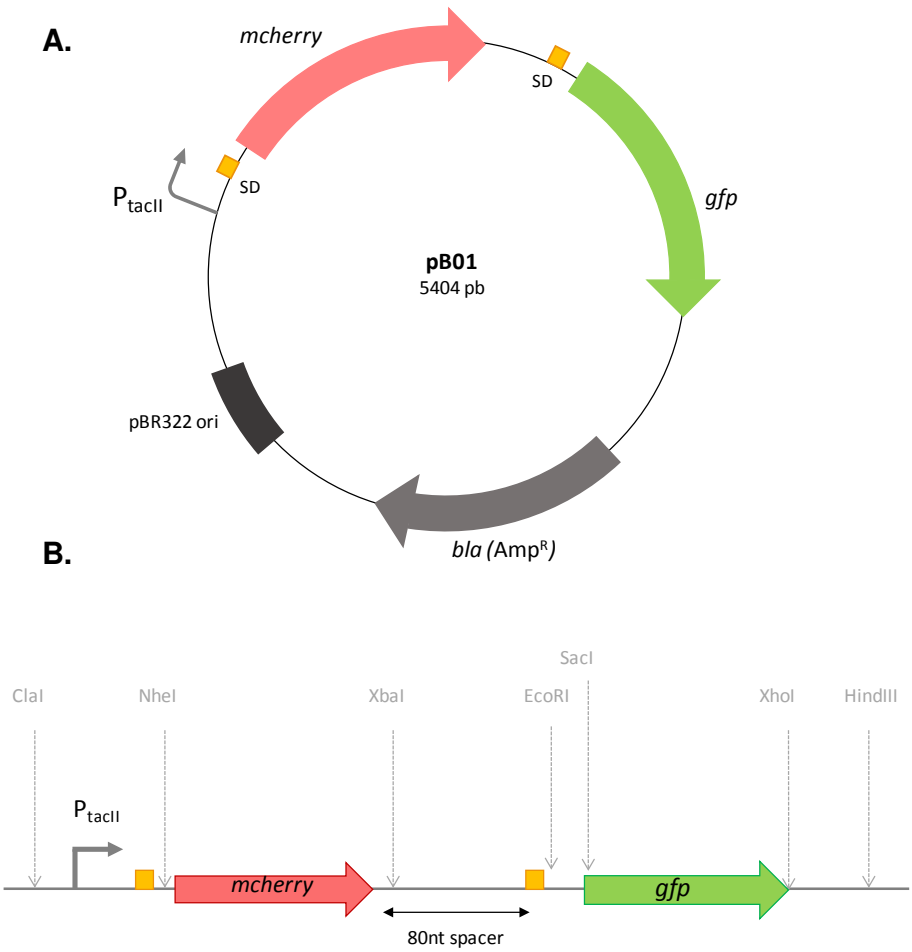

Figure 15: Schematic representation of pB01 plasmid (A) and general organization the dual fluorescent reporter with *mcherry* and *gfp* coding sequences (B). Restriction sites used for the cloning are indicated by grey dashed arrows. Red box: mcherry coding sequence, green box: *gfp* coding sequence, PtacII: constitutive promoter, yellow box: Shine-Dalgarno sequence.

To test whether both fluorescent proteins can be expressed from pB01, the plasmid was transformed in MG1655. Cells were cultured in M9 glucose at 37°C until they reached the exponential phase (OD_{600} of 0.5) and fluorescence was measured. GFP fluorescence normalized by OD_{600} reached a value of 1113+/-187 GFP relative fluorescence units ($_{GFP}$RLU) and mCherry fluorescence was 9562+/-990 mCherry relative fluorescence units ($_{mC}$RLU). Thus, both proteins are produced from pB01. As mCherry is meant to be used as internal control, we calculated the ratio of GFP/mCherry which was about 0.12 for pB01.

- Programmed frameshifting

Programmed frameshifting uses slippery sequences to disrupt codon-anticodon interactions and promote re-association of the aminoacyl tRNA with an overlapping codon. As a consequence, ribosomes shift from one frame to another. Such signals for ribosomal frameshifting are present within the mRNA sequence and their efficiency in frameshifting can be improved by internal SD-like sequences and stem loops. To study programmed frameshifting, we inserted variant sequences of the genes *dnaX* or *prfB* upstream of *gfp* (between *EcoR*I and *Sac*I restriction sites) (Figure 16). In both constructions, the ATG start codon was removed from *gfp* coding sequence.

In plasmid pB14prfB, we inserted the first 79 nt of *prfB* gene of *E. coli* (Figure 16.C). The slippery site of this gene is located at position 63 of which sequence is CUU-UGA with an in frame UGA stop codon. Frameshifting at this site makes the ribosome decode the UUU codon (+1 frame) and thus permits translation of the whole protein. There is an SD-like sequence (AGGGGG) upstream of the slippery site promoting the repositioning of the ribosome in the second frame of translation. Plasmid pB14prfB bears those signals and the coding sequence of GFP (deleted of its endogenous start codon) is not in frame. The ribosomes must shift to the second frame of translation to produce GFP. Thus, translation of active GFP from pB14prfB reflects +1 *prfB* dependent frameshifting.

The *E. coli dnaX* gene contains the slippery sequence A-AAA-AAG driving the ribosome to change to the -1 frame and read AAA codon instead of AAG. Immediately downstream of this site, there is a stop codon in the third frame of translation. Thus, the -1 frameshift event causes early termination of translation. Supplementary features are necessary for efficient *dnaX* frameshifting: upstream of the slippery site there is an internal SD-like sequence, while downstream there is a stem loop. In plasmid pB11dnaX, we introduced a 107 nt insert upstream of GFP coding sequence (deleted of its ATG) (Figure 16.D). The insert contains an ATG initiation codon and the signals for *dnaX* dependant frameshifting namely the slippery sequence, the SD-like sequence and the stem loop. The -1 frame stop codon was mutated (TGA to cGA) and we inserted an additional in frame stop codon after the stem loop. Thus, in pB11dnaX, GFP coding sequence is in the third frame of translation and its production requires -1 frameshifting.

pB14prfB and pB11dnaX were transformed in MG1655 to check for GFP production. MG1655 harbouring pB14prfB showed a GFP fluorescence of 7367+/-620 GFP $_{GFP}$RLU and mCherry of 9150+/-214 mCherry $_{mC}$RLU. It resulted in a GFP/mCherry ratio of 0.8+/-0.08. Concerning pB11dnaX, MG1655 exhibited values of 2362+/-720 $_{GFP}$RLU and 16940+/-4730 $_{mC}$RLU. The GFP/mCherry ratio with pB11dnaX was then about 0.14+/-0.004.

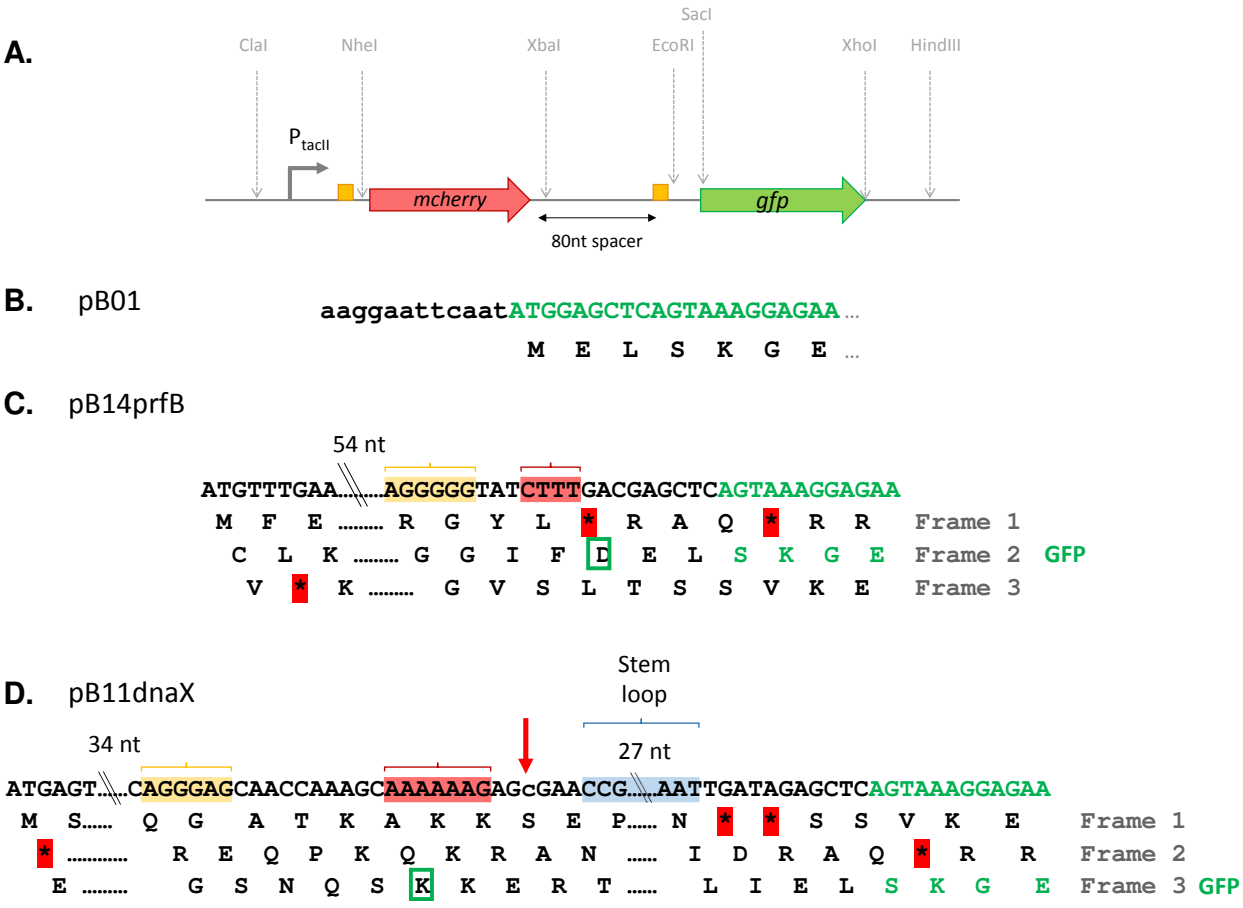

Figure 16: Nucleotidic sequence inserted upstream of *gfp* to promote programmed frameshifting in pB14prfB and pB11dnaX. (A) Organization of pB01 and (B) sequence of *gfp* in pB01. Nucleotidic sequence upstream of *gfp* gene in pB14prfB (C) and pB11dnaX (D). The inserts were introduced between EcoRI and SacI sites. The different features necessary for frameshifting are indicated in boxes. Yellow boxes: SD-like sequence, red boxes: slippery sequence, blue box: stem loop. Translation frames are indicated below the nucleotidic sequence, the aminoacid in a green empty box is the first one which is incorporated following a frameshift. GFP sequence is written in green. Stop codons are highlighted in red.

Thus, programmed frameshifting was very efficient using *prfB* and *dnaX* sequences leading to detectable fluorescence signals. Moreover, ratios obtained from pB14prfB were higher than those from pB11dnaX. This difference was expected due to the bias induced by *prfB* regulation. Indeed, as *prfB* frameshifting relies on low concentration of RF2, we can assume that production of *gfp* mRNA exhibiting prfB signals leads to a titration of RF2 of which, content is not sufficient to inhibit frameshifting.

- Spontaneous frameshifting

We also built two reporters of spontaneous ribosomal frameshifting (pB18gfp+1 and pB19gfp-1) (Figure 17). In pB18gfp+1, a single nucleotide was added in *gfp* coding sequence at position 15; at the opposite, in pB19gfp-1, one nucleotide was removed at position 14 (see Figure 17.B and C). As a consequence the coding frame is changed to frame 2 in pB18gfp+1 and frame 3 in pB19gfp-1. Those mutations were inserted upstream of a hairpin (depicted in yellow in Figure 17) that could potentially slow down ribosomes and lead to a better frameshifting efficiency. Moreover, the beginning of the sequence (first 14 nucleotides) is the same for all 3 constructs and they all exhibit stop codons in the second and third frames of translation (red stars in Figure 17). As a consequence, we can assume that translation starts at the ATG in the first frame for all constructs and to translate an active GFP from pB18gfp+1 and pB19gfp-1, ribosomes need to shift to resume the coding frame (frame 2 or 3 respectively). Moreover, that frameshift has to happen before the eleventh codon for valine. Indeed, the first β-barrel (highlighted in green in Figure 17) starts at this position and is necessary for GFP fluorescence. Indeed, several studies analysed GFP fluorescence after mutagenesis and deletion of NH2 extremity and they all agree that β-barrel is essential and does not tolerate any mutation or deletion.

When transformed in MG1655, pB18gfp+1 and pB19gfp-1 did not lead to a significant production of GFP: values of GFP fluorescence reached 39.6+/-12 and 31.7+/-11.5 respectively. This low fluorescence led to GFP/mCherry ratios of 0.005 for pB18gfp+1 and 0.004 for pB19gfp-1 (while GFP/mCherry ratio from pB01 was about 0.12). Spontaneous frameshifting is a rare event happening with a probability

of 10^{-5} per codon, thus we can expect that it is hardly measurable *in vivo*. However, *gfp* sequence from pB18gfp+1 and pB19gfp-1 were subsequently used for *in vitro* translation assays.

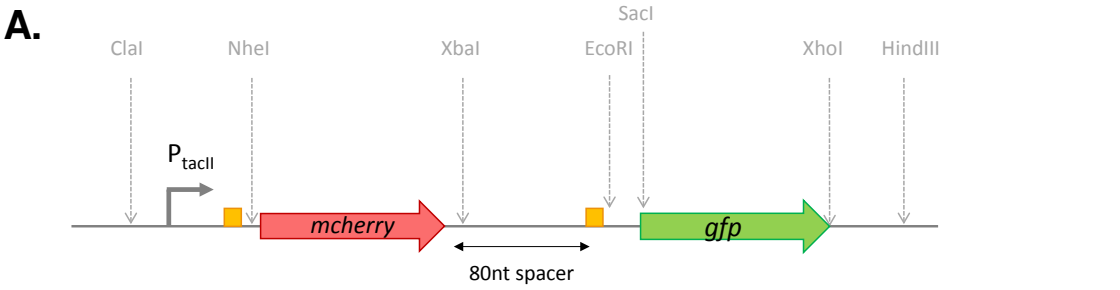

Figure 17: Coding sequence (first 50 nucleotides) of GFP from plasmids pB01, pB18gfp+1 and pB19gfp-1. (A) Organization of the dual fluorescent reporter pB01 and (B) coding sequence of GFP. GFP sequence was modified to build plasmids pB18gfp+1 and pB19gfp-1. Insertion of a single nucleotide in pB18gfp+1 (C) is highlighted in blue and location of the single nucleotide deletion in pB19gfp-1 (D) is indicated by an arrow. Nucleotidic sequence is indicated, the sequence of a hairpin is highlighted in yellow. Above, the three different frames of translation are represented. Stop codons are highlighted in red, the first amino acids of the first β-barrel of GFP is highlighted in green.

3.2. Lack of methylation m^3U1498 affects maintenance of the reading frame

a. Absence of RsmE does not impair growth or fitness

The methyltransferase RsmE was discovered quite recently and thus only a few groups studied the effects of RsmE knockout. We compared growth of an *E. coli* wild type strain, MG1655, with the isogenic mutant *ΔrsmE*. When cultured at 30°C in minimal medium M9 glucose, growth rates of both strains were similar: 0.58+/-0.03 h^{-1} for the wild type and 0.58+/-0.06 h^{-1} for the mutant. This is in accordance with a previous study that also observed a comparable growth in M9 glucose and in LB at various temperatures (25°C, 37°C and 42°C) (Basturea *et al.*, 2006). They also showed a deficiency in fitness of the mutant strain when grown together with the wild type strain in LB.

We also analysed the ability of *ΔrsmE* mutant to grow in competition with the wild type. To do so, we used MG6416 and *ΔrsmE*::kan strains and cultured them in minimal medium M9 glucose in either single or co-cultures. When the cultures reached exponential phase, 24h- and 48h- stationary phases, cells from the three cultures were diluted and the serial dilutions were spotted on several M9 glucose plates and incubated at 30°C. To analyse growth in stressful conditions, some plates were incubated at 43°C and 16°C and other plates containing stresses (such as NaCl to induce osmotic stress or plumbagin for oxidative stress) at 30°C. After 24h incubation, pictures of the plates were taken (Figure 18). No difference was observed between cells plated from exponential or stationary phases, thus only results from 24h-cultures are presented here. When MG6416 and *ΔrsmE*::kan were cultured together (Figure 18, bottom panel) at 30°C, we did not detect difference in the bacterial load. So, in those conditions, *ΔrsmE* mutant does not seem to have a defect in competitive growth. In addition, MG6416 and *ΔrsmE*::kan have similar behaviours when grown in the different stressful conditions, indicating that *ΔrsmE*::kan is able to efficiently adapt to those conditions.

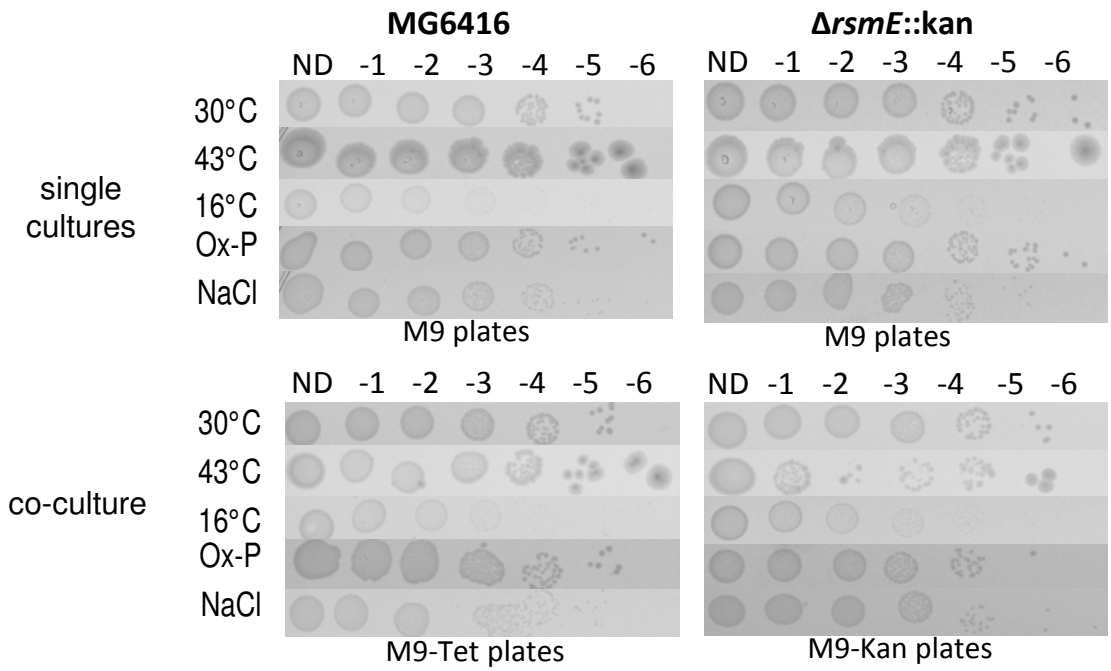

Figure 18: Adaptation of MG6416 and Δ*rsmE*::kan strains to various conditions. Spots of 10-fold serial dilutions of cells grown in single (top panels) or co-cultures (bottom panels) for 24h. M9–Glc plates were incubated at different temperatures (30°C, 43°C for 24h or 16°C for 48h), plates containing either plumbagin (0,2mM; Ox-P) or NaCl (0,5M; NaCl) were incubated at 30°C during 24h.

b. Lack of RsmE promotes translation of leaderless mRNA under heat shock

Even if lack of RsmE does not induce a difference in growth, we hypothesized that translation could be affected by growth conditions. We postulated that the possible effects of methylations could be more pronounced under stressful conditions. To assess translation of the different strains we used pF38lacZSD carrying a canonical *lacZ* (Figure 14.A). Transcription of the reporter is induced by the addition of arabinose in the growth medium. Translation of lacZ mRNA is not regulated and depicts canonical translation: the mRNA exhibits an SD sequence upstream of the AUG start codon. Consequently, pF38lacZSD was used as a control for translation efficiency in each strain.

We also analysed the influence of rRNA methylations on leaderless mRNA translation. We used pF45lacZLL plasmid carrying a leaderless *lacZ* reporter: arabinose induced transcription directly starts at the ATG initiation codon resulting in the production of an mRNA that completely lacks 5' UTR and so does not possess any SD sequence (Figure 14.B).

Wild type (MG6416) and *ΔrsmE* 6420 mutants were transformed with pF38lacZSD or pF45lacZLL and cultured in M9 glucose until they reached exponential phase (OD_{600} of 0.5). Afterwards, those precultures were washed and the cells were resuspended in M9 supplemented with L-arabinose to induce the transcription of the reporter. Indeed, *lacZ* is transcribed from P_{BAD} promoter which is induced by CRP-cAMP. The transition from a medium containing glucose to one with arabinose leads the cells to adapt their metabolism and thus it induces a longer time for full induction of the reporter. Therefore, the cultures were grown for 1h30 in M9 L-arabinose in order to obtain the best yield of reporter production.

During this incubation, cultures underwent different growth conditions such as control condition at 30°C, osmotic stress (at 30°C), oxidative stress (at 30°C), heat stress (43°C) or cold stress (20°C). Afterwards, samples were taken and β-Galactosidase activity of the reporters was assayed.

After 1h30 incubation with stresses, bacteria divided exponentially meaning they were adapted to those conditions. As a consequence, those assays give information about long-term adaptation rather than an immediate short-term stress response.

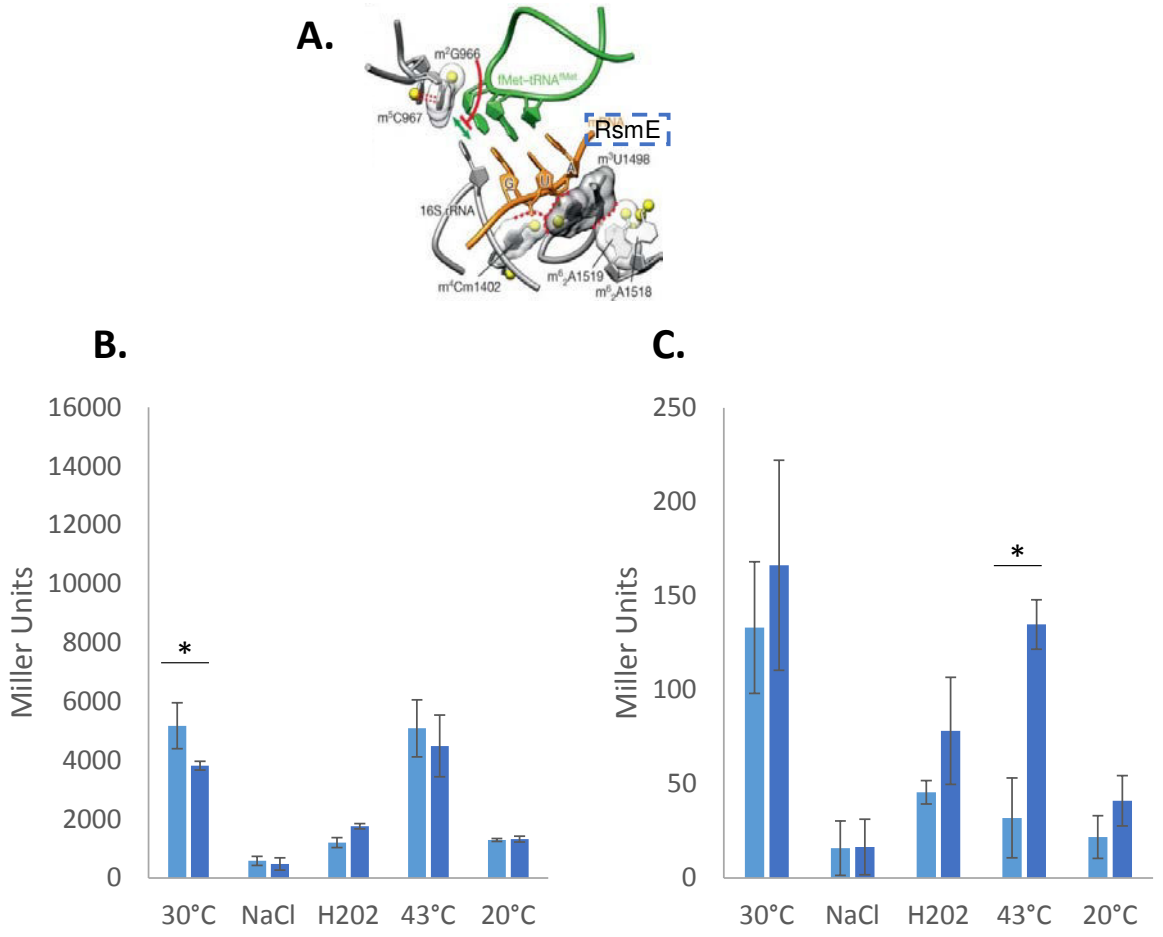

Figure 19: Effect of the lack of methylation m^3U1498 on translation of a canonical and a leaderless *lacZ* reporter. A. Decoding centre, the dashed box indicates the localization of m^3U1498 methylated by RsmE (adapted from Fischer *et al.*, 2015). β-Galactosidase assays in MG6416 (MG1655 Δ*lacZ)* (light blue) and Δ*rsmE* 6420 (dark blue) transformed with pF38lacZSD (B) or with pF45lacZLL (C). Different conditions were applied for 1h30 to the cultures: 30°C (control condition), 0.5 M NaCl, 10 mM H_2O_2, 43°C or 20 °C. The average (+/- standard deviation) of three independent experiments is represented. The star above the values indicates a significant difference according to t-test (p-value lower than 0.05).

In control condition (at 30°C), *ΔrsmE* 6420 had a lower level of translation of the canonical lacZ mRNA than the wild type: β-Galactosidase activity of MG6416 reached 5172+/-780 Miller Units and that of the *ΔrsmE* 6420 3818 +/- 145 Miller units (Figure 19.B). Moreover, with the exception of heat stress, stresses negatively impacted translation in both strains. In fact, β-Galactosidase activity of the two strains drastically reduced after exposure to NaCl (582 +/- 154 Miller Units in the wild type

and 476 +/- 200 in *ΔrsmE* 6420), H_2O_2 (1200 +/- 170 Miller Units in the wild type and 1700 +/- 90 in *ΔrsmE* 6420) and 20°C (around 1300 Miller units in both strains). Nevertheless, the mutant exhibited similar levels of translation than the wild type in those conditions. At 43°C, translation of *lacZ* in the two strains was not changed compared with levels at 30°C (5086 +/- 900 Miller units in MG6416 and 4500 +/- 1000 Miller units in *ΔrsmE* 6420). Methylation m^3U1498 could permit a better efficiency of the ribosomes in translation under normal conditions but not under stressful conditions.

We were able to detect translation of the leaderless *lacZ* reporter (Figure 19.C). Translation of leaderless *lacZ* is less efficient than for the canonical mRNA but is significant, even if the reporter is not a natural leaderless mRNA. As we can see in Figure 19.C, β-Galactosidase activity was similar in both strains at 30°C: 133 +/- 35 in wild type and 160 +/-55 in the mutant. Addition of NaCl or H_2O_2 and incubation at 20°C led to a decrease of β-Galactosidase activity: around 15 +/-10 Miller units in NaCl assay for both strains and 50+/-10 and 80 +/- 30 Miller units at 20°C for wild type and Δ*rsmE* respectively. At 43°C, the mutant *ΔrsmE* 6420 exhibited the same level of translation than at 30°C while it decreased drastically in the wild type (Figure 19.C). Lack of methylation m^3U1498 does not impact translation of leaderless mRNAs under normal conditions but improved it at 43°C.

c. *RsmE impacts translational frameshifting* in vivo *and* in vitro

As *ΔrsmE* mutant strain seems to have a slight but significant impact on translation, we hypothesized that it could also be more error-prone, for instance in maintenance of the reading frame. We also aimed to study how stressful conditions impact maintenance of the reading frame in strains lacking methylations.

To investigate further frameshifting in the mutant strains, we used plasmids pB01, pB18gfp+1, pB19gfp-1, pB11dnaX and pB14prfB. Those plasmids were transformed in MG1655 and in isogenic mutant strains *ΔrsmA, ΔrsmB, ΔrsmD, ΔrsmE and ΔrsmH*. Cells expressed both fluorescent reporters constitutively from the plasmids. Therefore, using this dual fluorescent system, there was no need to change media nor a delay for induction as for β-Galactosidase assays. Thus, using those constructs we investigated short term adaptation to stresses. To do so, wild

type and mutant strains transformed with each plasmid were cultured until they reached exponential phase (OD_{600} of 0.5) and stresses were applied for 20 min.

We analysed ratios of GFP/mCherry fluorescence. Thus, GFP expression due to frameshifting is normalized by canonical expression of mCherry in every condition and for each strain. Those ratios permitted us to directly compare frameshifting between mutants and wild type which was used as a reference.

To validate the system, we checked for constitutive expression of mCherry and GFP from pB01 in the wild type and in the mutants.

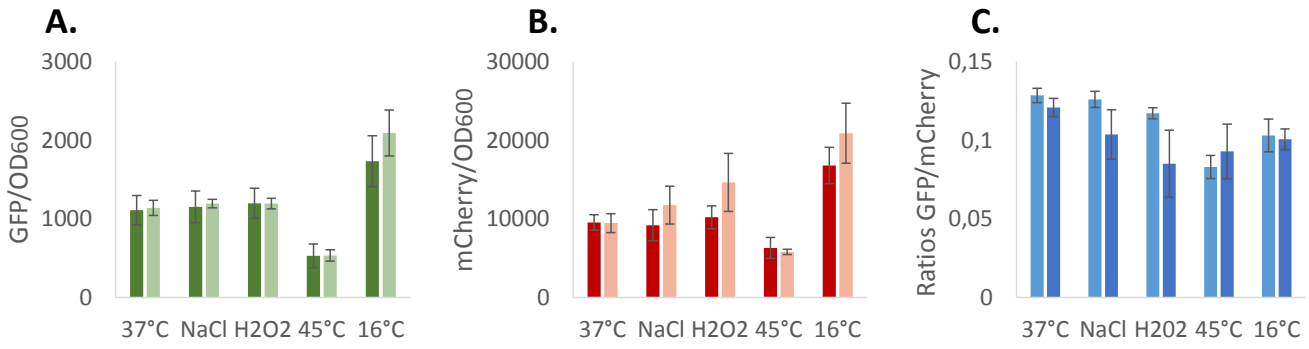

Figure 20: Fluorescence of GFP and mCherry produced from pB01 plasmid. A. GFP fluorescence normalized by OD_{600} of MG1655 (dark green) and *ΔrsmE* (light green). B. mCherry fluorescence normalized by OD_{600} of MG1655 (dark red) and *ΔrsmE* (pink). C. Ratios of GFP/mCherry in MG1655 (light blue) and *ΔrsmE* (dark blue). Cells were grown until OD_{600}=0.5 and were then submitted to various conditions for 20 min: 37°C (control conditions), 0.3 M NaCl, 10 mM H2O2, 45°C or 16°C. Values represent the average (+/- standard deviation) of three independent experiments and a star indicates a significant difference according to t-test (p-value lower than 0.05).

As we can see in Figure 20 A. and B., both strains exhibited similar levels of GFP or mCherry fluorescence in every condition. For instance, at 37°C, GFP fluorescence was 1113+/-187 $_{GFP}$RLU in the wild type and 1140+/-96 $_{GFP}$RLU in *ΔrsmE.* We can notice that translation of the two fluorescent proteins was not impaired by the addition of NaCl or H_2O_2 but was reduced by half after exposure at 45°C. On the other hand, at 16°C the mutant and the wild type had higher

fluorescence levels of GFP and mCherry compared to those observed in control conditions (37°C). In Figure 20 C., ratios of GFP/mCherry are represented.

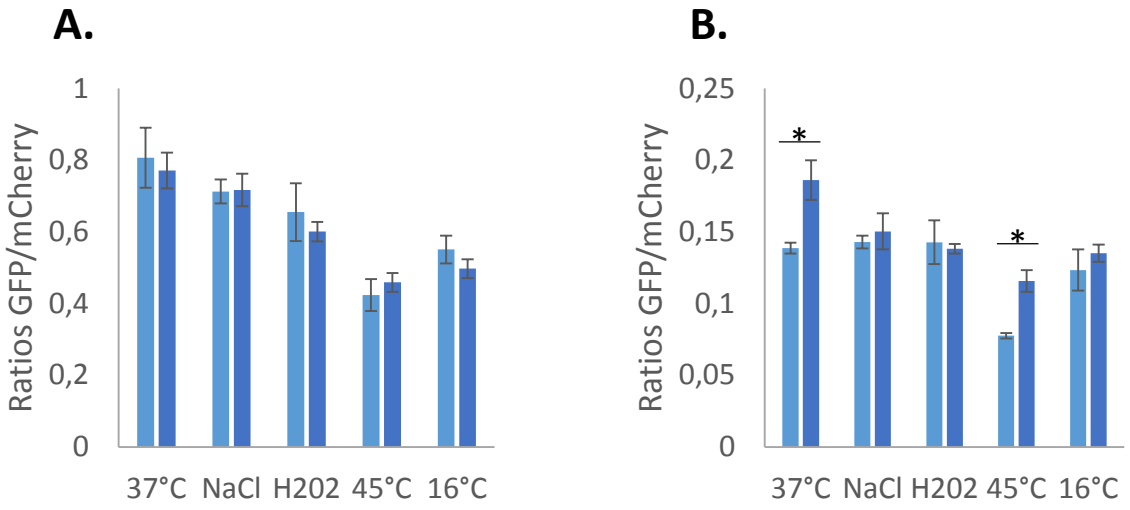

Figure 21: Effect of the lack of m^3U1498 on *prfB* and *dnaX* frameshifting *in vivo.* Ratios of fluorescence of GFP/mCherry in MG1655 (light blue) and *ΔrsmE* (dark blue) transformed with pB14prfB (A) and pB11dnaX (B). Cells were grown until OD_{600}=0.5 and were then submitted to various conditions for 20 min: 37°C (control conditions), 0.3 M NaCl, 10 mM H_2O_2, 45°C, 16°C. Values represent the average (+/- standard deviation) of three independent experiments and a star indicates a significant difference according to t-test (p-value lower than 0.05).

Programmed frameshifting was very efficient using *prfB* and *dnaX* sequences leading to detectable fluorescence signals (Figure 21). *prfB* frameshifting in MG1655 and in *ΔrsmE* is depicted in Figure 21.A. As we can see, fluorescence ratios were equivalent in the mutant and in the wild type in all conditions. As an example, values of GFP/mCherry ratios at 37°C were 0.81 +/- 0.08 in wild type and 0.77 +/- 0.05 in *ΔrsmE.* Thus, lack of RsmE does not impact *prfB* +1 frameshifting under normal or stressful conditions.

In contrast, *ΔrsmE* had a higher level of translation of *dnaX* frameshifting reporter at 37°C (GFP/mCherry ratios: 0.14 +/- 0.004 in wild type and 0.19 +/- 0.014 in *ΔrsmE*) and at 45°C (GFP/mCherry ratios: 0.08 +/- 0.002 in wild type and 0.12 +/- 0.008 in *ΔrsmE*) (Figure 21.B). Thus, m^3U1498 reduces *dnaX* -1 frameshifting and its lack partially suppresses its inhibitory effect at higher temperature.

GFP produced from plasmids pB18gfp+1 and pB19gfp-1 represents spontaneous frameshifting. Indeed, coding sequence of GFP was modified by addition or removal of one nucleotide, changing the frame of translation to the second (+1) or third one (-1) respectively. However, those plasmids did not lead to a significant GFP production in any strains (MG1655 and isogenic *rsm* mutant strains) (not shown). Thus to investigate spontaneous frameshifting, we purified ribosomes from *Δrsm* mutants and from the wild type and tested them for *in vitro* translation.

We amplified *gfp* sequence from pB01, pB18gfp+1 and pB19gfp-1 to produce templates for *in vitro* transcription. The three different RNAs obtained were *in vitro* translated by ribosomes lacking methylation (purified from the mutant strains) or wild type ribosomes. Fluorescence of GFP was then measured to evaluate levels of canonical translation of GFP (gfp0) and spontaneous frameshifting (gfp+1 and gfp-1).

A.

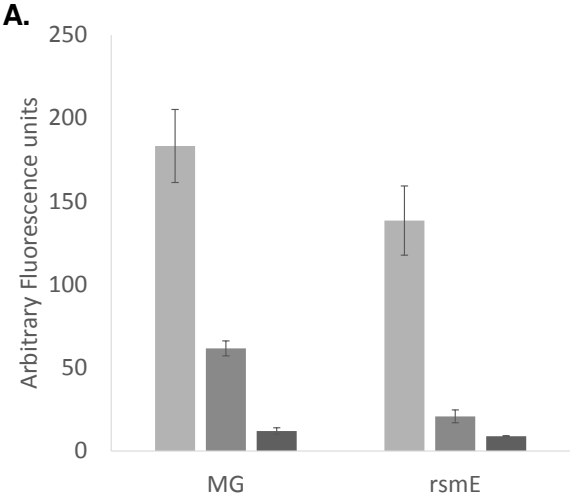

B.

	Frameshifting rates	
	Rate +1	Rate -1
MG1655	0,34 ± 0,05	0,065 ± 0,005
ΔrsmE	**0,15 ± 0,007**	0,065 ± 0,012

Figure 22: *In vitro* translation with ribosomes purified from MG1655 and Δ*rsmE*. A. Translation of three different RNA reporters gfp0 (light grey), gfp+1 (grey), gfp-1 (dark grey) by ribosomes from MG1655 (MG) and Δ*rsmE.* B. Table of frameshifting rates calculated from values obtained *via in vitro* translation: Rate +1 = (translation of gfp+1)/(translation of gfp0); and Rate -1 = (translation of gfp-1)/(translation of gfp0). Values represent the average (+/- standard deviation) of three independent experiments and a star indicates a significant difference according to t-test (p-value lower than 0.05).

Using *in vitro* produced GFP, we were able to successfully detect fluorescence using canonical mRNA (gfp0) and even frameshifting reporters (gfp+1 and gfp-1) (Figure 22). Moreover, the results obtained using true triplicates had a low variance meaning the assay is reproducible and results are very robust.

As we can see in Figure 22, frameshifting in the +1 direction is rather frequent in those conditions: it was about 1/3 (frameshifting rate: 0.34+/-0,005) compared with canonical translation with wild type ribosomes. However, frameshifting in -1 direction was much lower with a rate of 0.065 with wild type ribosomes. Ribosomes lacking m^3U1498 translated canonical gfp0 mRNA as efficiently as wild type ribosomes: levels of fluorescence were 138.5+/-21 and 183+/-22 arbitrary fluorescence units (AFU) respectively (Figure 22.A). Translation of the frameshifting reporter gfp+1 was also significantly affected when performed by ribosomes from *ΔrsmE*. Indeed, they exhibited +1 frameshifting rate about twice less (frameshifting rate: 0.15+/-0.007) than the wild type ribosomes (frameshifting rate: 0.34+/-0.05) while rate of -1 frameshifting was similar with ribosomes from both strains (Figure 22.B). We could conclude that m^3U1498 makes the ribosomes more prone to +1 frameshifting.

- **Conclusion**

m^3U1498 contacts the mRNA thus its loss could influence mRNA binding, translation initiation, interactions with the anticodon and so decoding. Here, we were able to show a slight difference in translation in *ΔrsmE* mutant *in vivo*. First, methylation at position m^3U1498 facilitates translation (Figure 19 B) and its absence does not impact translation after exposure to stresses. This modification does not influence translation of leaderless mRNA either under various conditions. However after heat stress, leaderless translation was not affected in *ΔrsmE* strain whereas it reduces dramatically in the wild type (Figure 19 C). The modification m^3U1498 does not impact *prfB* +1 frameshifting but reduces *dnaX* -1 frameshifting (Figure 21). At the opposite, ribosomes lacking m^3U1498 are more prone to spontaneous frameshifting to the second frame (+1) while frameshifting to the third frame (-1) is not impacted *in vitro.*

3.3. Lack of methylation m^5C967 impacts canonical translation

a. Absence of RsmB impacts adaptation to cold and heat stresses

Lack of RsmB does not have an impact on growth, the *ΔrsmB* mutant strain had a similar growth rate (of 0.55+/-0.03 h^{-1}) than the wild type (0.58+/-0.04 h^{-1}) in minimal medium M9 glucose at 30°C.

The competitive growth of the mutant and the wild type was also analysed. *ΔrsmB::*kan mutant and MG6416 were grown in M9 glucose in single and co-cultures and cells were diluted and spotted on M9 glucose agar plates (Figure 23). First, when both strains were grown together (bottom panel, first line), they exhibited a similar bacterial load than in single cultures (top panel, first line), indicating that *ΔrsmB::*kan mutant does not have a competition defect at 30°C. Concerning adaptation of MG6416 and *ΔrsmB::*kan to stresses, the two strains had similar reduction of bacterial load, when grown in presence of NaCl or plumbagin (Ox-P). However, *ΔrsmB::*kan seemed to be more sensitive to temperature stresses after growth in co-culture. Indeed, a reduction of 1 to 2 log was observed when *ΔrsmB*::kan cells are spotted on M9-Glc agar plates and incubated at 16°C or at 43°C. In conclusion, *ΔrsmB* is able to compete when grown with the wild type but is more sensitive to cold and heat stresses which is in accordance with Burakovsky *et al*., 2012 who observed that *ΔrsmBD* double mutant was cold sensitive.

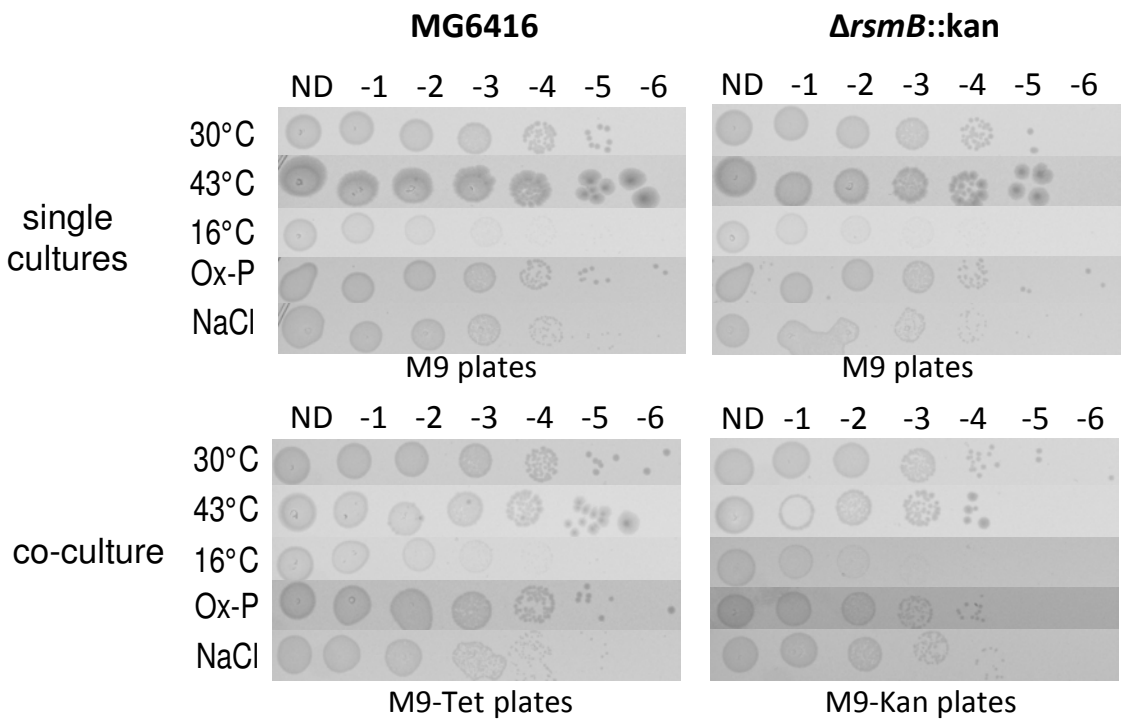

Figure 23: Adaptation of MG6416 and Δ*rsmB*::kan to various conditions. Spots of 10-fold serial dilutions of cells grown in single (top panels) or co-cultures (bottom panels) for 24h. M9–Glc plates were incubated at different temperatures (30°C, 43°C for 24h or 16°C for 48h), plates containing either plumbagin (0,2mM; Ox-P) or NaCl (0,5M; NaCl) were incubated at 30°C during 24h.

b. RsmB affects translation

Under control conditions (30°C), *ΔrsmB* 6418 translated canonical lacZ mRNA about twice more than the wild type: 11339 +/- 2184 Miller Units in the mutant and 5172+/-780 Miller Units for the MG6416 (Figure 24.B). Methylation m^5C967 seems to reduce translation in those conditions.

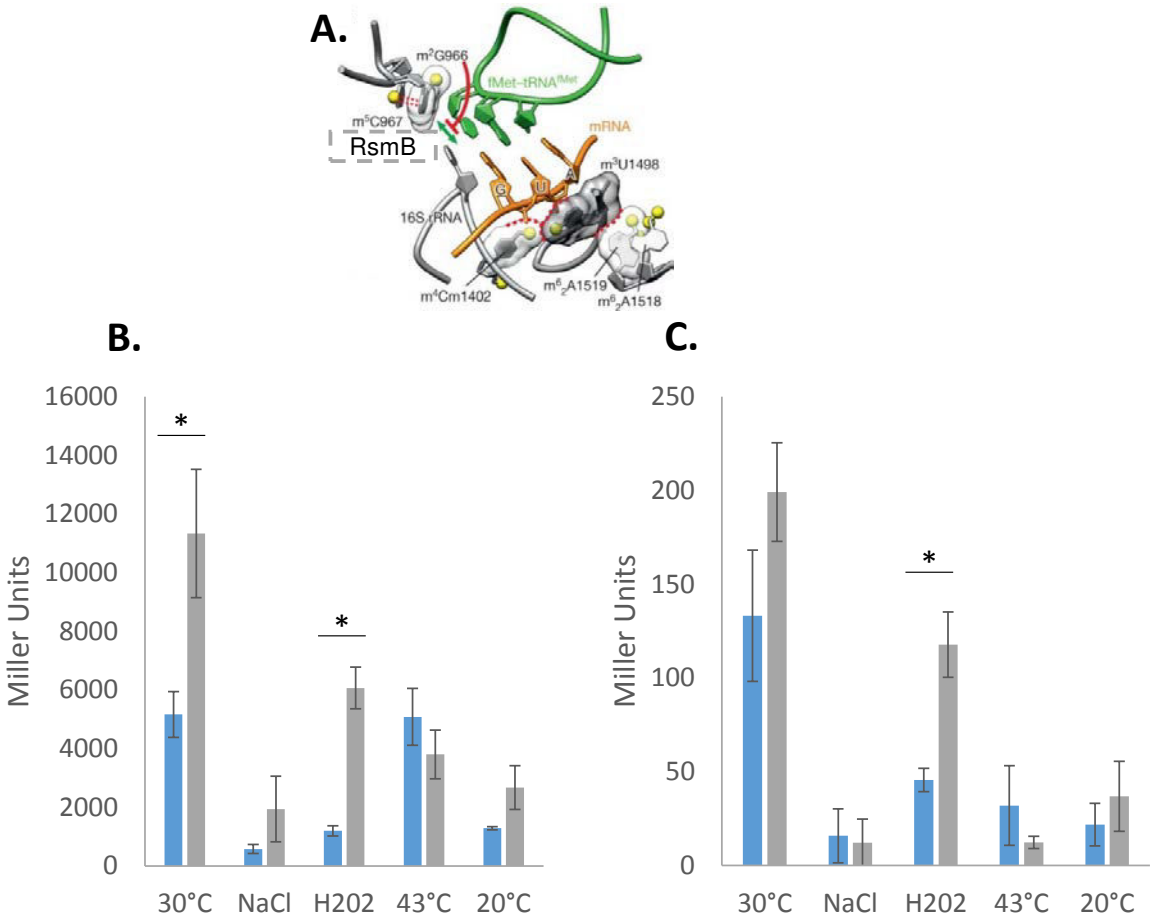

Figure 24: Effect of the lack of methylation m^5C967 on translation of a canonical and a leaderless *lacZ* reporter. A. Decoding centre, the dashed box indicates the localization of m^5C967 methylated by RsmB (adapted from Fischer et al, 2015). β-Galactosidase activity in MG6416 (light blue) and Δ*rsmB* 6418 (grey) transformed with pF38lacZSD (B) or with pF45lacZLL (C). Different conditions were applied for 1h30 to the cultures: 30°C (control condition), 0.5 M NaCl, 10 mM H_2O_2, 43°C or 20 °C. The average (+/- standard deviation) of three independent experiments is represented. The star above the values indicates a significant difference according to t-test (p-value lower than 0.05).

Exposure to stresses had distinctive impact in the mutant and the wild type strains (1202 +/- 171 Miller Units in the wild type and 6070 +/- 710 in *ΔrsmB* 6418). H_2O_2 oxidative stress led to an equivalent reduction of β-Galactosidase activity in both strains meaning that translation is more efficient in the mutant strain but is lower due to H_2O_2 (1202 +/- 171 Miller Units in the wild type and 6070 +/- 710 in *ΔrsmB* 6418). In contrast, translation of the reporter drastically reduced in both strains under osmotic stress (NaCl) (582 +/- 154 Miller Units in the wild type and 1946 +/- 1118 in *ΔrsmB* 6418) and cold stress at 20°C (1293 +/- 52 Miller Units in the wild type and 2681 +/- 747 in *ΔrsmB* 6418) and no significant difference was detected. After a heat stress at 43°C, β-Galactosidase activity reduced dramatically to 3809 +/- 832 Miller Units in *ΔrsmB* 6418 while translation in the wild type was not impacted (5087 +/- 972 Miller Units) compared to that at 30°C.Thus translation is more affected in the mutant than in the wild type after exposure to osmotic, heat and cold stresses.

Translation of the leaderless lacZ reporter was slightly higher at 30°C in Δ*rsmB* 6418 than in the wild type (133 +/- 35 Miller Units in the wild type and 199 +/- 26 in ΔrsmB 6418, with a marginal p-value of 0.0586) (Figure 24.C). No significant difference between the two strains was observed in the other conditions except for H_2O_2 stress for which Δ*rsmB* 6418 had a higher level of translation (46 +/- 6 Miller Units in the wild type and 118 +/- 17 in *ΔrsmB* 6418). Leaderless translation seems to be facilitated by the absence of m^5C967 under normal conditions and oxidative stress.

c. *Lack of RsmB results in higher -1 programmed frameshifting* in vivo

Fluorescence of the two reporters from pB01 was the same in *ΔrsmB* and wild type strains in all conditions except at 16°C in which mCherry fluorescence was lower in the mutant. This led to higher GFP/mCherry ratios at 16°C (not shown).

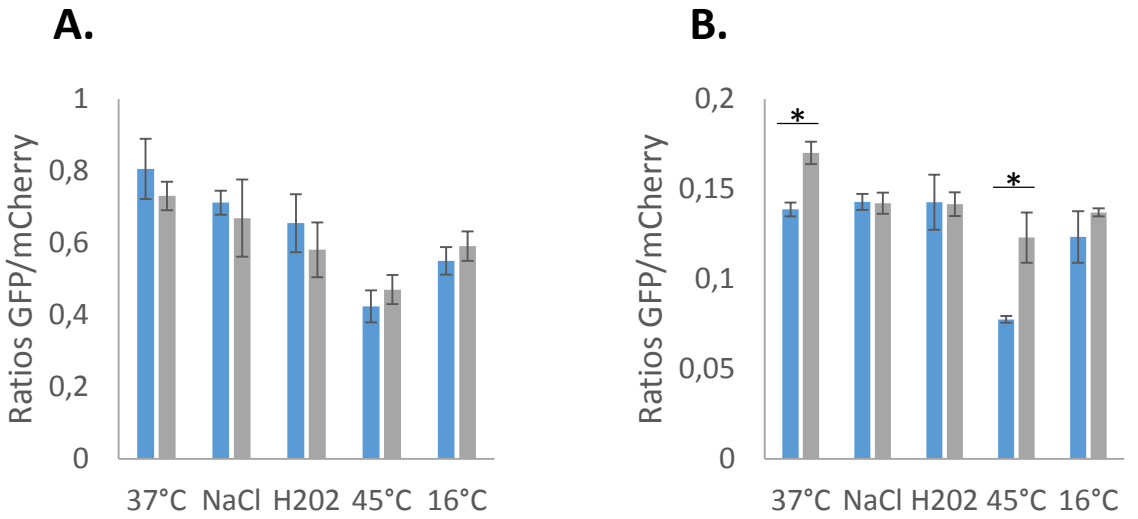

Figure 25: Effect of the lack of m^5C967 on *prfB* and *dnaX* programmed frameshifting *in vivo.* Ratios of fluorescence of GFP/mCherry in MG1655 (light blue) and *ΔrsmB* (grey) transformed with pB14prfB (A) and pB11dnaX (B). Cells were grown until OD_{600}=0.5 and were then submitted to various conditions for 20 min: 37°C (control conditions), 0.3 M NaCl, 10 mM H_2O_2, 45°C, 16°C. Values represent the average (+/- standard deviation) of three independent experiments and a star indicates a significant difference according to t-test (p-value lower than 0.05).

Concerning *prfB* dependant frameshifting (Figure 25.A), relative fluorescence in the wild type and in *ΔrsmB* were similar in all conditions. At the opposite, *dnaX* frameshifting was higher in the mutant at 37°C (0.14 +/- 0.004 in wild type and 0.17 +/- 0.006 in *ΔrsmB*) and after a heat stress at 45°C (0.08 +/- 0.002 in wild type and 0.12 +/- 0.014 in *ΔrsmB*) (Figure 25.B). *ΔrsmB* seems to be more prone to *dnaX* -1 dependant frameshifting.

A.

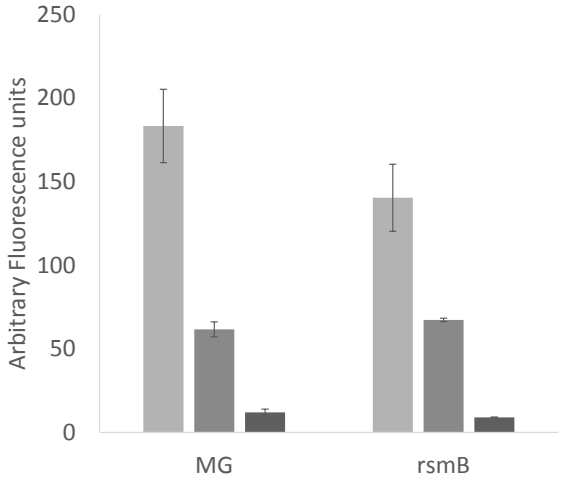

B.

	Frameshifting rates	
	Rate +1	Rate -1
MG1655	0,34 ± 0,05	0,065 ± 0,005
ΔrsmB	**0,49 ± 0,069**	0,065± 0,008

Figure 26: *In vitro* translation with ribosomes purified from MG1655 and *ΔrsmB*. A. Translation of three different RNA reporters gfp0 (light grey), gfp+1 (grey), gfp-1 (dark grey) by ribosomes from MG1655 (MG) and Δ*rsmB.* B. Table of frameshifting rates calculated from values obtained *via in vitro* translation: Rate +1 = (translation of gfp+1)/(translation of gfp0); and Rate -1 = (translation of gfp-1)/(translation of gfp0). Values represent the average (+/- standard deviation) of three independent experiments and a star values in bold indicate a significant difference according to t-test (p-value lower than 0.05).

Using *in vitro* translation assays (Figure 26), we could not detect any difference in translation of the canonical reporter (gfp0) by ribosomes from *ΔrsmB* (0.141 +/-20 AFU) or wild type (183+/-22 AFU). However the rate of +1 frameshifting was significantly higher with ribosomes lacking m^5C967 while -1 frameshifting rates were similar (Figure 26. B).

- **Conclusion**

In conclusion, lack of m^5C967 led to higher levels of translation of canonical and leaderless mRNAs under control conditions (Figure 24). Stresses impacted canonical and leaderless translation in *ΔrsmB* more severely than in the wild type with the exception of oxidative stress. The absence of m^5C967 modification also affected frameshifting: *in vivo, dnaX* -1 programmed frameshifting was higher in *ΔrsmB* (Figure 25) while *in vitro,* it led to more shifts to the +1 frame (frame 2) (Figure 26). However, previous studies showed that lack of *rsmB* did not impact canonical translation nor frameshifting (Arora *et al.*, 2013b).

3.4. Lack of methylation m^2G966 enhances translation

a. Absence of RsmD leads to cold sensitivity

Wild type and *ΔrsmD* mutant had similar growth rates when grown at 30°C in M9 glucose: 0.56 +/-0.05 h^{-1} for *ΔrsmD* and 0.58 +/-0.04 h^{-1} for the wild type.

Concerning competitive growth, *ΔrsmD*::kan did not show any defect, when grown together with MG6416 (Figure 27, bottom panels) compared to growth in single culture. Concerning adaptation to stresses, *ΔrsmD*::kan showed a higher sensitivity to NaCl and to 16°C especially when exposure followed the co-culture.

Thus, *ΔrsmD*::kan is more sensitive to cold stress which is in agreement with Burakovsky *et al.*, (2012) who observed that the double mutant *ΔrsmBrsmD* was cold sensitive. Moreover, *ΔrsmD*::kan seems to have a deficiency in osmotic stress adaptation.

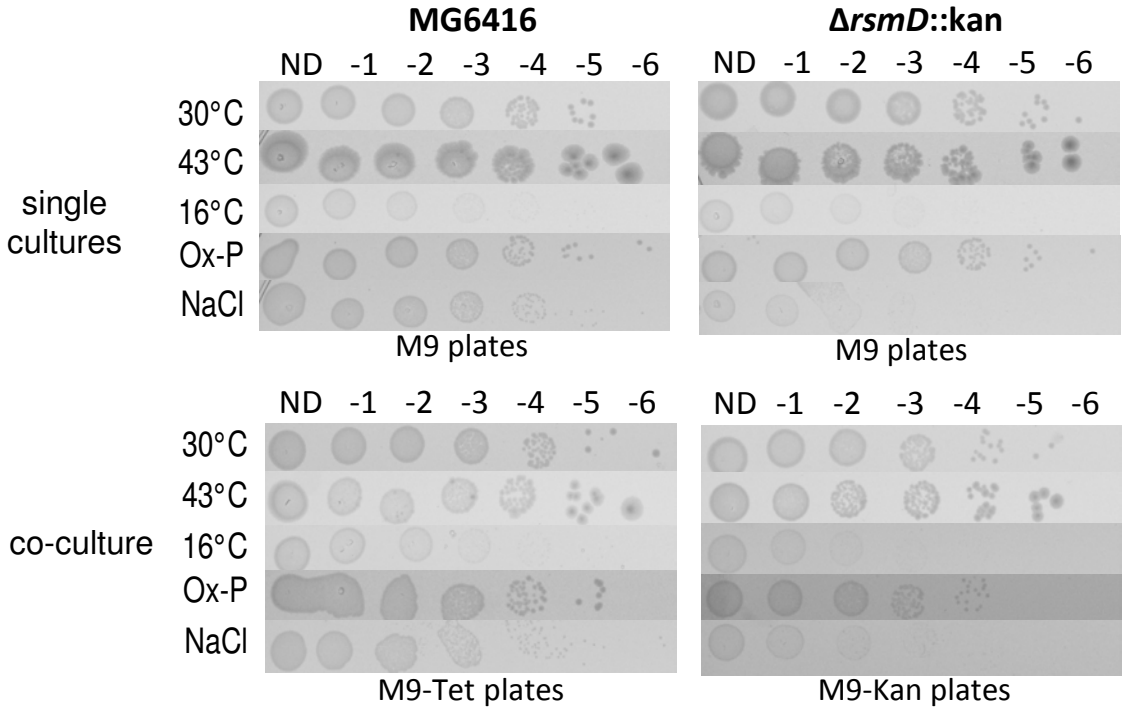

Figure 27: Adaptation of MG6416 and Δ*rsmD*::kan to various conditions. Spots of 10-fold serial dilutions of cells grown in single (top panels) or co-cultures (bottom panels) for 24h. M9–Glc plates were incubated at different temperatures (30°C, 43°C for 24h or 16°C for 48h), plates containing either plumbagin (0,2mM; Ox-P) or NaCl (0,5M; NaCl) were incubated at 30°C during 24h.

b. Lack of RsmD results in higher levels of translation

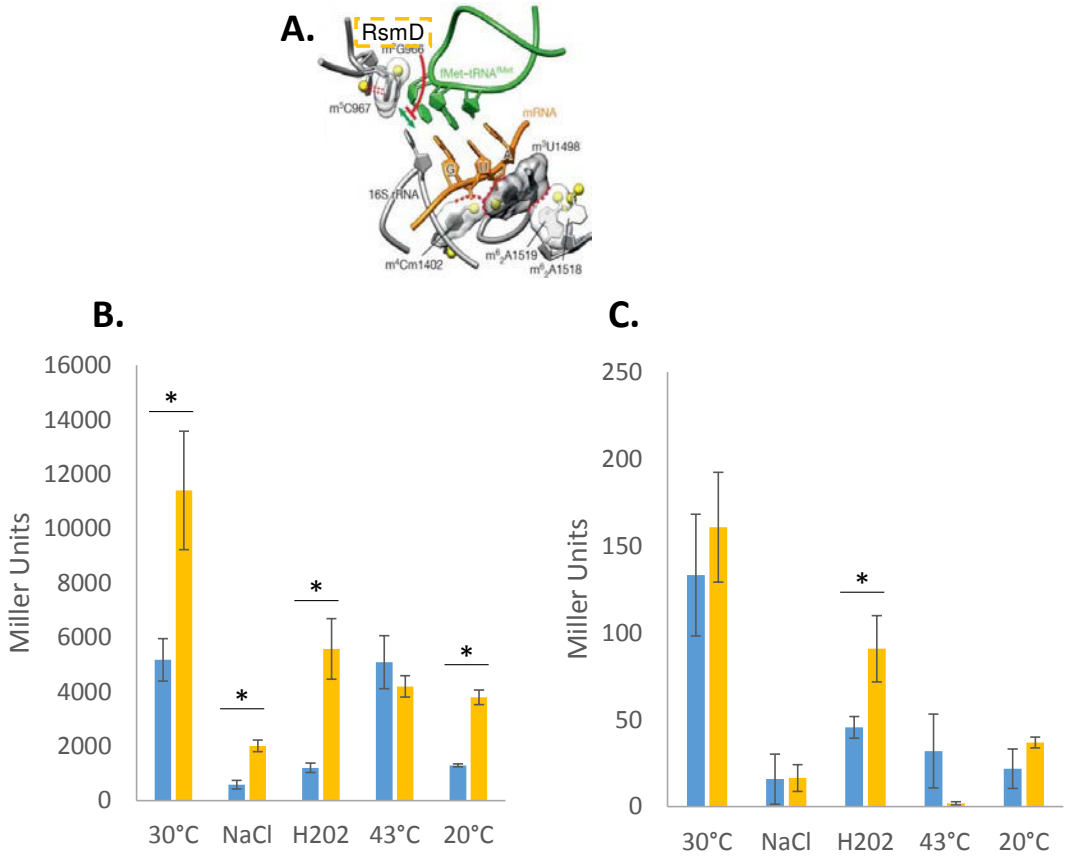

Figure 28: Effect of the lack of methylation m^2G966 on translation of a canonical and a leaderless *lacZ* reporter. A. Decoding centre, the dashed box indicates the localization of m^2G966 methylated by RsmD (adapted from Fischer et al, 2015). β-Galactosidase assays in MG6416 (light blue) and *ΔrsmD* 6419 (yellow) transformed with pF38lacZSD (B) or with pF45lacZLL (C). Different conditions were applied for 1h30 to the cultures: M9 (control condition), 0.5 M NaCl, 10 mM H_2O_2, 43°C or 20 °C. The average (+/- standard deviation) of three independent experiments is represented. The star above the values indicates a significant difference according to t-test (p-value lower than 0.05).

Concerning canonical translation, the mutant *ΔrsmD* 6419 exhibited a higher β-Galactosidase activity (11403 +/- 2176 Miller units) than the wild type (5172 +/- 780 Miller units) under control conditions (30°C) (Figure 28.B). We also observed a higher activity in the mutant after exposure to NaCl (582 +/- 154 Miller Units in the wild type and 2008 +/- 211 in *ΔrsmD* 6419), H_2O_2 (1202 +/- 171 Miller Units in the wild type

and 5573 +/- 1112 in *ΔrsmD* 6419) and 20°C (1293 +/- 52 Miller Units in the wild type and 3795 +/- 269 in *ΔrsmD* 6419) although translation of both strains decreased proportionally. At 43°C, while translation in the wild type strain was not changed, that of *ΔrsmD* 6419 was reduced about twice (4194 +/- 393 Miller units) compared to its β-Galactosidase activity at 30°C.

Regarding translation of the leaderless reporter (Figure 28.C), no significant difference was observed between the two strains except for H_2O_2 stress in which β-Galactosidase activity was higher in Δ*rsmD* 6419 (46 +/- 6 Miller Units in the wild type and 91 +/- 19 in *ΔrsmD* 6419). While translation of canonical mRNA was more efficient in the mutant Δ*rsmD* 6419 it is not the case for leaderless mRNA. However, under oxidative stress, lack of RsmD led to higher translation of canonical and leaderless mRNAs. Absence of methylation at position m^2G966 is detrimental for translation at 43°C.

c. RsmD does not play a significant role in translational frameshifting

When transformed with pB01, wild type and *ΔrsmD* showed similar levels of GFP and mCherry fluorescence in all conditions (not shown).

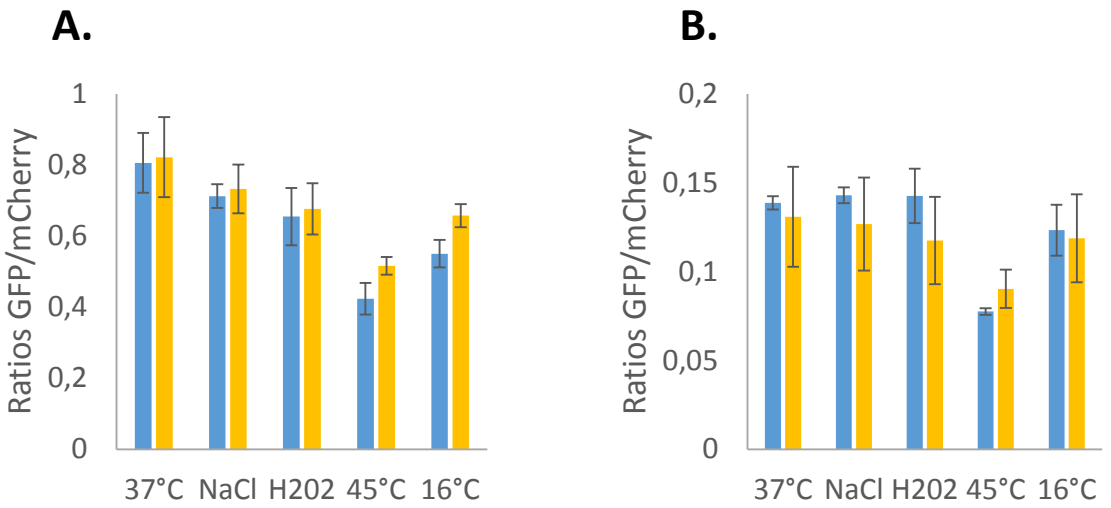

Figure 29: Effect of the lack of m^2G966 on *prfB* and *dnaX* frameshifting *in vivo.* Ratios of fluorescence of GFP/mCherry in MG1655 (light blue) and *ΔrsmD* (yellow) transformed with pB14prfB (A) and pB11dnaX (B). Cells were grown until OD_{600}=0.5 and were then submitted to various conditions for 20 min: 37°C (control conditions), 0.3 M NaCl, 10 mM H_2O_2, 45°C, 16°C. Values represent the average (+/- standard deviation) of three independent experiments and a star indicates a significant difference according to t-test (p-value lower than 0.05).

Lack of m^2G966 does not impact *prfB* nor *dnaX* programmed frameshifting (Figure 29. A and B). Indeed, we could not detect differences of fluorescence ratios between *ΔrsmD* and the wild type when transformed with pB14prfB and pB11dnaX.

In contrast, *in vitro* translation of canonical mRNA (gfp0) was slightly lower with ribosomes lacking methylation m^2G966 (126 +/- 10 AFU) compared to the wild types ones (183 +/- 22 AFU). However, both exhibited the same rates of +1 and -1 frameshifting (Figure 30. B).

A.

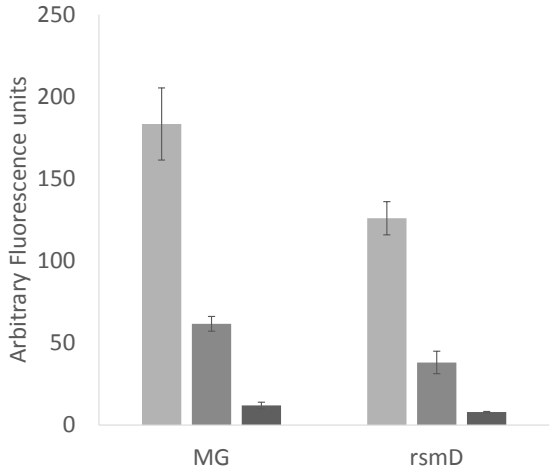

B.

	Frameshifting rates	
	Rate +1	Rate -1
MG1655	0,34 ± 0,05	0,065 ± 0,005
ΔrsmD	0,31 ± 0,078	0,063 ± 0,002

Figure 30: *In vitro* translation with ribosomes purified from MG1655 and *ΔrsmD*. A. Translation of three different RNA reporters gfp0 (light grey), gfp+1 (grey), gfp-1 (dark grey) by ribosomes from MG1655 (MG) and Δ*rsmD.* B. Table of frameshifting rates calculated from values obtained *via in vitro* translation: Rate +1 = (translation of gfp+1)/(translation of gfp0); and Rate -1 = (translation of gfp-1)/(translation of gfp0). Values represent the average (+/- standard deviation) of three independent experiments and a star indicates a significant difference according to t-test (p-value lower than 0.05).

- **Conclusion**

In *ΔrsmD* mutant strain, we were able to show that canonical translation was higher than in the wild type. However, under heat stress, translation was impacted in both strains and the effects were more severe in the mutant (Figure 28). Moreover, lack of modification did not impact programmed frameshifting (Figure 29) or frameshifting *in vitro* (Figure 30). Those results are in contrast with previous studies that showed that canonical translation in *ΔrsmD* was similar than in the wild type and that +1 and -1 frameshifting rates were lower in the mutant (Arora *et al.*, 2013b).

3.5. Absence of $m^6{}_2$1518 and $m^6{}_2$1519 increases frameshifting errors

a. Lack of RsmA induces a cold sensitivity

The wild type and *ΔrsmA* mutant strain grew similarly, indeed they exhibited similar growth rates when cultured in M9 glucose at 30°C (0.58 +/-0.04 h^{-1} for the wild type and 0.54 +/- 0.05 h^{-1} for *ΔrsmA*).

We also analysed growth of *ΔrsmA*::kan in competition with the wild type MG6416 and its adaptation to stresses (Figure 31). No difference was observed between bacterial loads of MG6416 or *ΔrsmA*::kan when grown together (bottom panel, lane 1). About adaptation to stresses, *ΔrsmA*::kan showed similar behaviour than the wild type, except after growth at 16°C. Indeed, *ΔrsmA*::kan bacterial load was reduced of 1 log at 16°C and this effect is more significant when cells from co-culture were plated. Thus, we can conclude that *ΔrsmA*::kan is more sensitive to cold stress, which is in agreement with previous studies (Connolly *et al.*, 2008).

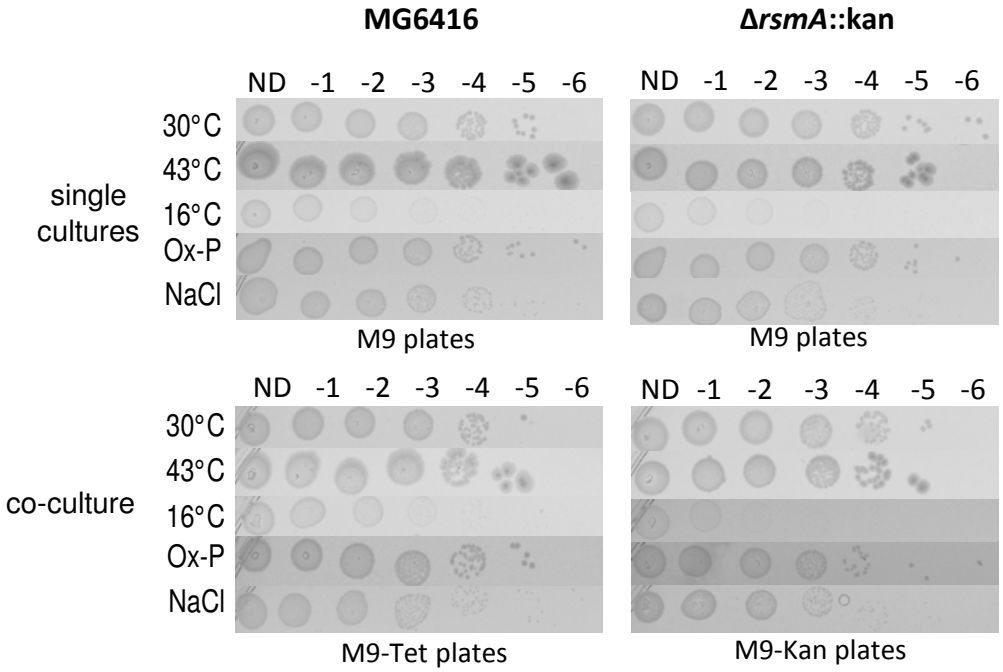

Figure 31: Adaptation of MG6416 and Δ*rsmA*::kan to various conditions. Spots of 10-fold serial dilutions of cells grown in single (top panels) or co-cultures (bottom panels) for 24h. M9–Glc plates were incubated at different temperatures (30°C, 43°C for 24h or 16°C for 48h), plates containing either plumbagin (0,2mM; Ox-P) or NaCl (0,5M; NaCl) were incubated at 30°C during 24h.

b. Translation is more efficient in ΔrsmA

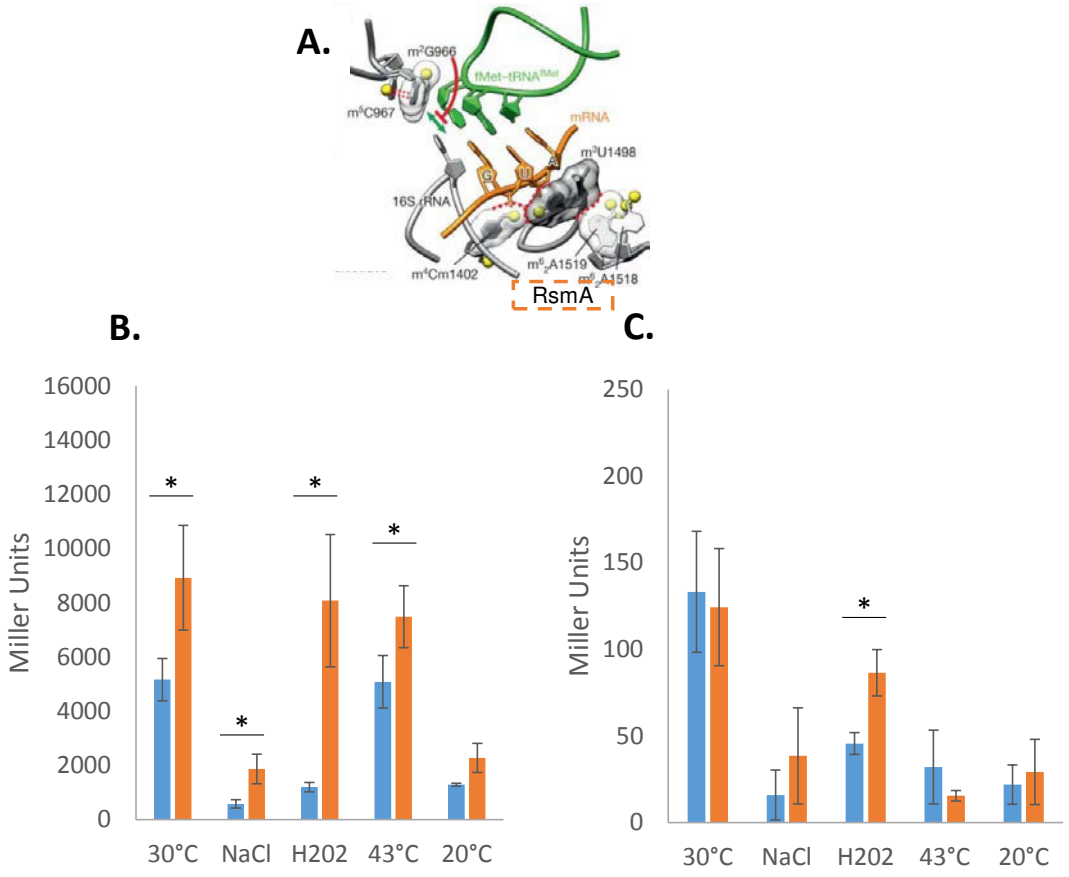

Figure 32: Effect of the lack of methylations $m^6_2$1518 and $m^6_2$1519 on translation of a canonical and a leaderless lacZ reporter. A. Decoding centre, the dashed box indicates the localization of $m^6_2$1518 and $m^6_2$1519 methylated by RsmA (adapted from Fischer *et al.*, 2015). β-Galactosidase assays in MG6416 (light blue) and *ΔrsmA* 6417 (orange) transformed with pF38lacZSD (B) or with pF45lacZLL (C). Different conditions were applied for 1h30 to the cultures: 30°C (control condition), 0.5 M NaCl, 10 mM H_2O_2, 43°C or 20 °C. The average (+/- standard deviation) of three independent experiments is represented. The star above the values indicates a significant difference according to t-test (p-value lower than 0.05).

In every condition, *ΔrsmA* 6417 exhibited higher levels of translation of canonical lacZ mRNA compared to the wild type strain (Figure 32. B). First, under control conditions (30°C), β-Galactosidase activity was higher in Δ*rsmA* 6417 than in the wild type (5172 +/- 780 Miller Units in wild type and 8926 +/- 1938 in *ΔrsmA* 6417). So the modifications added by RsmA inhibit canonical translation in those conditions

Translation of both strains was impacted after an osmotic stress (NaCl): β-Galactosidase activities reached 582 +/- 154 and 1868 +/- 547 Miller Units respectively for wild type and *ΔrsmA* 6417. Cold stress (20°C) also reduced translation of both strains (12932 +/- 52 Miller Units in wild type and 2280 +/- 536 in *ΔrsmA* 6417). However, after a heat shock at 43°C, both strains had similar β-Galactosidase activity than at 37°C (5087 +/- 972 Miller Units in wild type and 7493 +/- 1144 in *ΔrsmA* 6417). In addition, while translation of the wild type dramatically reduced after H_2O_2 oxidative stress, translation in the mutant strain was not affected and showed similar activity than in control condition (1202 +/- 171 Miller Units in wild type and 8084 +/- 2441 Miller Units in *ΔrsmA* 6417). Absence of methylations $m^6{}_2$1518 and $m^6{}_2$1519 has a positive effect on translation after exposure to stresses, especially after oxidative stress.

Concerning translation of leaderless *lacZ* mRNA (Figure 32. C), levels of β-Galactosidase activity in the two strains were similar at 37°C (133 +/- 35 Miller Units in wild type and 124 +/- 34 in *ΔrsmA* 6417). Their levels reduced after osmotic stress (NaCl) (16 +/- 14 Miller Units in wild type *versus* 38 +/- 28 in *ΔrsmA* 6417), at 43°C (32 +/- 21 Miller Units in wild type and 15 +/- 3 in *ΔrsmA* 6417) or 20°C (22 +/- 11 Miller Units in wild type and 19 +/- 19 in *ΔrsmA* 6417) and no difference were detected. Exposure to H_2O_2 did not affect translation significantly in *ΔrsmA* 6417 while β-Galactosidase activity in the wild type decreased a lot (46 +/- 6 Miller Units in wild type *versus* 86 +/- 13 in *ΔrsmA* 6417). Methylations $m^6{}_2$1518 and $m^6{}_2$1519 do not have an effect on translation of leaderless mRNAs except after oxidative stress in which condition their absence is stimulatory.

c. Lack of RsmA has an impact on frame maintenance

When transformed with pB01, wild type and *ΔrsmA* showed similar levels of GFP and mCherry fluorescence in all conditions (not shown).

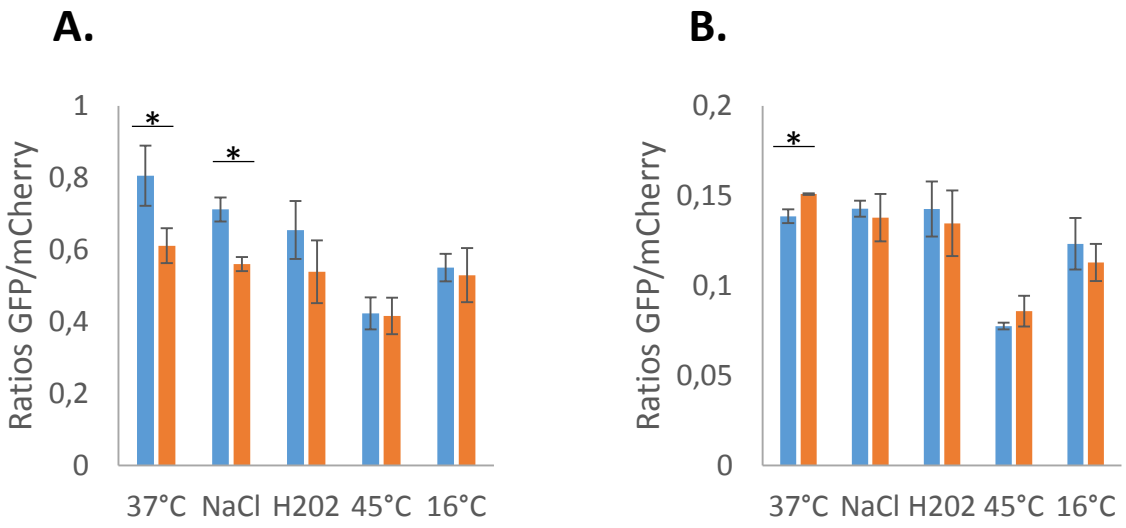

Figure 33: Effect of the lack of $m^6_2$1518 and $m^6_2$1519 on (A) *prfB* and (B) *dnaX* dependent frameshifting *in vivo*. Ratios of fluorescence of GFP/mCherry in MG1655 (light blue) and *ΔrsmA* (orange) transformed with pB14prfB (A) and pB11dnaX (B). Cells were grown until OD_{600}=0.5 and were then submitted to various conditions for 20 min: 37°C (control conditions), 0.3 M NaCl, 10 mM H_2O_2, 45°C, 16°C. Values represent the average (+/- standard deviation) of three independent experiments and a star indicates a significant difference according to t-test (p-value lower than 0.05).

Figure 33.A depicts fluorescence ratios in the wild type and in *ΔrsmA* transformed with pB14prfB. At 37°C *ΔrsmA* exhibited lower ratios than in the wild type (0.81 +/- 0.08 in wild type and 0.61 +/- 0.05 in *ΔrsmA*), similar results were observed after NaCl addition (0.71 +/- 0.03 in wild type and 0.56 +/- 0.02 in *ΔrsmA*). Hence, lack of RsmA reduces *prfB* +1 frameshifting. In contrast, compared to the wild type at 37°C, Δ*rsmA* harboured a slightly but significantly higher GFP/mCherry ratio when transformed with pB11dnaX (0.14 +/- 0.004 in wild type and 0.15 +/- 0.001 in *ΔrsmA*) (Figure 33.B).

A.

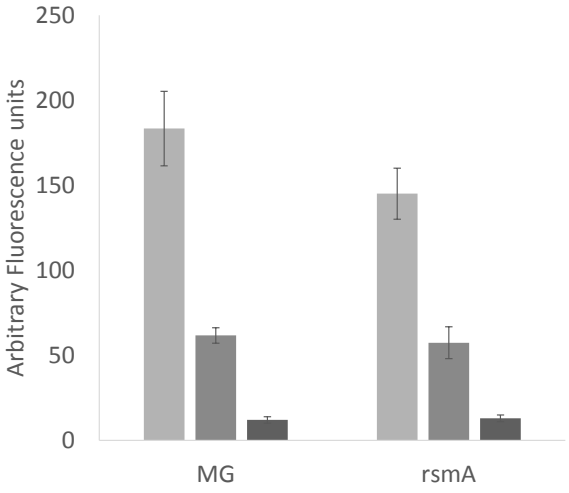

B.

	Frameshifting rates	
	Rate +1	Rate -1
MG1655	0,34 ± 0,05	0,065 ± 0,005
ΔrsmA	0,40 ± 0,066	**0,09 ± 0,015**

Figure 34: *In vitro* translation with ribosomes purified from MG1655 and Δ*rsmA*. A. Translation of three different RNA reporters gfp0 (light grey), gfp+1 (grey), gfp-1 (dark grey) by ribosomes from MG1655 (MG) and *ΔrsmA*. B. Table of frameshifting rates calculated from values obtained *via in vitro* translation: Rate +1 = (translation of gfp+1)/(translation of gfp0); and Rate -1 = (translation of gfp-1)/(translation of gfp0). Values represent the average (+/- standard deviation) of three independent experiments and a star or values in bold indicate a significant difference according to t-test (p-value lower than 0.05).

In vitro, ribosomes lacking modifications $m^6{}_2$1518 and $m^6{}_2$1519 translated gfp0 canonical reporter as efficiently as wild type ribosomes: 0.145+/-15 and 0.183+/-22 AFU respectively (Figure 34.A). No difference in +1 frameshifting rate was detected but the rate of -1 frameshifting significantly increased with ribosomes purified from the mutant strain (Figure 34.B).

- **Conclusion**

Lack of RsmA leads to higher level of canonical translation compared to the wild type in our conditions (Figure 32). Nevertheless, previous studies did not detect differences in canonical translation between the mutant and the wild type (O'Connor *et al.*, 1997, van Buul *et al.*, 1984). Translation in *ΔrsmA* mutant strain is not affected by oxidative stress or heat stress. Modifications $m^6{}_2$1518 and $m^6{}_2$1519 seem to influence frameshifting: in the mutant strain, levels of *prfB* frameshifting were lower while *dnaX* frameshifting increased (Figure 33) and, *in vitro*, ribosomes lacking those dimethylations exhibited higher rates of -1 frameshifting but similar rates for +1 frameshifting (Figure 34).

3.6. Lack of base methylation $m^4Cm1402$ has strong effects on translation

a. Absence of RsmH does not alter growth but impairs fitness

Lack of RsmH does not impact growth: when cultured in M9 glucose at 30°C, Δ*rsmH* had a growth rate of 0.56+/-0.05 h^{-1} similar of that of the wild type (0.58 +/- 0.04 h^{-1}).

The ability of Δ*rsmH* to compete with the wild type and adapt to various stresses was also studied. Concerning competitive growth of Δ*rsmH::*kan *versus* MG6416, Δ*rsmH::*kan exhibited a drastic reduction of the bacterial load following the co-culture (Figure 35, bottom panel). Adaptation of Δ*rsmH::*kan was also extremely challenged after the co-culture. However, when grown as a single culture, Δ*rsmH::*kan was able to efficiently adapt to various stressful conditions (43°C, Plumbagin, NaCl) but exhibited a reduction of the bacterial load of 1 to 2 log at 16°C compared to MG6416. Thus, Δ*rsmH* has a fitness deficiency and is cold sensitive.

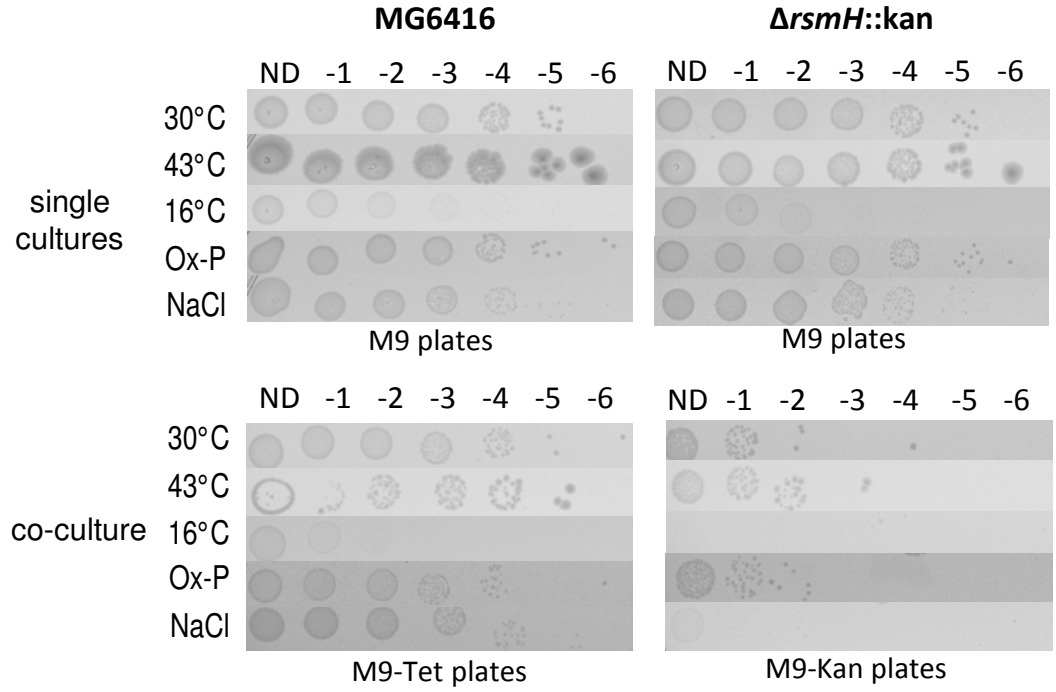

Figure 35: Adaptation of MG6416 and Δ*rsmH*::kan to various conditions. Spots of 10-fold serial dilutions of cells grown in single (top panels) or co-cultures (bottom panels) for 24h. M9–Glc plates were incubated at different temperatures (30°C, 43°C for 24h or 16°C for 48h), plates containing either plumbagin (0,2mM; Ox-P) or NaCl (0,5M; NaCl) were incubated at 30°C during 24h.

b. Lack of RsmH impacts strongly translation and ribosomal frameshifting in vitro

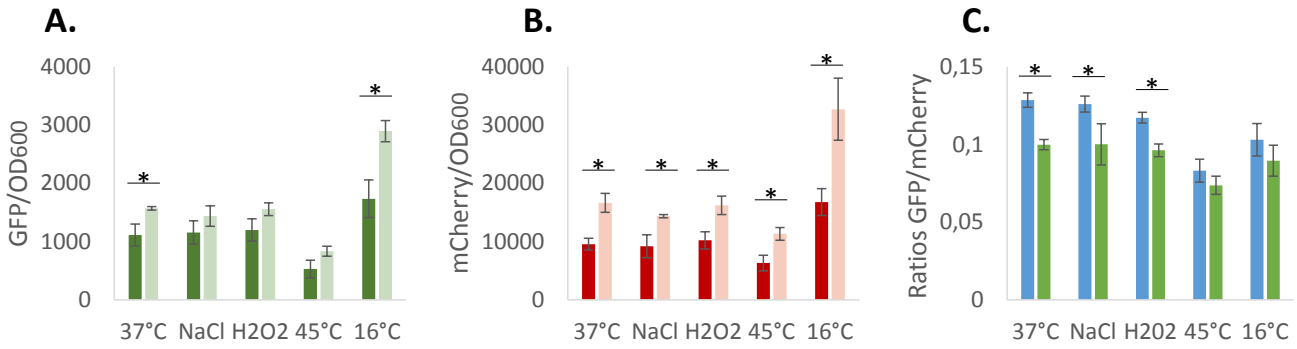

Figure 36: Fluorescence of GFP and mCherry produced from pB01 plasmid. A. GFP fluorescence normalized by OD_{600} of MG1655 (dark green) and *ΔrsmH* (light green). B. mCherry fluorescence normalized by OD_{600} of MG1655 (dark red) and *ΔrsmH* (pink). C. Ratios of GFP/mCherry in MG1655 (light blue) and *ΔrsmH* (green). Cells were grown until OD_{600}=0.5 and were then submitted to various conditions for 20 min: 37°C (control condition), 0.3 M NaCl, 10 mM H_2O_2, 45°C or 16°C. Values represent the average (+/- standard deviation) of three independent experiments and a star indicates a significant difference according to t-test (p-value lower than 0.05).

As we can see in Figure 36, mCherry and GFP expression from pB01 in *ΔrsmH* mutant were different than in the wild type (Figure 36.A and B). Indeed, the mutant exhibited higher levels of fluorescence of both proteins: for instance, when cells were cultured at 37°C, values of GFP/OD_{600} reached 1572+/-31 $_{GFP}$RLU in *ΔrsmH* and 1112+/-187 in MG1655 while values of mCherry/OD_{600} were about 16670+/-1625 $_{mC}$RLU and 9562+/-990 $_{mC}$RLU in *ΔrsmH* and the wild type respectively. The difference was not proportional and led to lower ratios of GFP/mCherry in *ΔrsmH* (0.099+/-0.003) compared to the wild type ones (0.127+/-0.006) (Figure 36.C). This interval between fluorescence ratios in *ΔrsmH* and MG1655 was also observed when the strains were transformed with pB14prfB and pB11dnaX (Figure 37).

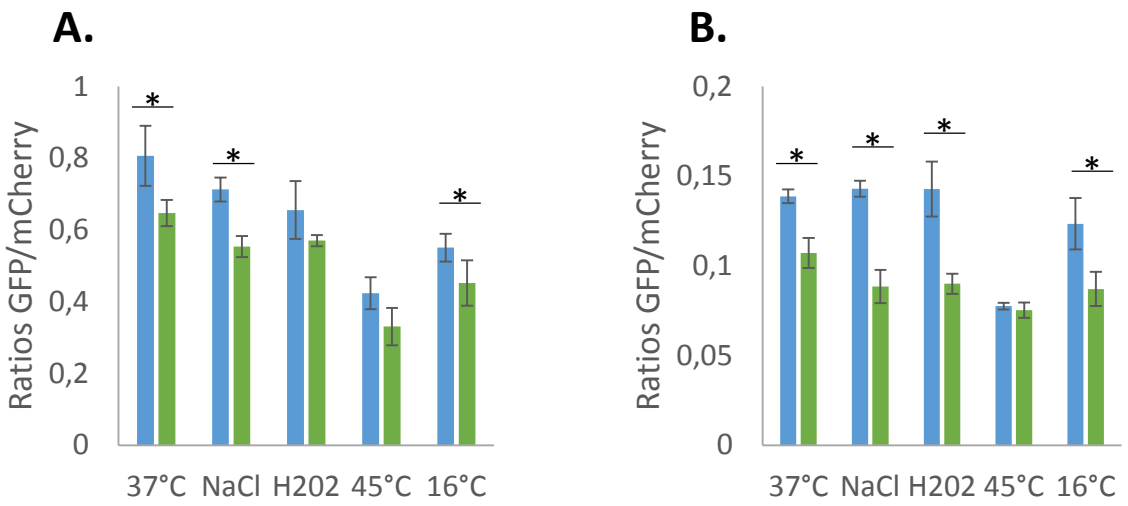

Figure 37: Effect of the lack of base methylation $m^4Cm1402$ on *prfB* and *dnaX* dependent frameshifting *in vivo*. Ratios of GFP/mCherry fluorescence in MG1655 (light blue) and Δ*rsmH* (green) transformed with pB14prfB (A) and pB11dnaX (B). Cells were grown until OD_{600}=0.5 and were then submitted to various conditions for 20 min: 37°C (control conditions), 0.3 M NaCl, 10 mM H_2O_2, 45°C, 16°C. Values represent the average (+/- standard deviation) of three independent experiments and a star indicates a significant difference according to t-test (p-value lower than 0.05).

Concerning *prfB* and *dnaX* frameshifting, *ΔrsmH* exhibited lower GFP/mCherry ratios than the wild type for both reporters (Figure 37). Nevertheless, as ratios were different also for pB01 control plasmid, it is hard to conclude on effect on the mutation on frameshifting. It is rather due to the artefact observed with the control.

The dual fluorescent system seems not to be adapted to analyse the effects of the methylation added by RsmH. However, *in vitro* translation can bring some information.

A.

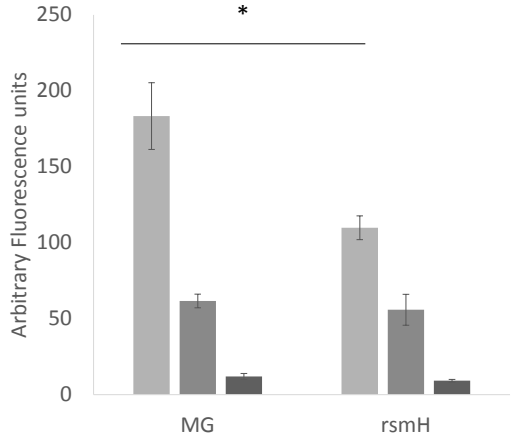

B.

	Frameshifting rates	
	Rate +1	Rate -1
MG1655	0,34 ± 0,05	0,065 ± 0,005
ΔrsmH	**0,51 ± 0,064**	**0,084 ± 0,004**

Figure 38: *In vitro* translation with ribosomes purified from MG1655 and Δ*rsmH*. A. Translation of three different RNA reporters gfp0 (light grey), gfp+1 (grey), gfp-1 (dark grey) by ribosomes from MG1655 (MG) and Δ*rsmH.* B. Table of frameshifting rates calculated from values obtained *via in vitro* translation: Rate +1 = (translation of gfp+1)/(translation of gfp0); and Rate -1 = (translation of gfp-1)/(translation of gfp0). Values represent the average (+/- standard deviation) of three independent experiments and a star indicates a significant difference according to t-test (p-value lower than 0.05).

Ribosomes purified from *ΔrsmH* showed a lower level of translation of gfp0 canonical reporter (110+/-8 AFU) compared with wild type ribosomes (183+/-22 AFU) (Figure 38.A). In addition, +1 and -1 frameshifting rates were higher with ribosomes from *ΔrsmH* compared to wild type ribosomes (Figure 29.B).

- **Conclusion**

Translation in *ΔrsmH* is strongly affected. *In vivo*, it seemed that translation was higher in *ΔrsmH* than in the wild type strain whereas *in vitro*, ribosomes purified from the mutant were less efficient than wild type ones (Figure 38). However, Kimura and Suzuki (2010) did not detect differences in canonical translation *in vivo*. It was not possible to assess frameshifting *in vivo*, but *in vitro* assays showed that +1 and -1 frameshifting is more important with ribosomes lacking the methylation added by RsmH.

4. Discussion

In this work, we focused on the six methylations located within the decoding centre of *Escherichia coli* catalysed by the methyltransferases RsmA, RsmB, RsmD, RsmE and RsmH. Those methylations appear to modulate the structure of this functional region of the ribosome by creating stacking and hydrophobic interactions. The network that methylations form is thought to influence mRNA interactions with the 16S rRNA, tRNA-16S interactions and interactions with initiation and elongation factors. Therefore, those modifications could influence docking of the mRNA, tRNA binding or codon-anticodon interactions and decoding. They could also affect functional activities of the ribosome such as accurate initiation, fidelity and efficiency. Moreover, most of the modifications within the decoding centre are conserved between bacteria and even archaea and eukaryotes (Sergiev *et al.*, 2018). This evolutionary conservation tends to highlight an important role of those methylations. However little is known about their physiological function and how they could help bacteria to cope with conditions they have to face constantly. Data showing some variations of expression and protein abundance of those methyltransferases during stressful conditions are very rare. But such variations, and potential changes in the global level of modifications within the ribosome, could implicate ribosomal modifications in translational regulation of stress response. Thus, we focused on methylations located in the decoding centre and aimed to evaluate different aspects related to stress sensitivity and ribosomal activity.

Methyltransferases are dispensable for growth and fitness

First, we successfully generated *E. coli* mutant strains with single knockouts of the methyltransferase of interest (Δ*rsmA,* Δ*rsmB,* Δ*rsmD,* Δ*rsmE* and Δ*rsmH)*. This reflects that methyltransferases are not essential for cell viability. In addition, the lack of one methylation does not influence growth in minimal medium. Moreover, Δ*rsmA,* Δ*rsmB,* Δ*rsmD* and Δ*rsmE* mutants are able to efficiently compete with the wild type when grown together. Nevertheless, Δ*rsmH* mutant has a deficiency in competitive growth, emphasizing the potential importance of this methylation. Thus, taken one by one, those modifications are not essential for bacteria viability or fitness.

Some studies pointed out the role of some methyltransferases (RsmA, RsmB and RsmH) as checkpoint in ribosome biogenesis due to their activity on precursor of

the 30S subunit (Connolly *et al.*, 2008). According to such point of view, we could expect a phenotypic impact as it has been shown for other enzymes implicated in ribosome biosynthesis (Boehringer *et al.*, 2012; Bunner *et al.*, 2010; Davis and Williamson, 2017). Moreover, in such mutants, immature and inactive subunits tend to accumulate. We did not detect such accumulation of free 30S and 50S during ribosome purification. As a consequence, we could assume that lack of one methyltransferase does not have such an impact on ribosome maturation under the growth conditions we used.

Lack of methyltransferases impacts canonical translation

Then, we addressed the question of the ribosome efficiency in translation when they lack one methylation. To do so, we generated several tools to analyse canonical translation either *in vitro* or *in vivo*. *In vivo,* we used two reporters (β-galactosidase and GFP) to assess canonical translation in the mutants and the wild type.

β-galactosidase was produced from a canonical *lacZ* gene of which, transcription was inducible. After 1h30 induction of reporter transcription, we detected significant differences in translation. At 30°C, mutant strains Δ*rsmA,* Δ*rsmB* and Δ*rsmD* have higher levels of translation than the wild type while translation in Δ*rsmE* is slightly lower. Thus, in this condition, methylation m^3U1498 permits a better efficiency of the ribosomes in translation. On the contrary, methylations catalysed by RsmA, RsmB and RsmD seem to reduce translation efficiency. However, previous studies did not detect any difference in canonical translation of the mutants Δ*rsmA,* Δ*rsmB* and Δ*rsmD* compared to the wild type (Arora *et al.*, 2013b, O'Connor *et al.*, 1997). Interestingly, they used different strains and growth conditions: cultures were made in LB, at 37°C and IPTG was used to induce the transcription of their reporter. The growth conditions we used to perform β-galactosidase assays were more constraining for the cells. Indeed, in our experiment, cells were cultured in minimal medium at 30°C and when they reached exponential phase, growth medium was changed for arabinose induction in order to purge glucose. As a consequence, bacteria had to adapt to the change of carbon source (arabinose *versus* glucose) thus other factors could also influence translation in those conditions and such effect would be added to the impact of lacking one methyltransferase.

Subsequently, we performed another assay of canonical translation, using the dual fluorescent reporter from pB01 plasmid. To measure fluorescence, bacteria were grown at 37°C until they reached exponential phase and fluorescent signals were detected directly in the culture avoiding any medium change. In those conditions, all strains exhibited similar levels of translation, except for Δ*rsmH*.

Hence, the experimental conditions of those two assays were different and bacteria were not in the same metabolic state. In β-galactosidase assays, bacteria had to adapt to a different medium, leading to a lag phase during which cells were not dividing but redirecting their metabolism. We did not analyse whether lack of methylation could influence lag phase. To evaluate translation in actively growing cells, measurements were performed after 1h30 incubation. On the other hand, concerning fluorescence assays, cells were grown in the same medium, until exponential phase, so mutants and wild type were actively dividing at the same rates. Taken together, those variations between the experiments could explain the differences in translation observed with the two reporters. As a consequence, we can consider that methyltransferases could participate to metabolic changes in modulating translation.

In vitro assays can give us information in a much simpler and controlled system. The Pure system for *in vitro* transcription/translation contains only the factors necessary for transcription (T7 polymerase, dNTPs...) and translation (IF, EF, RF, tRNAs, amino acids...). In this system, ribosomes are in excess and transcription and translation are not coupled. In fact, T7 RNA polymerase is highly active and overloads the translational machinery by running ahead of the translating ribosomes (Lopez *et al.*, 1994). This phenomenon leaves part of mRNAs free of ribosomes and so they may fold in complex structures which could impact translation efficiency. Moreover if the defect of one methylation induces a slowdown of transcription, it could impact translational efficiency. We used a canonical *gfp* mRNA (derived from *gfp* from pB01) to measure translation performed by ribosomes lacking one methylation in comparison with wild type ones. Ribosomes purified from Δ*rsmA,* Δ*rsmB,* Δ*rsmD* and Δ*rsmE* show similar translational activity than wild type ones. However, ribosomes from Δ*rsmH* are about twice less efficient than wild type

ribosomes. Such results are similar to those obtained with the dual fluorescent reporter.

In conclusion, in controlled environments, ribosomes lacking methylation do not impact translation with the exception of Δ*rsmH* ribosomes. Nevertheless, a metabolic switch has consequences on translation performed by ribosomes lacking one methylation. So it seems that lack of RsmA, RsmB or RsmD influences translation in conditions of metabolism challenge (such as medium change) while, in more favourable growth conditions, it does not impact translation. The methylations catalysed by methyltransferases RsmA, RsmB, RsmD are, in fact, modifications that negatively regulate the translation, or specifically modulate it.

The methylations of the decoding centre form two different platforms: m^5C967 and m^2G966 are involved in contact with tRNA (Burakovsky *et al.*, 2012) while mRNA contacts $m^4Cm1402$ and m^3U1498 which form a hydrophobic network together with $m^6{}_2A1518$ and $m^6{}_2A1519$ (Figure 7) (Kimura and Suzuki, 2010, Fischer *et al.*, 2015). As a consequence, we could expect that absence of one methylation would disturb interaction with the mRNA (deletion of RsmA, RsmE or RsmH) or with the tRNA (RsmB or RsmD) and so our results showing higher translation in some mutants could be surprising. In helix 31, methylation m^2G966 forms interactions with the tRNA and m^5C967 allows m^2G966 correct orientation. Lack of either modification could have consequences on tRNA binding. They have been shown to facilitate initiation of translation *in vitro*, probably by promoting binding of the initiator $tRNA^{fMet}$ (Burakovsky *et al.*, 2012). On the other hand ribosomes containing single mutations of G966 or C967 were considered as hyperactive (Saraiya *et al.*, 2008). Taken together, those data are in accordance with our results: *in vitro,* translation tends to be lower with ribosomes lacking one of those methylations while *in vivo* we observed higher translation levels. Dimethylations $m^6{}_2A1518$ and $m^6{}_2A1519$ were shown to participate in the correct formation of helices 44 and 45 (Demirci *et al.*, 2010). Lacking those dimethylations could then disrupt the structure of the decoding centre and the interactions with the mRNA which could make the ribosome more prone to translation with non-AUG initiation codons (O'Connor *et al.*, 1997) or with non-cognate initiator tRNA (Das *et al.*, 2008). Methylation m^3U1498 is located at the elbow between helices 44 and 45. Its absence seems more critical for translation

than lacking modifications of nucleotides A1518 and A1519. Indeed lack of m^3U1498 induces a faint decrease in the translation efficiency. We could hypothesize that lacking RsmE modification disrupts the network of hydrophobic interactions (formed with $m^4Cm1402$, $m^6{}_2A1518$ and $m^6{}_2A1519$) and affects the stability of the mRNA binding and the accurate placement of the initiator tRNA (Das *et al.*, 2008; Fischer *et al.*, 2015).

Lack of methylation can improve translation under stressful conditions

Subsequently, we studied the impact of methylations on canonical translation using the same reporters (β-galactosidase and dual fluorescent) under stressful conditions such as osmotic, oxidative, heat or cold stresses. Using those genetic tools, we investigated long term adaptation and immediate stress response.

- Long term adaptation response

When cells underwent a long exposure to stresses, we were able to see differences in translation. In fact, for β-galactosidase assays, the cultures were submitted to those stresses for 1h30 (during induction) and so allowing us to analyse the long term adaptation of the strains to those conditions. Interestingly, lack of different methylations had distinctive consequences on translation upon oxidative and heat stresses.

Concerning heat stress, canonical translation in the strains Δ*rsmB* and Δ*rsmD* decreased compared to normal conditions and to the wild type strain. Consequently, methylations m^5C967 and m^2G966 (catalysed by RsmB and RsmD) are critical for canonical translation during heat stress. Concerning Δ*rsmA,* Δ*rsmE* and wild type, heat stress does not impact translation in those strains compared with levels at 30°C. As methylations are implied in maintaining RNA structure, we could suppose that such role is important at elevated temperature. Interestingly it seems that methylations of RsmB and RsmD are of particular relevance at this temperature. Absence of either RsmB or RsmD modification could impact the overall structure of the decoding centre and destabilize interactions with tRNA or translation factors leading to a decrease in translation. Heat stress induces erroneous dissociation of tRNA (Jiang *et al.*, 2009) which could strengthen the structural effects due to lack of m^5C967 and m^2G966. Moreover, dissociation of tRNA results in empty A-site,

connecting heat stress response with stringent response (Harcum and Bentley, 1999).

Concerning oxidative stress, it negatively impacted canonical translation in every strain with the exception of Δ*rsmA.* Thus lack of $m^6{}_2$A1518 and $m^6{}_2$A1519 makes the ribosomes more resistant to oxidative stress.

Osmotic and cold stresses impacted all strains similarly, mutants and wild type which is consistent with previous studies (Brigotti *et al.*, 2003; Dai *et al.*, 2018; Zhang *et al.*, 2018).

- Immediate stress response

We examined the immediate stress response 20 min after the application of stressful conditions (osmotic, oxidative, heat or cold stresses) using the dual fluorescent reporters system from pB01. In those conditions, translation is not impacted by the lack of methylation or by stresses, with the exception of heat and cold shock. In fact, the mutant and the wild type strains did not show any differences of fluorescence of mCherry or GFP synthesis. In all strains, osmotic and oxidative stresses did not impact translation while heat shock led to a reduction of both fluorescent proteins and cold shock induced higher levels of GFP and mCherry. At 45°C, fluorescence levels of both proteins were lower and cells were growing. Thus we could suspect that the plasmid was unstable at this temperature leading to a dilution of GFP and mCherry among cell division. At the opposite, at 16°C, cells were not growing thus there was no such dilution.

- Translation of leaderless mRNAs during stress

Leaderless mRNAs have been described being more abundant after stresses (Moll and Engelberg-Kulka, 2012; Vesper *et al.*, 2011). Using a leaderless version of *lacZ*, we were able to evaluate leaderless translation in the wild type and mutant strains in the same conditions as for described above β-galactosidase.

At 30°C, all mutants were capable of translating leaderless lacZ at the same level as the wild type. Nevertheless, stresses impacted the wild type and the mutants in a different way. Indeed, after heat stress, leaderless translation reduced drastically in the wild type, as well as in strains Δ*rsmA,* Δ*rsmB* and Δ*rsmD* while it was not impacted in *ΔrsmE*. Translation of leaderless *lacZ* mRNA under oxidative stress was

dramatically affected in the wild type and Δ*rsmE* while in the other mutant strains it slightly reduced. The absence of RsmA, RsmB or RsmD led to similar results for both canonical and leaderless translation under oxidative or heat stress. However, in *ΔrsmE* mutant, lack of m^3U1498 is not detrimental at 43°C for canonical translation but seems to confer an advantage in leaderless translation.

Lack of methylation has distinctive impact on frameshifting

Frameshifting was studied in different contexts. On the one hand, we used reporters of *dnaX* and *prfB* programmed frameshifting *in vivo,* leading to high rates of ribosomal shift. On the other hand we also used reporters of spontaneous frameshifting. *In vivo*, we could not detect fluorescent signals from the reporters of spontaneous frameshifting and so we tested such frameshifing in *in vitro* assays.

Spontaneous frameshifting is a rather rare event (10^{-5} per codon) this is probably why we could not detect it *in vivo*. However, *in vitro* translation of frameshift reporters permitted to analyse this phenomenon. Indeed, the probability of a ribosomal frameshift is much higher *in vitro*: using wild type ribosomes, rates of frameshift increased up to one third when the ribosome moves to the second frame of translation (called +1) and 1/15 for a shift to the third frame (called -1). In those conditions, the -1 frameshift rate was less frequent than the +1 rate. Concerning -1 rate, ribosomes purified from Δ*rsmA* and Δ*rsmH* were more prone to this error than wild type ribosomes. About frameshifting to the second frame (+1), ribosomes from Δ*rsmE* were less susceptible whereas ribosomes from Δ*rsmB* and Δ*rsmH* exhibited higher +1 rate. Ribosomes from Δ*rsmD* did not differ from the wild type ones. With the exception of Δ*rsmE* ribosomes, the ribosomes purified from the other mutant strains seem to be more prone to frameshifting errors.

We used the signals of *dnaX* -1 dependant frameshifting to study how the absence of methylation could impact it. Compared to the wild type strain, *dnaX* frameshifting in Δ*rsmD* was similar while Δ*rsmA,* Δ*rsmB* had higher levels of -1 programmed frameshifting and was higher in Δ*rsmE*.

Concerning *prfB* programmed frameshifting, we only detected difference in Δ*rsmA* in which *prfB* frameshifting was lower. Taken together, those two experiments seem to show that Δ*rsmA,* Δ*rsmB,* and *ΔrsmH* are generally more error-prone than

the wild type, whereas ribosomes lacking m^3U1498 (Δ*rsmE)* proceed translation with less error.

Methyltransferases as ribosomal regulators?

We demonstrated that absence of $m^6{}_2A1518$ and $m^6{}_2A1519$ (catalysed by RsmA) is not deleterious for the bacteria and can even be beneficial for translation at 30°C as well as for long-term adaptation to oxidative and heat stresses. Concerning methylations m^5C967 and m^2G966, their lack induces higher levels of translation at 30°C and after oxidative stress but this beneficial effect is lost after heat stress. Modification m^5C967 is described as allowing correct orientation of m^2G966 which is in contact with tRNA, this is in agreement with our results as Δ*rsmB* and Δ*rsmD* mutants exhibits very similar translation patterns. Interestingly, absence of RsmE modification, m^3U1498, does not impact levels of translation but leads to a certain decrease of ribosomal frameshifting. Deletion of RsmH leads to a fitness deficiency, to lower translation levels and higher ribosomal frameshifting *in vitro.* Hence, this modification seems to be of particular importance for the bacteria.

Thus, methylations of the decoding centre impact differently translation regarding the conditions. But can we consider methylations and methyltransferases as stress response modulators? Little is known about the overall level of methylations in the ribosome. We can suppose that there are subpopulations of undermodified ribosomes within the cell. Those ribosomes could bring advantages during specific stressfull conditions, but they would be present in very small proportions. Moreover, we lack information about the expression of methyltransferases during growth and stresses, since data concerning their expression came from global transcriptome analysis. Even if the expression of some methyltransferases changes upon stress, ribosomes fully modified or undermodified are already present. There are several possibilities, for instance if expression increases following exposure stress, (i) the methyltransferase acts on 30S precursor (like RsmA and RsmB) and thus can only modify neo-synthesized ribosomes, (ii) the methyltransferase acts on 30S subunit (like RsmD, RsmE and RsmH) and can modify all ribosomes, neo-synthesized and potential unmethylated ones. Moreover, so far, no bacterial demethylase of rRNA has been discovered therefore rRNA methylations are supposed to be permanent.

Hence, the system of rRNA modification can be considered as static but compensated by the degradation of ribosomes.

In addition, we must take into account that various factors and not only the absence of methylations affect ribosomes during stress. We compared the effects of stresses between wild type and mutant strains, but we cannot exclude that methylations and stress factors act synergistically or in opposite ways on ribosome efficiency. The other actors of translation *in vivo* (tRNA, aminoacyl tRNA synthetases, initiation factors, elongation factors….) are also affected by stress. Therefore *in vitro* analysis appears as a solution to determine the impact of ribosome methylations, provided that all factors associated with ribosomes during stress are eliminated during ribosomes purification. *In vivo*, all those factors and their effects also influence the analysis of the effects of *rsm* mutations on translation under stressful conditions. Moreover, other systems can also impact translation in such conditions. This is particularly true for toxin-antitoxin modules that are induced by stress and can affect translation for instance with endoribonuclease toxins which degrade bulk mRNAs or redirect translation.

IV. Chapter II : Characterization of HicAB toxin-antitoxin system of *Sinorhizobium meliloti*

1. Introduction

Upon stressful conditions, TA modules are induced and the toxin can exert its deleterious actions. Toxins have many cellular targets, and, interestingly, the majority of type II TA systems impacts translation (Harms *et al.*, 2018). Among those type II TA, the well-known MazF was shown to exert a crucial role during stress adaptation *via* generation of stress ribosomes depleted of the anti-SD sequence and of leaderless mRNAs specifically translated by this specific subpopulation of ribosomes (Vesper *et al.*, 2011). Other toxins are mRNA interferases and affect translation by degrading bulk mRNAs.

A major problem in the study of TA modules resides in regulation of the toxin production. Indeed, as the toxin effect is buffered by the antitoxin, to overcome this antagonist effect, most studies analyse the toxin effect by overproducing it. However, such overproduction results in growth arrest: homeostasis is unbalanced too drastically leading to unfavourable conditions.

Thus, the use of a heterologous toxin allows using mild conditions more compatible with physiological studies. As a consequence, we aimed to study the putative TA system HicAB of *Sinorhizobium meliloti* and we analysed it in *Escherichia coli*. We showed that HicAB of *S. meliloti* is a functional TA system, HicA is an RNAse and HicAB complex is affected by stress.

2. HicAB study

This work, named “Characterization of HicAB toxin-antitoxin module of *Sinorhizobium meliloti”* has been submitted to BMC Microbiology and is presented in this section.

Sujet : Confirmation of your submission to BMC Microbiology – MCRO-D-18-00573
De : "BMC Microbiology Editorial Office" <em@editorialmanager.com>
Date : 23/09/2018 23:29
Pour : "Gwennola Ermel" <gwennola.ermel@univ-rennes1.fr>

MCRO-D-18-00573
Characterization of HicAB toxin-antitoxin module of Sinorhizobium meliloti
Manon Thomet; Annie Trautwetter; Gwennola Ermel; Carlos Blanco
BMC Microbiology

Dear Dr Ermel,

Thank you for submitting your manuscript 'Characterization of HicAB toxin-antitoxin module of Sinorhizobium meliloti ' to BMC Microbiology.

The submission id is: MCRO-D-18-00573
Please refer to this number in any future correspondence.

Characterization of HicAB toxin-antitoxin module of *Sinorhizobium meliloti*

Authors:

Manon THOMET, Annie TRAUTWETTER, Gwennola ERMEl, Carlos BLANCO

Institution address:

Ribosome, bacteria and stress Team, Univ. Rennes, CNRS, Institut de Génétique et de Développement de Rennes (IGDR), UMR6290, F35000 Rennes, France.

Email addresses:

manon.thomet@univ-rennes1.fr, annie.trautwetter@univ-rennes1.fr, gwennola.ermel@univ-rennes1.fr, carlos.blanco@univ-rennes1.fr

Corresponding author:

Gwennola ERMEL

ABSTRACT

Background:

Toxin-antitoxin (TA) systems are little genetic units generally composed of two genes encoding antitoxin and toxin. These systems are known to be involved in many functions that can lead to growth arrest and cell death. Among the different types of TA systems, the type II gathers together systems where the antitoxin directly binds and inhibits the toxin. Among

these type II TA systems, the HicAB module is widely distributed in free-living Bacteria and Archaea and the toxin HicA functions via RNA binding and cleavage. The genome of the symbiotic *Sinorhyzobium meliloti* encodes numerous TA systems and only a few of them are functional. Among the predicted TA systems, there is one homologous to HicAB modules.

Results:

In this study, we characterize the HicAB toxin-antitoxin module of *S. meliloti*. The production of the HicA of *S. meliloti* in *Escherichia coli* cells abolishes growth and decreases cell viability. We show that expression of the HicB of *S. meliloti* counteracts HicA toxicity. The results of double hybrid assays and co-purification experiments allow demonstrating the interaction of HicB with the toxin HicA. Purified HicA, but not HicAB complex, is able to degrade ribosomal RNA in vitro. The analysis of separated domains of HicB protein permits us to define the antitoxin activity and the operator-binding domain.

Conclusions:

This study points out the first characterization of the HicAB system of the symbiotic *S. meliloti* whereas HicA is a toxin with ribonuclease activity and HicB has two domains: the COOH-terminal one that binds the operator and the NH2-terminal one that inhibits the toxin.

KEYWORDS

Toxin antitoxin, hicAB, BACTH, DNA binding, *Sinorhizobium meliloti,* RNase

BACKGROUND

Toxin antitoxin modules (TA) play important roles in plasmids and prophage stability and are also important actors in bacterial physiology [1]. Canonical TA modules encode a bacterial toxin and a more labile antitoxin in an operon, the antitoxin typically represses the transcription of the operon. The degradation of the antitoxin relieves repression and releases the toxin [2]. The antitoxin could be an RNA molecule (types I and III of TA systems) that controls the level of the toxin protein by either blocking translation of the toxin mRNA or impeding the toxin protein. The nature of the antitoxins may also be proteins that inhibit the toxin by direct interaction or as a hindrance to the effect on the targets (types II and IV of TA systems) [1]. Another types V and VI were described recently. The antitoxin GhoS, , which cleaves the mRNA of the toxin GhoT, is classified in the type V of TA system [3]. The type VI corresponds to the antitoxin that presents the toxin to the proteolytic complex ClpXP [4].

The expressions of TA modules are induced by stress [5]. The links between TA modules and adaptation to stresses are numerous such as the coordination of metabolism with the external supply of nutrients [6] and the increase of membrane permeability due to the delivery of the GraT toxin for example [7]. Whereas the TA systems remain quiescent under favourable growth conditions because of the antagonist action of the antitoxin, under stress, the antitoxins are degraded, allowing the toxins to inhibit essential cellular processes. This inhibition ensues in rapid growth arrest [8] and development of stress-tolerant dormant state [9]. The actions of the toxins are diversified: cleavage, modification and degradation of the cellular targets and, finally hamper the bacterial physiology. Numerous toxins are ribosome-dependent or -independent endonucleases. Other actions of the toxins are described such as the post-translational modification of the targets or the depolarization of the bacterial membrane leading to the arrest of the ATP synthesis [1]. The toxins could have either indirect effects *i.e.* MqsR, which is a ribosome independent mRNA interferase, cleaves the *ygiS*

mRNA resulting in increased bile tolerance [10]; or domino effects where one toxin could control another TA module: MqsR cleaves antitoxin *ghoS-ghoT* mRNA in the *ghoS* coding region leading to the enhancement of *ghoT* coding region [11]. The physiological consequence of TA expression could also result of a direct role of the antitoxin on targets other than its cognate toxin: MqsA and DinJ antitoxins are able to repress *rpoS* gene, affecting the general stress response [12, 13]. TA modules are involved in the virulence of *Salmonella* [14], *Haemophilus influenza* [15] and *Staphylococcus aureus* [16]. Many of them are implicated in persistence [1] and are considered as targets for antibacterial development.

The HicAB system belonging to the type II TA systems are found in many bacteria and archaea and has been shown to be involved in the stress response virulence and persistence [17-20]. The first identification of *hicAB* was done in *Haemophilus influenza* [21] and the term *hic* came from the localization near the pathogenicity island *hif*. Then *hicAB* operons were identified in other bacteria such as *Escherichia coli*, *Burkholderia pseudomallei*, *Yersinia pestis*, *Pseudomonas aeruginosa* and the structure of HicAB was determined in *Yersinia pestis* and *Streptococcus pneumoniae* [17, 22-24]. In *E. coli* K12, the *hicAB* locus encodes the toxin HicA that cleaves mRNAs and also the tmRNA by a ribosome-independent manner, and the antitoxin HicB [25].

In *Sinorhizobium meliloti* 53 TA modules were predicted [26], only a few of them were characterized. NtpP/R and VapB/C are involved in symbiotic efficiency [27, 28]. Systematic deletion of TA loci in megaplasmids pSymA and pSymB shows that the deletion of some of them affects growth [29], suggesting that part of them is not functional. In this study, we focused on the TA module HicAB of *S. meliloti* corresponding to SMc04441 and SMc04269 hypothetical proteins as defined by Capela et al.,[30]. The HicAB modules are highly subjected to horizontal gene transfer and are widely distributed in free-living Bacteria- and

Archaea-species, and are not found in genomes of obligate parasites and symbionts [24] such as *S. meliloti*. Moreover, this HicAB module is involved in virulence and adaptative traits: attenuated virulence of *Y. pestis* mutants [31] development of persister cells in the bacteria *B. pseudomaellei* [17]; adaptation to extracellular stresses in *E. coli* [19]. In this study, we show that the operon consisting of the ORFs SMc04441 and SMc04269 in *S. meliloti* encodes a TA module composed of the functional toxin HicA and antitoxin HicB.

RESULTS

hicAB of *S. meliloti* encodes a functional TA system

In order to study the HicAB module of *S. meliloti*, we assumed that several TA systems could be active in heterologous bacteria [32]. Considering this hypothesis that the TA systems possess a relatively broad host range, we examined the functionality of the HicAB module of *S. meliloti* by constructing a conditional system for the expressions of HicA and HicB in *Escherichia coli*.

The *hicA* ORF of *S. meliloti*, cloned in the pBB-HicA allows the production of HicA under control of the P_{BAD} promoter. After induction with arabinose, the influence of the expression of HicA on cell growth was investigated in *E. coli* strain MG1655 (Fig. 1). Cells carrying the empty pBBara expression vector showed no difference in growth or in viability when they were either induced or not by arabinose. When cells harbouring pBB-HicA were grown without arabinose, they exhibited the same growth pattern estimated by turbidity (OD_{570nm}) but when HicA production was induced, growth was abolished (Fig. 1.A). Moreover, the number of CFU dramatically reduced after induction and continuously decreased throughout time representative of the lethal effect of the toxin (Fig. 1.B).

To investigate whether HicB could alleviate HicA toxicity, *hicB* ORF was cloned in the plasmid pNDM220. This vector is compatible with pBBara and the expression of HicB is inducible with IPTG. Plasmid derivatives from both vectors were introduced in *trans* and induced simultaneously in *E. coli*. After two hours of induction, cells carrying the empty vector pNDM220 and pBB-HicA exhibited lethality (Fig. 1. C, line B) whereas in cells harbouring pBB-HicA and pNDM-hicB for which the simultaneous production of HicA and HicB reduced drastically HicA lethal effect (Fig. 1. C, line D).

HicB binds to *hicAB* promoter region

In type II TA systems the transcription of both toxin and antitoxin are autoregulated: the antitoxin binds to the promoter of the TA operon and thus inhibits transcription of both toxin and antitoxin [1]. To study HicB interaction with *hicAB* promoter, we performed an electrophoretic mobility shift assay (EMSA) using purified His-tagged HicB and a 223 bp sequence containing the promoter of genes *hicAB*, which was previously characterized [33, 34] (Fig. 2). An upshifted band appeared faintly with a low concentration (50 nM) of HicB and was clearly present with the highest concentrations (from 0,25 to 1 μM) of HicB. These results demonstrate that the HicB protein of *S. meliloti* binds to the *hicAB* promoter region.

HicB interacts with HicA

To assess HicA-HicB protein interactions, we used the bacterial two-hybrid system (BACTH) in *E. coli cya* strain BTH101. BACTH relies on the recovery of *Bordetella pertussis* adenylate cyclase whose domains T18 and T25 are split and can be fused with proteins [35]. HicA and HicB were alternatively fused to the NH2 and COOH ends of T18 and T25 domains in different combinations, for which β-galactosidase assays were monitored (Fig.S1). All the combinations between HicA and HicB showed significant β-galactosidase

activities in regards to those determined with empty vectors without any fused protein and self-interactions of HicA. High β-galactosidase activity was detected in cells producing T25-HicA and T18-HicB reflecting HicA-HicB interaction (Fig. 3.A). Although HicA does not self-interact the co-expression of T25-HicB and T18-HicB resulted in high levels of β-galactosidase activity (Fig. 3.A) suggesting HicB self-interaction and a possible dimeric organization of the protein.

To confirm HicA-HicB interaction, we performed co-purification experiments. A synthetic *hicAstrep-hicBhis* operon (Fig. S2) was introduced in pET22b(+) vector leading to the productions of strep-tagged HicA and his-tagged HicB at their COOH ends. After IPTG induction, the produced proteins were alternatively purified on IMAC chromatography and on Strep-Tactin resins. In both cases HicA and HicB were co-purified (Fig. 3.B).

These data indicate that *S. meliloti* HicA and HicB interact, as expected for a toxin-antitoxin system. Moreover HicB would be a multimeric protein while HicA behaves as a monomer as this has been shown using the two-hybrid assays and described for HicAB in *Y. pestis* [22].

Antitoxin stability and toxin purification

Toxins are stable proteins while antitoxins are targeted by proteases such as the Lon protease or by ClpP associated with either ClpA or ClpX [2]. Proteases synthesis is induced by stresses such as osmotic and starvation ones. Thus we hypothesized that the strains expressing toxin and antitoxin must have their growth affected by stress while it would not be affected in non-stressing medium. The *E. coli* strain MG1655 containing both pBB-hicA and pNDM-hicB, or both pBB-hicA and pNDM220, or both pBBara and pNDM220 vectors as controls, was grown in M63 medium after induction of *hicA* and *hicB*. The sole induction of HicA and HicB production did not affect growth (data not shown). When osmotic stress was performed by the addition of NaCl to growth medium, a growth arrest of the strain expressing

toxin and antitoxin was observed after induction while strains containing empty vectors still grew (data not shown) but the cell survival was affected after stress application (Fig.4 A). Concerning the strain containing both pBB-hicA and pNDM220, defect of growth was observed after arabinose induction leading to the production of the toxin HicA. A concentration of 0.5M NaCl in M63 medium amplified this defect of growth.

The extraction of proteins was performed in *E. coli* BL21 cells harbouring pETHicAStrepHicBHis 3 h after IPTG induction, and 4 h after NaCl addition (*i.e.* 7h after induction); proteins were loaded on Strep-Tactin column that traps the strep-tagged toxin. Toxin and antitoxin were eluted from extracts of non-salted cultures (Fig. 4 B) while only toxin was eluted from salted cultures (Fig. 4 C). These data show that the antitoxin produced before NaCl addition is degraded during salt stress adaptation.

To determine the toxic effect of HicA, RNase activity of purified proteins was analysed. Extracts of cells cultured in M63 medium that contained the HicA-HicB complex did not show RNase activity against ribosomal RNAs. In contrast ribosomal RNAs were fully degraded by purified HicA originated from cells cultured in M63 medium containing 0.5M NaCl after 1h at 37°C (Fig. 4 D).

These results show that contrary to HicB, HicA ribonuclease is not degraded by proteases induced by osmotic stress [1, 2]. This allows a simple toxin purification protocol that did not need protein denaturation and renaturation as described for other HicA proteins.

HicB is composed of two functional modules

The structure of HicAB was determined in *Y. pestis* and *S. pneumoniae*. In both bacteria, HicA and HicB structures are very close [22, 23]. In these bacteria, HicA is a monomer while HicB is dimeric or tetrameric. This antitoxin is composed of two domains linked by a hinge, a NH2 domain interacting with HicA toxin and a COOH domain possessing a ribbon-helix-

188 helix (RHH) motif that interacts with the operator. HicB3 of *Y. pestis* dimerizes through the
189 RHH domain while HicB of *S. pneumoniae* dimerizes through the NH2 domain.

190 Clustall alignments of *S. meliloti* HicA with HicA of *E. coli*, *Y. pestis* and *S. pneumoniae*,
191 show that all the proteins are very closed (Fig. S3), the conserved residues important for the
192 activity are conserved in *S. meliloti* HicA. In contrast, Clustall alignments of HicB show that
193 the amino acids are less conserved in HicB proteins (Fig. S3). Structure prediction of *S.*
194 *meliloti* with Phyre server shows that its structure is close to that of *Y. pestis* and *S.*
195 *pneumoniae*, main differences were observed in the hinge region (Fig. S4 and Fig. S5).

196 The two domains (RHH for C-terminal and COG for N-terminal domains) were cloned in
197 pBBara, the hinge region was conserved in both constructs. The arabinose induction of the
198 two domains does not induce toxicity in *E. coli* cells (data not shown). Thus, the sequences
199 corresponding to the two domains were separately cloned into pNDM vector and introduced
200 in *E. coli* with pBB-HicA. After induction with arabinose and IPTG, toxicity was observed
201 when HicA and HicB-RHH were produced simultaneously (Fig. 1 C lane C). In contrast
202 expression of HicB-COG domain abolishes HicA toxicity (Fig. 1C lane E). The antitoxin
203 effect is greater than that observed with HicB (Fig. 1C lane E). Interaction of the HicB NH2-
204 domain with HicA was confirmed by BACTH analysis (Fig. 5 and S6). The HicB COG
205 domain must multimerize as deduced from the high ß-galactosidase activity observed in
206 HicB-COG self-interaction in BACTH assays (Fig. 5 and S5). Moreover, this HicB-COG was
207 unable to interact with HicB-RHH domain in BACTH assays. The HicB RHH domain was
208 purified and used in EMSA studies with HicB binding region. It bound operator sequence as
209 efficiently as HicB protein (Fig. 5). The analysis of BACTH assays showed that RHH domain
210 dimerizes, a feature necessary for efficient binding to the operator.

211

DISCUSSION

Numerous TA modules exist in *Bacteria* and *Archaea* and are related to numerous functions that allow the control of growth arrest or death when cells adapt to variable environments. Among numerous TA modules, the type II HicAB is widely distributed in the genomes of many bacteria, especially in free-living bacteria but was studied in few of them [17, 20, 22-25, 36]. In the nitrogen-fixing soil bacterium *S. meliloti*, , numerous TA modules were predicted [24, 26] and one TA module, encoded by *smc04441/smc04269*, showed homologies with *hicAB* loci [30]. A few of TA modules have been characterized: NtpRP, VapBC on the chromosome and four other ones from the megaplasmids [26-29] . Nevertheless, the deletion of many others predicted modules had no phenotypes, thus bioinformatics characterization is not sufficient to conclude on the functionality of TA modules. In this study, we demonstrate that the HicAB module of *S. meliloti* is functional using *E. coli* as a host and conditional expression systems for verification of this heterogenic TA module. This strategy has been successful for the characterization of TA modules of bacteria such as *Bacillus anthracis*, *S. pneumonia*, *Streptococcus mutans* and *Pseudomonas aeruginosa* [20, 37, 38].

The expression of HicA toxin under the control of the arabinose promoter in *E. coli* permits us to show that HicA toxin provoked a decrease of the viability of bacteria after the induction by arabinose (Fig. 1B). The toxicity of HicA was prevented by the simultaneous expression of HicB antitoxin (Fig. 1C). The interactions between the two proteins were confirmed by the two hybrid assays using the BACTH system [35] whatever the combination using HicA or HicB (Fig. 3A and Fig. S1). The co-purification of strep-tagged HicA and His-tagged HicB using affinity chromatographies on either Nickel or Strep-Tactin resins is another argument in favour of HicA-HicB interaction (Fig. 3B). Furthermore, these experiments allow us to reveal a self-interaction and a possible dimerization of HicB (Fig. S1). These data indicate that *S.*

236 *meliloti* HicA and HicB interact, as expected for a toxin-antitoxin system. Moreover there are
237 evidence that HicB would be a multimeric protein while HicA behaves as a monomer, as
238 described for HicAB in *Y. pestis* [22]. The purified His-tagged HicB bound to the promoter of
239 genes *hicAB* (Fig. 2A). Thus the HicB protein of *S. meliloti* binds to the *hicAB* promoter
240 region such as the antitoxins HicB of other bacteria [22, 39].

241 The operon organization, HicB binding to the promoter of the operon, the protein interactions
242 and the antagonist effect of HicB to counteract the toxic effect of HicA are elements that
243 allow to identify the locus *smc04441/smc04269* as a locus that encodes the type II HicAB
244 module in the symbiotic nitrogen-fixing soil bacterium *S. meliloti*.

245 The simultaneous induction of HicA and HicB affected growth only when osmotic stress was
246 applied by the addition of NaCl to the medium (Fig. 4A), meaning that the HicB antitoxin
247 was digested by osmotic stress-induced proteases such as Lon or ClpP as this phenomenon
248 has been observed for other antitoxins [1, 2]. This particularity was used to purify the HicA
249 toxin only (Fig. 4C) using a simple protocol. The HicA protein of *S. meliloti* was shown to be
250 a ribonuclease that degraded ribosomal RNAs (Fig. 4D). RNA cleavage would block
251 translation and cause primarily a growth arrest and finally a decrease of cell viability [25].

252 The analysis of the predicted structure of HicB showed a NH2 domain with homologies to
253 the domain of HicB of *S. pneumoniae* and *Y. pestis*, interacting with HicA toxin and a COOH
254 domain possessing a potential ribbon-helix-helix motif, binding promoter that is less
255 conserved (Fig. S2). The different experiments permitted to show that the two domains are
256 active independently: the NH2 domain of HicB interacts with the toxin HicA and the COOH
257 domain of HicB binds to the promoter of *hicAB* operon. Moreover, these two domains
258 potentially showed self-interaction and a possible dimerization. HicB of *Y. pestis* and *S*
259 *pneumoniae* possess only one dimerization domain, but not in the same region. Isolated

domains of *S. meliloti* have both the hinge region, nevertheless we could exclude that it is responsible for dimerization since no interaction was observed between NH2 and COOH domains. Thus *S. meliloti* HicB must have a slightly different structure with two interaction regions between monomers. Alternatively, HicB of the other bacteria also has the same ability to dimerize through two regions, but only one is used depending of experimental conditions that were different for *Y. pestis* and *S. pneumoniae* [22, 23].

CONCLUSION

In this study we prove the biochemical properties of HicA and HicB proteins of *S. meliloti*. Purified HicA has an RNAse activity; HicB is a DNA binding protein. Both proteins interact and this interaction via the NH2 domain of HicB abolishes the RNAse activity of the toxin. The following work, which is in progress, would have to determine the physiological importance of HicAB TA module in *S. meliloti*.

METHODS

Bacterial strains and culture conditions

E. coli and *S. meliloti* strains are listed in table 1.They were grown in LB medium at 37°C. For the selection of *E. coli* transformants, antibiotics (Sigma-Aldrich) were added: ampicillin (50 µg/mL), kanamycin (50 µg/mL), neomycin (50 µg/mL), chloramphenicol (25 µg/mL) and tetracycline (10 µg/mL). For the culture of *S. meliloti* strain 102F34, streptomycin was used at 100 µg/ml.

DNA manipulations

Chromosomal and plasmid DNA isolations were undertaken according to the standard procedures [40]. Sequencing was performed by Eurofins.

Plasmids, synthetic genes and primers

The plasmids and oligonucleotides that were used in this study are listed in tables 2 and 3. The synthetic genes are described in figure S2.

A new vector, pBBara was constructed: the *Nsi*I-*Hin*dIII fragment carrying *araC*, *araO* was liberated from pBAD24and introduced between the corresponding sites of pBBR1-MCS2, which was reported to have five to ten copies per chromosome/cell in *E. coli* [41].

In order to express HicA, the *hicA* sequence was amplified from genomic DNA of *S meliloti* strain 102F34 using the primers toxpBAD-A (carrying a *Nhe*I site) and toxpBAD-B (carrying a *Sal*I site). After restriction, the PCR fragment was introduced between the corresponding sites of pBBara, giving the pBB-HicA plasmid.

For the expression of HicA-StrepTag and HicB-6HisTag, a synthetic *hicAB* operon was synthesized (Eurofins Genomics) (Fig. S2) with a *Nde*I restriction site at the initiation codon of *hicA*, a Strep-Tag (WSHPQFE) at the COOH extremity of *hicA*, a *Xho*I site at stop codon of *hicB* in order to allow the expression of a 6His-Tag after the insertion of the fragment into the pET22b(+) vector between the *Nde*I and *Xho*I sites. This construct was named pETHicAStrepHicBHis.

The plasmid pET-HicB contains the HicB ORF, which was amplified by PCR from *S. meliloti* genomic DNA using the primers (HicBNde, HicBXho) and inserted into the pET22b(+) vector between the restriction sites *Nde*I and *Xho*I, introducing a 6His-Tag at the COOH extremity of HicB

The COG1598 (NH2-terminal extremity) and the RHH1 (COOH-terminal extremity) domains of HicB were obtained using amplification with HicBNH2Nde/HicBNH2Xho and RHHNde/HicBXho respectively and introduced into pET22b(+) vector yielding pET-COG and pET-RHH respectively.

Primers PET-BglII and PET-EcoRI were used to amplify the sequence of interest from pET-HicB, pET-RHH and pET-COG1598. The amplicons were digested with *Bgl*II and *Eco*RI and cloned between the *Eco*RI and *Bam*HI sites of pNDM220, yielding pNDM-HicB, pNDM-COG and pNDM-RHH respectively.

Purification of HicA and HicB

The pET22b(+) expression vector possesses a T7 promoter controlled by LacI. All its derivatives were transformed in BL21 cells. pET-HicB, pET-RHH and pET-COG1598 transformants were grown in LB medium to an OD_{570nm} of 0.6, IPTG was added at 1mM and incubation was continued for 4h. Cells were collected by centrifugation (5000g 15 min), washed (Tris-HCl 20 mM, NaCl 500 mM, imidazole 5 mM, pH 8), resuspended in the same buffer, broken in a French press (8,6 10^6 N m^{-2}) and centrifuged (20 000 g, 30 min). Protein extracts were loaded on a Ni-NTA agarose resin (Qiagen), washed with 60 mM imidazole buffer and proteins eluted with 200 mM imidazole buffer. Proteins were dialysed against PBS buffer.

BL21 containing pETHicAStrepHicBHis was grown in LB medium to an OD_{570nm} of 0.6 before 1 mM IPTG was added for protein induction. For purification of HicA-HicB complex, the bacterial cells were harvested 3 hours later. For HicA purification 1M NaCl was added 3h after induction with IPTG and incubation was continued for 4h. The purification steps were identical to those described above. Alternatively protein extract was loaded on a Strep-Tactin resin (IBA Lifesciences), and eluted with 2.5 mM desthiobiothin

328 **RNase assay**

329 *E. coli* ribosomes were purified on 10-40% sucrose gradients. Collected fractions containing
330 70S ribosomes were centrifuged (150 000 g, 2h) and 70S particles re-suspended in 50 mM
331 TRIS pH 7.5, NaCl 0.75 M, MgSO4 10 mM. RNA was extracted with Trizol (Thermo Fisher
332 Scientific) and re-suspended in PBS buffer.

333 HicA and HicAB complexes were purified on Strep-Tactin resin (IBA Lifesciences) and
334 resuspended in PBS buffer. Ribosomal RNA (130 pM) and proteins (20 nM) were incubated
335 at 37°C for 1h and RNA was analysed on bleach agarose gels [42].

336 **EMSA**

337 A 221 bp DNA fragment embedding *hicAB* promoter (-213. +8) was amplified and labelled
338 using PCR with EMSAD and EMSAR primers in the presence of $[\alpha^{32}]$P dCTP. The binding
339 reaction was performed in a 20 µl reaction volume containing10 mM TRIS-HCl pH 7.5, 50
340 mM NaCl, 1 mM DTT, 300 µg ml^{-1} BSA the labelled DNA fragment and the purified HicB-
341 His6 or RHH-6His.

342 The reaction was incubated 30 min at 25 °C followed by the addition of 2 µl of 50% glycerol
343 and electrophoresis through a 5% native polyacrylamide gel at 170 V cm^{-1} in TAE buffer (20
344 mM Tris, 40 mM acetate, 1 mM EDTA, pH7.5). The gel was then dried and revealed by
345 autoradiography.

346 **BACTH analysis**

347 HicA and HicB ORFs were amplified by PCR using ToxXbaT/ToxEcoT and
348 DopXba/DopEcoT primer pairs for HicA and HicB respectively and cloned into pKT25,
349 pKNT25, pUT18 and pUT18C vectors between *Xba*I and *Eco*RI restriction sites. Strain
350 BTH101 was transformed with a combination of one pUT (18 or 18C) derivative and a pKT

(or pKNT) derivative in order to obtain all the combinations to analyse HicA-HicA, HicB-HicB and HicA-HicB interactions. pKT25-ZIP and pUT18-ZIP were used as reference for positive interaction and pKT25 and pUT18 as control for the absence of interaction. BTH101 transformants were grown in LB or M63 medium containing 10 mM glycerol as growth substrate. β-galactosidase enzymatic activity was assayed after induction with 1mM IPTG according to [43].

HicB COG1598 and RHH1 domains were cloned into pKT25, pKNT25, pUT18 and pUT18C using DopXbaT/COGEco and RHHXba/DopEcoT primer pairs. BACTH analysis was performed as described for HicA-HicB interaction.

ABBREVIATIONS

BACTH: bacterial adenylate cyclase two-hybrid

BSA: bovine serum albumin

CFU: colony forming units

COG: clusters of orthologous groups

EMSA: electrophoretic mobility shift assay

IPTG: isopropyl β-D-1-thiogalactopyranoside

OD570nm : optical density measured at 570 nm

ON: overnight

PBS: phosphate-buffered saline

PCR: polymerase chain reaction

RHH: ribbon-helix-helix

DECLARATIONS

Acknowledgements

We sincerely thank Sylvie Georgeault, Marie-Christine Savary and Lydie Jose-Teixeira-Pinault from the IGDR for technical assistance. We also thank Prof. Reynald Gillet (University of Rennes1) head of IGDR, for his general support and for proofreading this manuscript.

Availability of data and materials

The datasets used and/or analyzed during the current study are available from the corresponding author on reasonable request.

Authors' contributions

MT, AT, GE and CB conceived and designed the experiments. AT and CB constructed all the plasmids used in this publication. MT and CB performed the protein purification and BACTH assays. MT and GE was involved in ribosome, rRNA purifications and RNase assays. CB and GE wrote the paper. All authors read and approved the final manuscript.

Ethics approval and consent to participate

The experiments conducted in this work do not include any human or animal subjects. We do not see any ethical issues.

Consent for publication

Not applicable.

Competing interests

The authors declare that they have no competing interest.

REFERENCES

1. Harms A, Brodersen DE, Mitarai N, Gerdes K. Toxins, Targets, and Triggers: An Overview of Toxin-Antitoxin Biology. Molecular Cell. 2018; 70(5):768-84.
2. Muthuramalingam M, White J, Bourne C. Toxin-Antitoxin Modules Are Pliable Switches Activated by Multiple Protease Pathways. Toxins. 2016; 8(7):214.
3. Wang X, Lord DM, Cheng H-Y, Osbourne DO, Hong SH, Sanchez-Torres V, Quiroga C, Zheng K, Herrmann T, Peti W *et al*. A new type V toxin-antitoxin system where mRNA for toxin GhoT is cleaved by antitoxin GhoS. Nat Chem Biol. 2012; 8:855-61.
4. Aakre Christopher D, Phung Tuyen N, Huang D, Laub Michael T. A Bacterial Toxin Inhibits DNA Replication Elongation through a Direct Interaction with the β Sliding Clamp. Mol Cell. 2013; 52(5):617-28.
5. Gerdes K, Christensen SK, Løbner-Olesen A. Prokaryotic toxin–antitoxin stress response loci. Nat Rev Microbiol. 2005; 3:371-82.
6. Gerdes K. Toxin-Antitoxin Modules May Regulate Synthesis of Macromolecules during Nutritional Stress. J Bacteriol. 2000; 182(3):561-72.
7. Tamman H, Ainelo A, Ainsaar K, Hõrak R. A Moderate Toxin, GraT, Modulates Growth Rate and Stress Tolerance of Pseudomonas putida. J Bacteriol. 2014; 196(1):157-69.
8. Page R, Peti W. Toxin-antitoxin systems in bacterial growth arrest and persistence. Nat Chem Biol. 2016; 12(4):208-14.
9. Hõrak R, Tamman H. Desperate times call for desperate measures: benefits and costs of toxin–antitoxin systems. Curr Genet. 2017; 63(1):69-74.

10. Kwan BW, Lord DM, Peti W, Page R, Benedik MJ, Wood TK. The MqsR/MqsA toxin/antitoxin system protects Escherichia coli during bile acid stress. Environ Microbiol. 2015; 17(9):3168-81.

11. Wang X, Lord DM, Hong SH, Peti W, Benedik MJ, Page R, Wood TK. Type II toxin/antitoxin MqsR/MqsA controls type V toxin/antitoxin GhoT/GhoS. Environ Microbiol. 2013; 15(6):1734-44.

12. Hu Y, Benedik MJ, Wood TK. Antitoxin DinJ influences the general stress response through transcript stabilizer CspE. Environ Microbiol. 2012; 14(3):669-79.

13. Wang X, Kim Y, Hoon Hong S, Ma Q, Brown BL, Pu M, Tarone AM, Benedik MJ, Peti W, Page R *et al*. Antitoxin MqsA Helps Mediate the Bacterial General Stress Response. Nat chem biol. 2011; 7(6):359-66.

14. De la Cruz MA, Zhao W, Farenc C, Gimenez G, Raoult D, Cambillau C, Gorvel J-P, Méresse S. A Toxin-Antitoxin Module of Salmonella Promotes Virulence in Mice. PLoS Pathog. 2013; 9(12):e1003827.

15. Ren D, Walker AN, Daines DA. Toxin-antitoxin loci vapBC-1 and vapXD contribute to survival and virulence in nontypeable Haemophilus influenzae. BMC Microbiol. 2012; 12:263.

16. Wen W, Liu B, Xue L, Zhu Z, Niu L, Sun B. Autoregulation and virulence control by the toxin-antitoxin system SavRS inStaphylococcus aureus. Infect Immun. 2018. doi: 10.1128/IAI.00032-18

17. Butt A, Higman Victoria A, Williams C, Crump Matthew P, Hemsley Claudia M, Harmer N, Titball Richard W. The HicA toxin from Burkholderia pseudomallei has a role in persister cell formation. Biochem J. 2014; 459(2):333-44.

443 18. Button JE, Silhavy TJ, Ruiz N. A Suppressor of Cell Death Caused by the Loss of σE
444 Downregulates Extracytoplasmic Stress Responses and Outer Membrane Vesicle
445 Production in Escherichia coli. J Bacteriol. 2007; 189(5):1523-30.
446 19. Daimon Y, Narita S-i, Akiyama Y. Activation of Toxin-Antitoxin System Toxins
447 Suppresses Lethality Caused by the Loss of σE in Escherichia coli. J Bacteriol. 2015;
448 197(14):2316-24.
449 20. Li G, Shen M, Lu S, Le S, Tan Y, Wang J, Zhao X, Shen W, Guo K, Yang Y *et al.*
450 Identification and Characterization of the HicAB Toxin-Antitoxin System in the
451 Opportunistic Pathogen Pseudomonas aeruginosa. Toxins. 2016; 8(4):113.
452 21. Mhlanga-Mutangadura T, Morlin G, Smith AL, Eisenstark A, Golomb M. Evolution
453 of the Major Pilus Gene Cluster of Haemophilus influenzae. J Bacteriol. 1998;
454 180(17):4693-703.
455 22. Bibi-Triki S, Li de la Sierra-Gallay I, Lazar N, Leroy A, Van Tilbeurgh H, Sebbane F,
456 Pradel E. Functional and Structural Analysis of HicA3-HicB3, a Novel Toxin-
457 Antitoxin System of Yersinia pestis. J Bacteriol. 2014; 196(21):3712-23.
458 23. Kim D-H, Kang S-M, Park SJ, Jin C, Yoon H-J, Lee B-J. Functional insights into
459 the Streptococcus pneumoniae HicBA toxin–antitoxin system based on a structural
460 study. Nucleic Acids Research. 2018; 46(12):6371-86.
461 24. Makarova KS, Grishin NV, Koonin EV. The HicAB cassette, a putative novel, RNA-
462 targeting toxin-antitoxin system in archaea and bacteria. Bioinformatics. 2006;
463 22(21):2581-84.
464 25. Jorgensen MG, Pandey DP, Jaskolska M, Gerdes K. HicA of Escherichia coli defines
465 a novel family of translation-independent mRNA interferases in bacteria and archaea.
466 J Bacteriol. 2009; 191(4):1191-99.

26. Sevin EW, Barloy-Hubler F. RASTA-Bacteria: a web-based tool for identifying toxin-antitoxin loci in prokaryotes. Genome Biol. 2007; 8(8):R155.

27. Bodogai M, Ferenczi S, Bashtovyy D, Miclea P, Papp P, Dusha I. The ntrPR Operon of Sinorhizobium meliloti Is Organized and Functions as a Toxin-Antitoxin Module. Mol Plant Microbe Interact 2006; 19(7):811-22.

28. Lipuma J, Cinege G, Bodogai M, Oláh B, Kiers A, Endre G, Dupont L, Dusha I. A vapBC-type toxin–antitoxin module of Sinorhizobium meliloti influences symbiotic efficiency and nodule senescence of Medicago sativa. Environ Microbiol. 2014; 16(12):3714-29.

29. Milunovic B, diCenzo GC, Morton RA, Finan TM. Cell Growth Inhibition upon Deletion of Four Toxin-Antitoxin Loci from the Megaplasmids of Sinorhizobium meliloti. J Bacteriol. 2014; 196(4):811-24.

30. Capela D, Barloy-Hubler F, Gouzy J, Bothe G, Ampe F, Batut J, Boistard P, Becker A, Boutry M, Cadieu E *et al*. Analysis of the chromosome sequence of the legume symbiont Sinorhizobium meliloti strain 1021. Proc Natl Acad Sci U S A. 2001; 98(17):9877-82.

31. Pradel E, Lemaitre N, Merchez M, Ricard I, Reboul A, Dewitte A, Sebbane F. New insights into how Yersinia pestis adapts to its mammalian host during bubonic plague. PLoS Pathog. 2014; 10(3):e1004029.

32. Buts L, Lah J, Dao-Thi M-H, Wyns L, Loris R. Toxin–antitoxin modules as bacterial metabolic stress managers. Trends Biochem Sci. 2005; 30(12):672-79.

33. Sallet E, Roux B, Sauviac L, Jardinaud MF, Carrere S, Faraut T, de Carvalho-Niebel F, Gouzy J, Gamas P, Capela D *et al*. Next-generation annotation of prokaryotic genomes with EuGene-P: application to Sinorhizobium meliloti 2011. DNA Res. 2013; 20(4):339-54.

34. Schlüter J-P, Reinkensmeier J, Barnett MJ, Lang C, Krol E, Giegerich R, Long SR, Becker A. Global mapping of transcription start sites and promoter motifs in the symbiotic α-proteobacterium Sinorhizobium meliloti 1021. BMC Genomics. 2013; 14:156-56.

35. Karimova G, Pidoux J, Ullmann A, Ladant D. A bacterial two-hybrid system based on a reconstituted signal transduction pathway. Proc Nat Acad Sci U S A. 1998; 95(10):5752-56.

36. Daimon Y, Narita S-i, Akiyama Y. Activation of TA system toxins suppresses lethality caused by the loss of σE in Escherichia coli. Journal of Bacteriology. 2015; 197(14):2316-24.

37. Agarwal S, Agarwal S, Bhatnagar R. Identification and characterization of a novel toxin–antitoxin module from Bacillus anthracis. FEBS Lett. 2007; 581(9):1727-34.

38. Nieto C, Cherny I, Khoo SK, de Lacoba MG, Chan WT, Yeo CC, Gazit E, Espinosa M. The yefM-yoeB Toxin-Antitoxin Systems of Escherichia coli and Streptococcus pneumoniae: Functional and Structural Correlation. J Bacteriol. 2007; 189(4):1266-78.

39. Turnbull KJ, Gerdes K. HicA toxin of Escherichia coli derepresses hicAB transcription to selectively produce HicB antitoxin. Mol Microbiol. 2017; 104(5):781-92.

40. Sambrook J, Fritsch EF, Maniatis T: Molecular cloning: a laboratory manual, 2nd ed., Cold Spring Harbor edn. New York: Cold Spring Harbor; 1989.

41. Kovach ME, Elzer PH, Hill DS, Robertson GT, Farris MA, Roop RM, Peterson KM. Four new derivatives of the broad-host-range cloning vector pBBR1MCS, carrying different antibiotic-resistance cassettes. Gene. 1995; 166:175-76.

42. Aranda PS, LaJoie DM, Jorcyk CL. Bleach gel: A simple agarose gel for analyzing RNA quality. Electrophoresis. 2012; 33(2):366-69.

43. Miller JH. Experiments in molecular genetics. Cold Spring Harbor Laboratory, Cold Spring Harbor, NY. 1972.

44. Jozefkowicz C, Brambilla S, Frare R, Stritzler M, Puente M, Piccinetti C, Soto G, Ayub N. Microevolution Rather than Large Genome Divergence Determines the Effectiveness of Legume-Rhizobia Symbiotic Interaction Under Field Conditions. J Mol Evol. 2017; 85(3-4):79-83.

45. Blattner FR, Plunkett G, 3rd, Bloch CA, Perna NT, Burland V, Riley M, Collado-Vides J, Glasner JD, Rode CK, Mayhew GF *et al*. The complete genome sequence of Escherichia coli K-12. Science. 1997; 277(5331):1453-62.

46. Studier WF, Moffat BA. Use of bacteriophage T7 RNA polymerase to direct selective high-level expression of cloned genes. J Mol Biol. 1986; 189:113-30.

47. Battesti A, Bouveret E. The bacterial two-hybrid system based on adenylate cyclase reconstitution in Escherichia coli. Methods. 2012; 58(4):325-34.

48. Guzman LM, Belin D, Carson MJ, Beckwith J. Tight regulation, modulation, and high-level expression by vectors containing the arabinose PBAD promoter. J Bacteriol. 1995; 177(14):4121-30.

49. Gotfredsen M, Gerdes K. The Escherichia coli relBE genes belong to a new toxin-antitoxin gene family. Mol Microbiol. 1998; 29(4):1065-76.

Table 1: Bacterial strains

Strains	Genotypes	References
S. meliloti		
102F34	WT SmR	[44]
E. coli		
MG1655	F^-, $lambda^-$, rph-1	[45]
BL21	*E. coli* B F^- *dcm ompT hsdS gal*λ(DE3)	[46]
BTH101	F′, *cya-99, araD139, galE15, galK16, rpsL1* (Str^R), *hsdR2, mcrA1, mcrB1, relA1*	[47]

Table 2: Plasmids used in this study

Names	Genotypes	References
pBAD24	ori ColE1 *araC*, P_{BAD} *bla*	[48]
pNDM220	Mini R1, *bla, lacI*^{q}, $P_{A1/O4/O3}$	[49]
pBBR1-MCS2	ori pBBR1, *lacZα, aphA*	[41]
pET22b(+)	ori ColE1, *bla, lac*I, T7p	Novagen
pKT25	ori P15A, *aac*, T25	[35]
pKNT25	ori P15A, *aac*, T25	[35]
pUT18	ori ColE1 *bla*, T18	[35]
pUT18C	ori ColE1 *bla*, T18	[35]
pKT25-Zip	ori P15A, *aac*, T25 :: Zip	[35]
pUT18C-Zip	ori ColE1 *bla*, T18 :: Zip	[35]
pBBara	pBBR1-MCS2, *araC*, P_{BAD}	
pBB-HicA	pBBR1-MCS2, *araC*, P_{BAD} -*hicA*	This study
pET-HicB	pET22 *hicB* 6 his	This study
pET-RHH	pET22 RHH1 6 his	This study
pET-COG	pET22 COG 6 his	This study
pETHicAStrepHicBHis	pET22 synthetic operon	This study
pNDM-HicB	pNDM220 *hicB*	This study
pNDM-COG	pNDM220 NH2 fragment of HicB (COG1598)	This study
pNDM-RHH	pNDM220 COOH fragment of HicB (RHH)	This study
pKThicA	pKT25 *hicA*	This study
pKThicB	pKT25 *hicB*	This study
pNThicA	pKNT25 *hicA*	This study
pNThicB	pKNT25 *hicB*	This study
pUThicA	pUT18 *hicA*	This study
pUThicB	pUT18 *hicB*	This study
pUChicA	pUT18C *hicA*	This study
pUChicB	pUT18C *hicB*	This study
pKTCOG	pKT25 COG1598	This study
pNTCOG	pKNT25 COG1598	This study
pKTRHH	pKT25 RHH1	This study
pNTRHH	pKNT25 RHH1	This study
pUTCOG	pUT18 COG1598	This study
pUCCOG	pUT18C COG1598	This study
pUTRHH	pUT18 RHH1	This study
pUCRHH	pUT18C RHH1	This study

Table 3: Oligonucleotides used in this study

Names	Sequences*	Restriction sites
Tox pBAD-A	TGGGCTAGCGTGTGTATTGTCGTATCAGATG	*Nhe*I
Tox pBAD-B	TGCCGTCGACTTACCTCAATTTCAAACC	*Sal*I
HicBNde	GAGGTAAGCATATGCGCAAC	*Nde*I
HicBXho	GGTATCTCGAGCACATTTTTG	*Xho*I
RHHNde	AGGTTCATATGTCCGACGCC	*Nde*I
ToxXbaT	CATCTAGAGAGCGGCGAC	*Xba*I
ToxEcoT	GAATTCCTCAATTTCAAACCG	*Eco*RI
DopXbaT	CCTCTAGACAACTATATCGG	*Xba*I
DopEcoT	AGGAATTCACATTTTTGCTGG	*Eco*RI
RHHXba	AATCTAGAATGTCCGACGCCGAGAACAGG	*Xba*I
COGEco	TAGAATTCCAACCTCAAGGGAGGAGGG	*Eco*RI
RHHNde	CGGTGAAAACATATGCAAAAAGAG	*Nde*I
HicBNH2Nde	GGCATATGCGCAACTATATCGGATTGATC	*Nde*I
HicBNH2Xho	CCCTCGAGTTCGGCGAAGGCATCTATC	*Xho*I
PET-Bgl	GGGGGGGAAGATCTAGAAATAATTTTGTTTAAC	*Bgl*II
PET-EcoRI	CGGGAATTCAGCAAAAAACCCCTCAAG	*Eco*RI
EMSAD	GATCCGACGGTTCGAGACCATCC	none
EMSAR	TCTTCGGGTGAGGAACGGTAACC	none

* the restriction sites are underlined

576 **Fig. 1. HicB prevents the toxicity of HicA in *E. coli*.**

577 *E. coli* strain MG1655 containing pBBara (squares) or pBB-HicA (circles) were precultured
578 in LB medium containing 10 mM glucose to an OD_{570nm} of 0.2. After centrifugation, cells
579 were suspended in LB medium containing 10 mM glucose (black symbols) or 10 mM
580 arabinose (white symbols). The growth of the strains was then followed for 3 h and estimated
581 using either turbidity (OD_{570nm}, A) or viable cell counts (log (CFU/mL), B). The panel C
582 corresponds to the numeration of the MG1655 cells containing pBBara + pNDM (A), pBB-
583 HicA + pNDM (B), pBB-HicA + pNDM-RHH (C), pBB-HicA + pNDM-HicB (D), pBB-
584 HicA + pNDM-COG (E) after 2h of arabinose induction in LB medium, the details of the
585 procedure were as in A. Tenfold dilutions were spotted on a LB plate and incubated for 48 hr.

586

587 **Fig.2. HicB binds hicAB promoter region.**

588 Gel mobility shift analysis of specific binding of the purified HicB to the promoter region of
589 *hicAB* operon. The probe, a 223 bp DNA fragment amplified by PCR, was incubated with
590 increasing amounts of purified HicB (0 to 1 µM) and submitted to electrophoresis in a 5%
591 PAGE in Tris acetate buffer pH 7.5. The position of the protein-DNA complex is indicated
592 by an arrow.

593

594 **Fig. 3.. HicB interacts with HicA**

595 **A** Two hybrid analysis of HicA and HicB interaction. HicB (black squares) and HicA (white
596 squares) were fused to T25 (white arrow) or T18 (grey arrow) catalytic domains of *Bordetella*
597 *pertussis* adenylate cyclase both at the N or C terminus of these domains. The whole set of
598 combinations is presented in Fig.S1. For this purpose *hicA* and *hicB* open reading frames

599 were amplified by PCR using ToxXba-ToxEco and DopXba-DopEco primers (Table 3). The
600 amplicons cleaved by *Xba*I and *Eco*RI were cloned into pKT25, pKNT25, pUT18 and
601 pUT18C, the resulting plasmids are listed in Table 2. After introduction of the different
602 recombinant plasmids into *E. coli* strain BTH101, β-galactosidase activities were assayed
603 after growth in LB medium containing 1 mM IPTG. Empty vectors pUT18 and pKNT25
604 were used to determine basal level of β-galactosidase activity and pKT25-Zip and pUT18C-
605 Zip as positive control of a high interaction. β-galactosidase activity (Miller units) is
606 indicated, results are the average of three independent experiments.

607 **B.** SDS-PAGE of both HicA-Strep and HicB-6His. A synthetic operon *hicA*-strep, *hicB*-6His
608 was cloned in pET22b(+). BL21 containing this plasmid was grown in LB medium to an
609 OD_{570nm} of 0.6, 1mM IPTG was added, and the growth of cells was carried on three hours
610 after induction. Cells were collected and broken, protein extract was applied to Ni affinity
611 chromatography using imidazole for elution (lane 1) and Strep-Tactin affinity
612 chromatography using desthiobiotin for elution (lane 2). The eluted proteins were resolved on
613 a 12.5% SDS PAGE.

614

615 **Fig.4 HicB stability and RNase assay**

616 Viable cell counts of cells of *E. coli* strain MG1655 containing pBBara and pNDM220, pBB-
617 hicA and pNDM-hicB or pBB-hicA and pNDM220 that were grown in M63 medium
618 containing or not 0.5 M NaCl (A). Strains were induced with 1mM arabinose and 1 mM
619 IPTG. Viable cell counts (ten fold dilutions) were determined throughout time, the figure
620 illustrates results obtained 3 h after induction.

621 Cells of *E. coli* strain BL21 containing pETHicAStrep-HicBHis grown in M63 medium were
622 induced with 1mM IPTG for 3h. Half of the culture was centrifuged and protein content was

623 loaded on Strep Tactin and eluted with 1 mM desthiobiotin (B). The other half of the culture
624 was added with 0.5M NaCl and incubation was extended for 4h, then the protein content was
625 loaded on Strep-Tactin and eluted with desthiobiotin (C). 20 µg of eluted proteins were
626 solved by SDS PAGE (B, C). The same amount of eluted proteins was incubated with
627 ribosomal RNAs 1h at 37°C and then loaded on 1% bleach agarose gel (D).

628

629 **Fig. 5. Functionnalities of HicB domains**

630 **A** DNA fragment coding for NH2 domain (COG1598) and COOH domain (RHH1) of HicB
631 were amplified by PCR and introduced into pUT18, pUT18C, pKT25 and pKNT25 vectors
632 allowing fusion of these domains with T25 and T18 fragments of *B. pertussis* adenylate
633 cyclase (All the combinations are shown in Fig. S1). Plasmids were introduced in *E. coli*
634 strain BTH101, and the cells were grown in LB medium containing 1mM IPTG and β-
635 galactosidase activity was assayed.

636 **B**. RHH1 domain binds operator sequence. Increasing amounts (0 to 5 µM) of RHH1 domain
637 fused to 6 His were incubated with the promoter region of *hicAB* operon (223 bp PCR
638 fragment used in Fig. 2). Then a 5% PAGE in Tris acetate buffer pH 7.5 was performed to
639 resolve the protein DNA complexes (indicated by an arrow).

640

641

642

643

644

645 **Additional files**

646 Additional file 1. HicA/HicB interaction analysis using the BACTH system

647 For analysis of interactions between HicA and HicB, either one of the plasmids pKThicA,
648 pNThicA, pKThicB, or pNThicB were transformed into the *E. coli* strain BTH101 reporter
649 strains (a *cya*-deficient strain), followed by secondary transformation of any of the following:
650 pUThicA, pUChicA, pUThiB, or pUThicB. Positive and negative controls were performed
651 using pNTZIP/pUCZIP and pKNT25/pUT18C sets respectively. Positive interactions allow
652 the reconstitution of adenylate cyclase activity and thus the expression of *lacZ* gene in the *cya*
653 strain BTH101. β–galactosidase activity (Miller units) is the mean of three independent
654 experiments.

655

656 Additional file 2. Nucleotide sequence of *hicA-hicB* synthetic operon introduced into
657 pEt22b(+).

658 HicA residues are highlighted in yellow, strep tag in pink, HicB in green and his tag in red.

659

660 Additional file 3. Alignments of HicA and HicB proteins with HicA and HicB homologues of
661 *E. coli*, *Y. pestis* and *S. pneumoniae* using Clustal Omega [1].

662

663 Additional file 4. Alignments of *S. meliloti* HicB with HicB of *S. pneumoniae* (A)and HicB3
664 of *Y. pestis* (B) using Phyre [2].

665

666 Additional file 5. *S. meliloti* HicB structure predicted by Phyre using HicB of *Y. pestis* and *S.*
667 *pneumoniae* as template.

668

669 Additional file 6. HicB domains interactions

For analysis of auto-interactions between HicB domains and their interaction with HicA, either one of the plasmids pKTCOG, pNTCOG, pKTRHH, pNTRHH, pKThicA or pNThicA were transformed into the *E. coli* strain BTH101 reporter strains (a *cya*-deficient strain), followed by secondary transformation of any of the following: pUTCOG, pUCCOG, pUTRHH, pUTCRHH or pUThicA. Positive and negative controls were performed using pNTZIP/pUCZIP and pKNT25/pUT18C sets respectively (not shown). Positive interactions allow the reconstitution of adenylate cyclase activity and thus the expression of *lacZ* gene in the *cya* strain BTH101. β–galactosidase activity (Miller units) is the mean of three independent experiments.

References of Additional files

1. Sievers F, Higgins DG. Clustal Omega for making accurate alignments of many protein sequences. Prot Sci. 2018; 27(1):135-45.

2. Kelley LA, Mezulis S, Yates CM, Wass MN, Sternberg MJE. The Phyre2 web portal for protein modeling, prediction and analysis. Nat Protoc. 2015; 10:845-58.

Figure 1

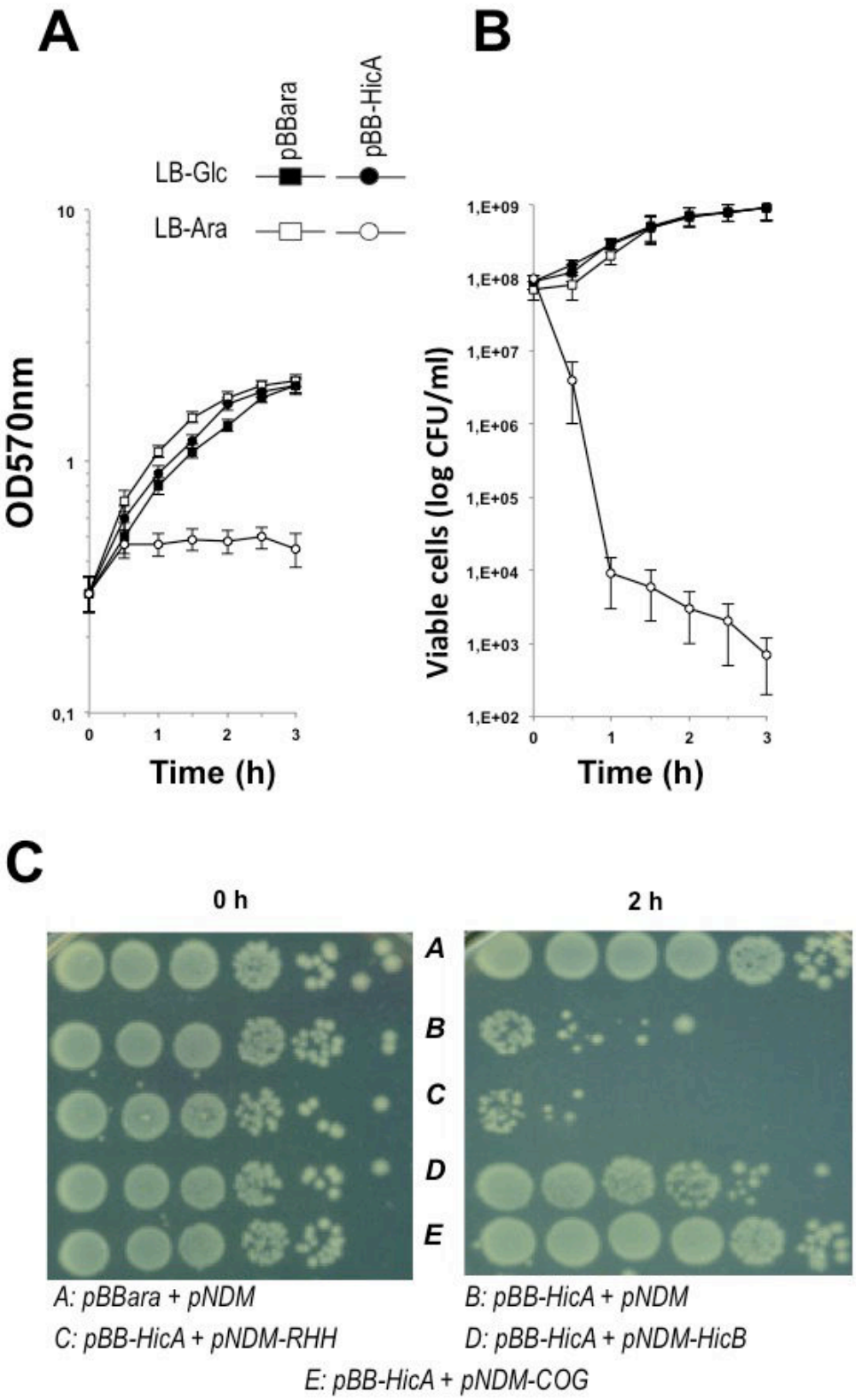
A
B
pBBara
pBB-HicA
LB-Glc
LB-Ara
OD570nm
Time (h)
Viable cells (log CFU/ml)
Time (h)
C
0 h
2 h
A
B
C
D
E
A: pBBara + pNDM
B: pBB-HicA + pNDM
C: pBB-HicA + pNDM-RHH
D: pBB-HicA + pNDM-HicB
E: pBB-HicA + pNDM-COG

Figure 2

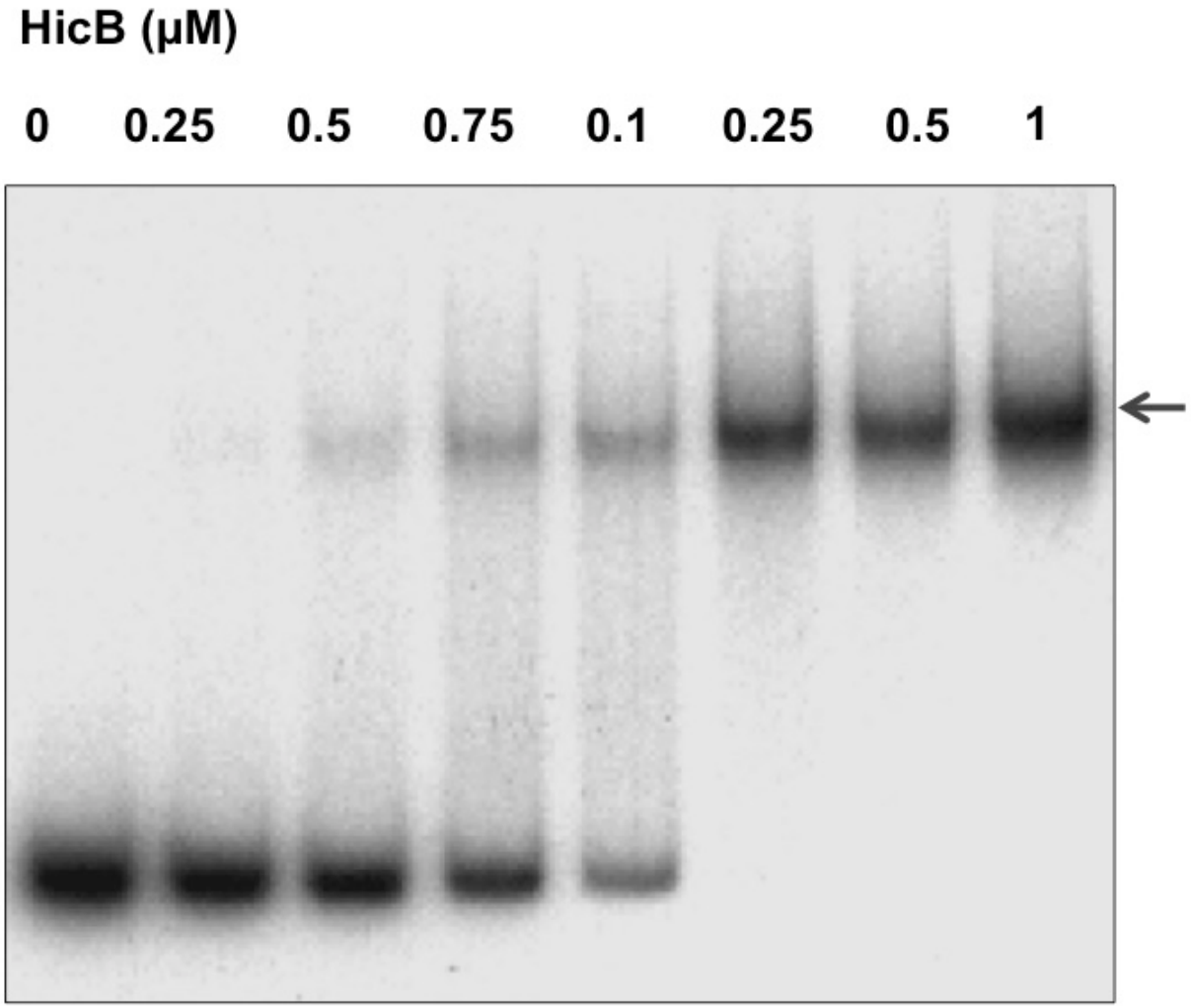

Figure 3

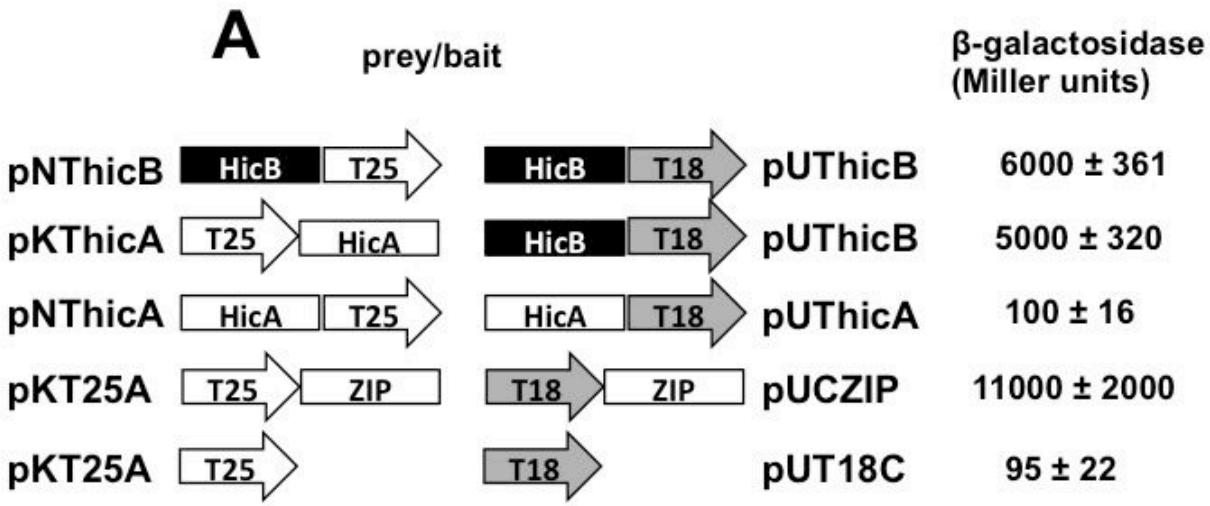
A
prey/bait
β-galactosidase
(Miller units)
pNThicB
HicB
T25
HicB
T18
pUThicB
6000 ± 361
pKThicA
T25
HicA
HicB
T18
pUThicB
5000 ± 320
pNThicA
HicA
T25
HicA
T18
pUThicA
100 ± 16
pKT25A
T25
ZIP
T18
ZIP
pUCZIP
11000 ± 2000
pKT25A
T25
T18
pUT18C
95 ± 22

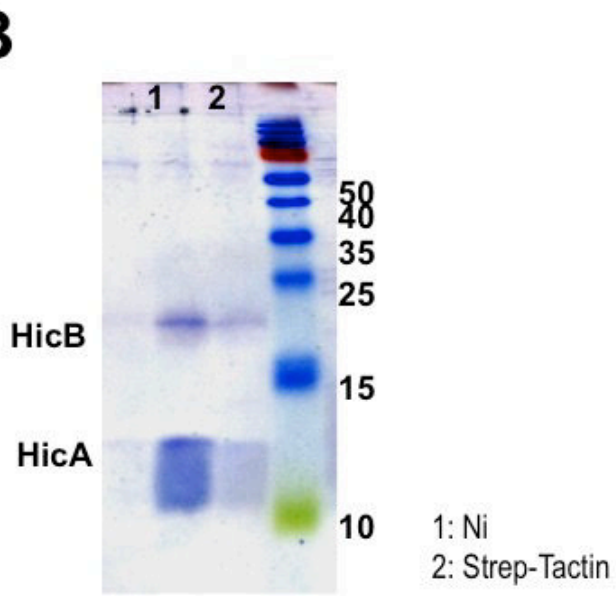
B
1
2
50
40
35
25
15
10
HicB
HicA
1: Ni
2: Strep-Tactin

Figure 4

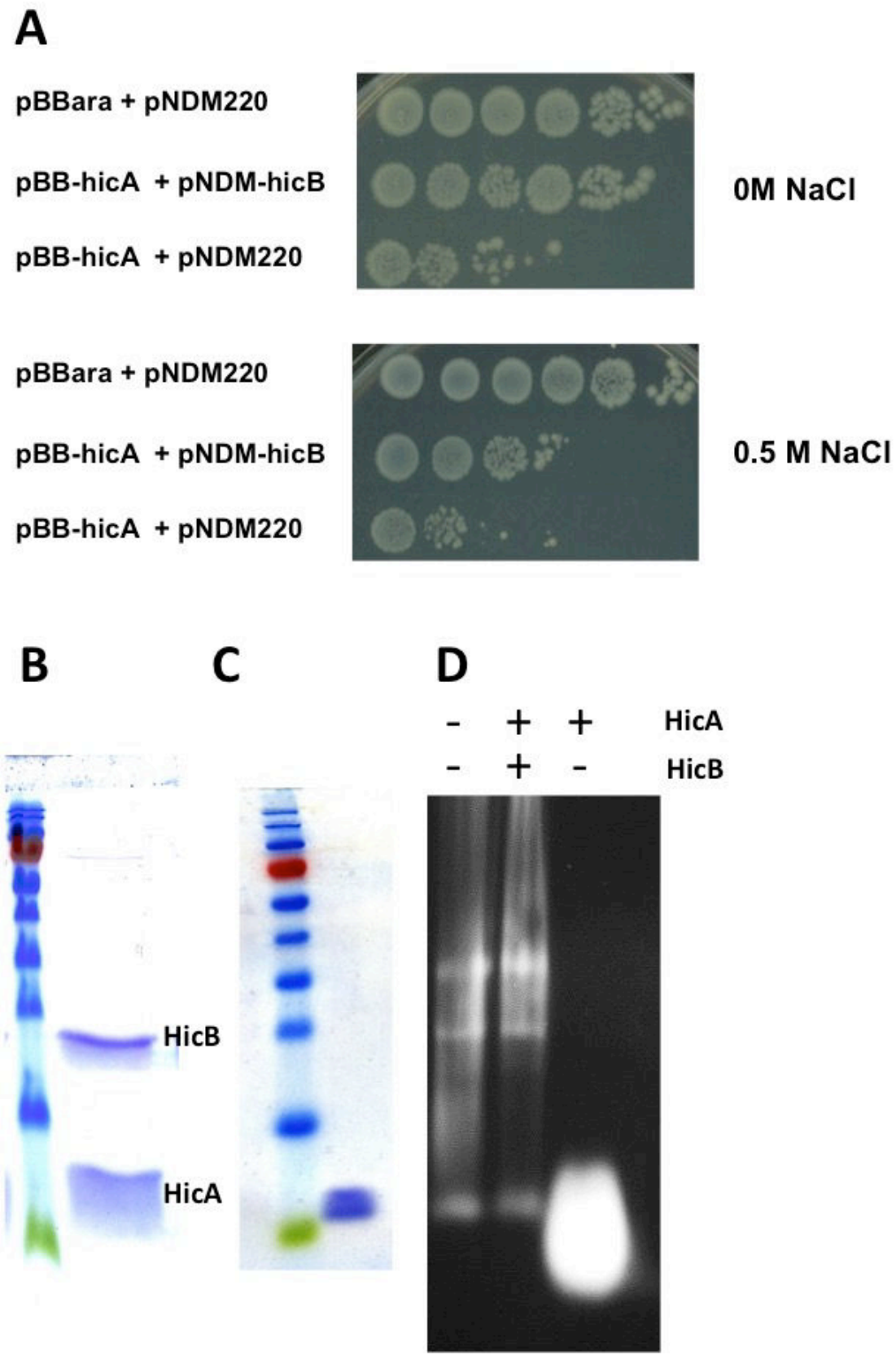
A
pBBara + pNDM220
pBB-hicA + pNDM-hicB
pBB-hicA + pNDM220
0M NaCl
pBBara + pNDM220
pBB-hicA + pNDM-hicB
pBB-hicA + pNDM220
0.5 M NaCl
B
C
D
HicB
HicA
- + + HicA
- + - HicB

Figure 5

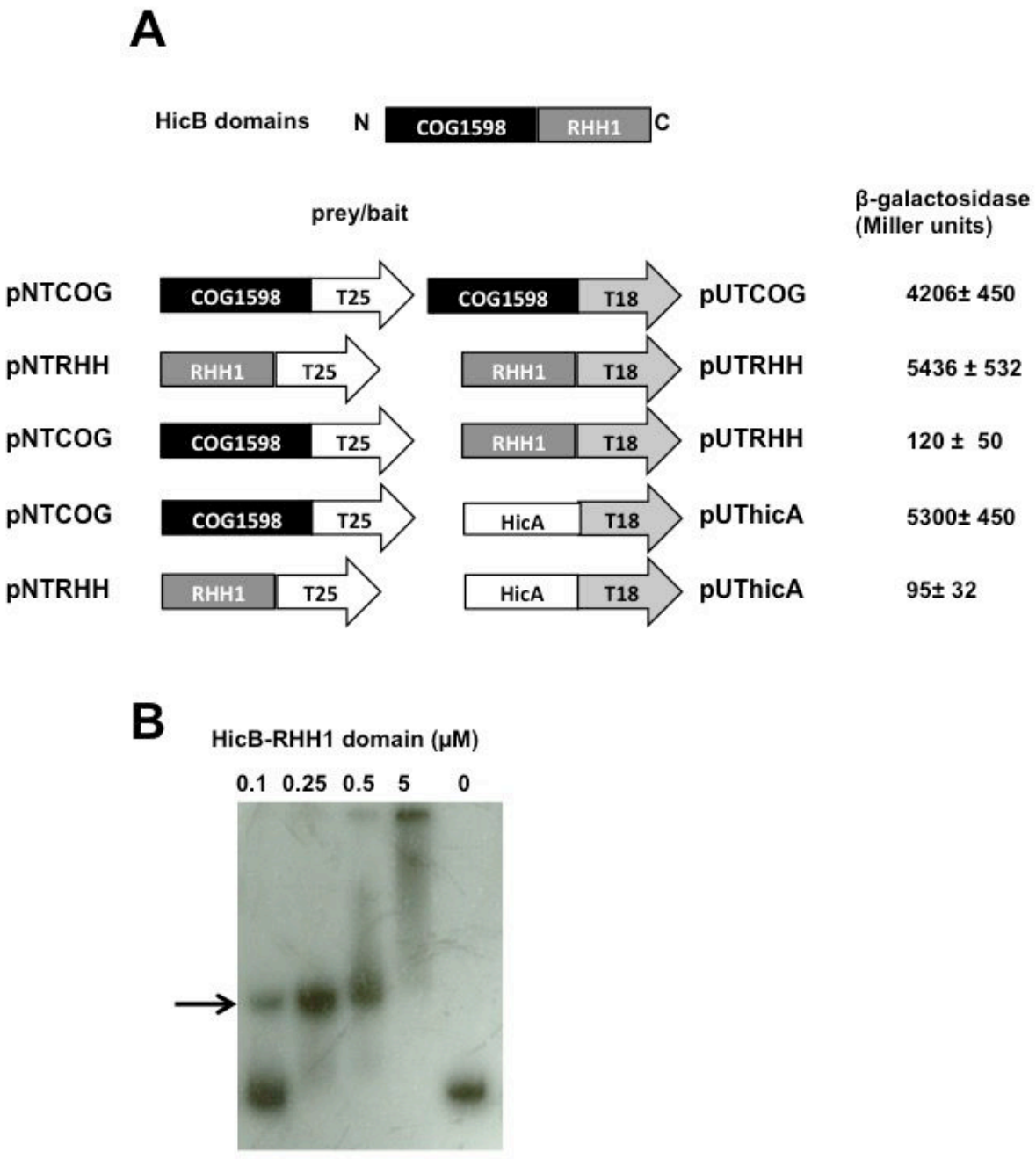
A
HicB domains
N
COG1598
RHH1
C
prey/bait
β-galactosidase
(Miller units)
pNTCOG
COG1598
T25
COG1598
T18
pUTCOG
4206± 450
pNTRHH
RHH1
T25
RHH1
T18
pUTRHH
5436 ± 532
pNTCOG
COG1598
T25
RHH1
T18
pUTRHH
120 ± 50
pNTCOG
COG1598
T25
HicA
T18
pUThicA
5300± 450
pNTRHH
RHH1
T25
HicA
T18
pUThicA
95± 32
B
HicB-RHH1 domain (μM)
0.1 0.25 0.5 5 0

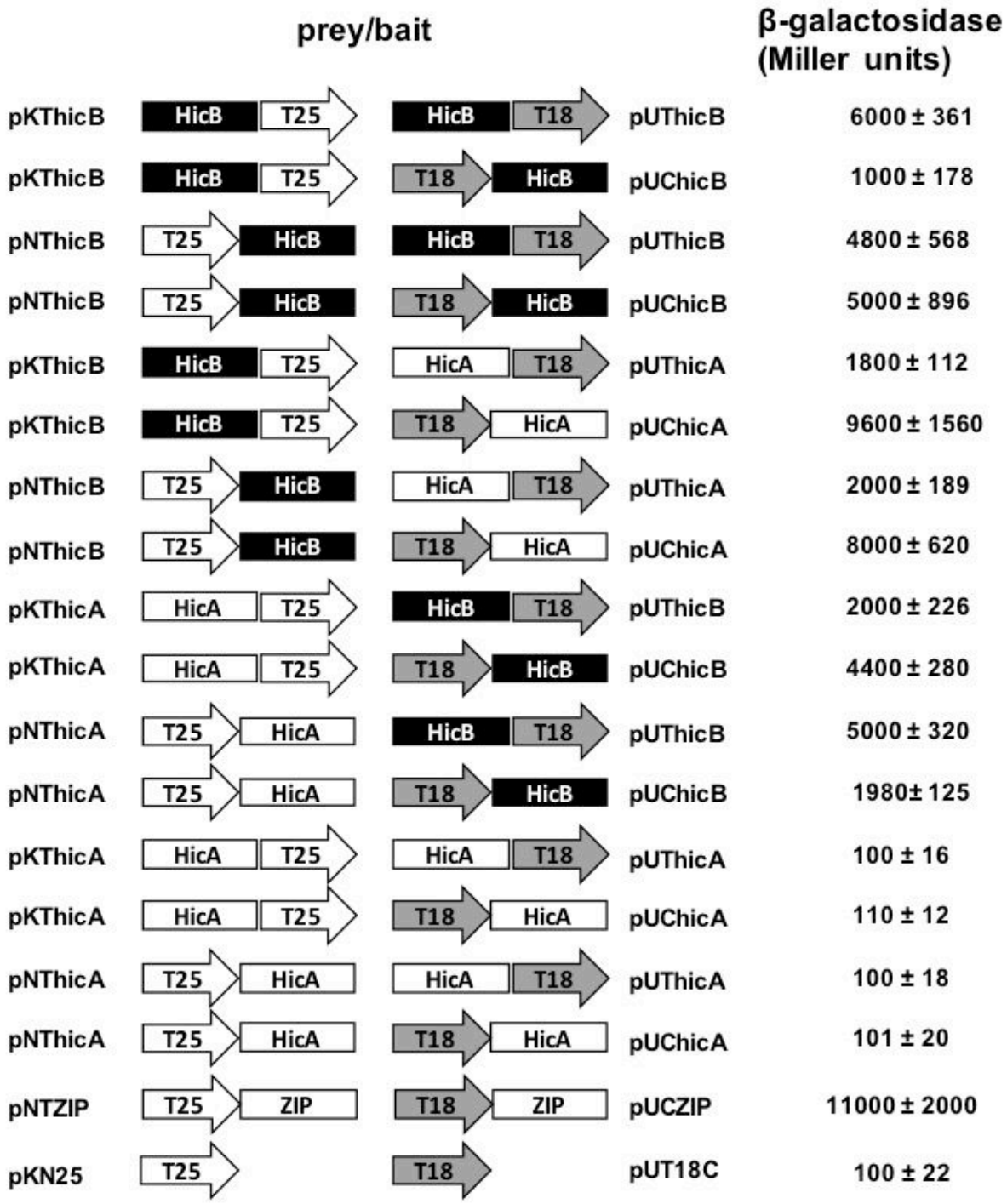
prey/bait
β-galactosidase (Miller units)
pKThicB HicB T25 HicB T18 pUThicB 6000 ± 361
pKThicB HicB T25 T18 HicB pUChicB 1000 ± 178
pNThicB T25 HicB HicB T18 pUThicB 4800 ± 568
pNThicB T25 HicB T18 HicB pUChicB 5000 ± 896
pKThicB HicB T25 HicA T18 pUThicA 1800 ± 112
pKThicB HicB T25 T18 HicA pUChicA 9600 ± 1560
pNThicB T25 HicB HicA T18 pUThicA 2000 ± 189
pNThicB T25 HicB T18 HicA pUChicA 8000 ± 620
pKThicA HicA T25 HicB T18 pUThicB 2000 ± 226
pKThicA HicA T25 T18 HicB pUChicB 4400 ± 280
pNThicA T25 HicA HicB T18 pUThicB 5000 ± 320
pNThicA T25 HicA T18 HicB pUChicB 1980± 125
pKThicA HicA T25 HicA T18 pUThicA 100 ± 16
pKThicA HicA T25 T18 HicA pUChicA 110 ± 12
pNThicA T25 HicA HicA T18 pUThicA 100 ± 18
pNThicA T25 HicA T18 HicA pUChicA 101 ± 20
pNTZIP T25 ZIP T18 ZIP pUCZIP 11000 ± 2000
pKN25 T25 T18 pUT18C 100 ± 22

Fig. S1

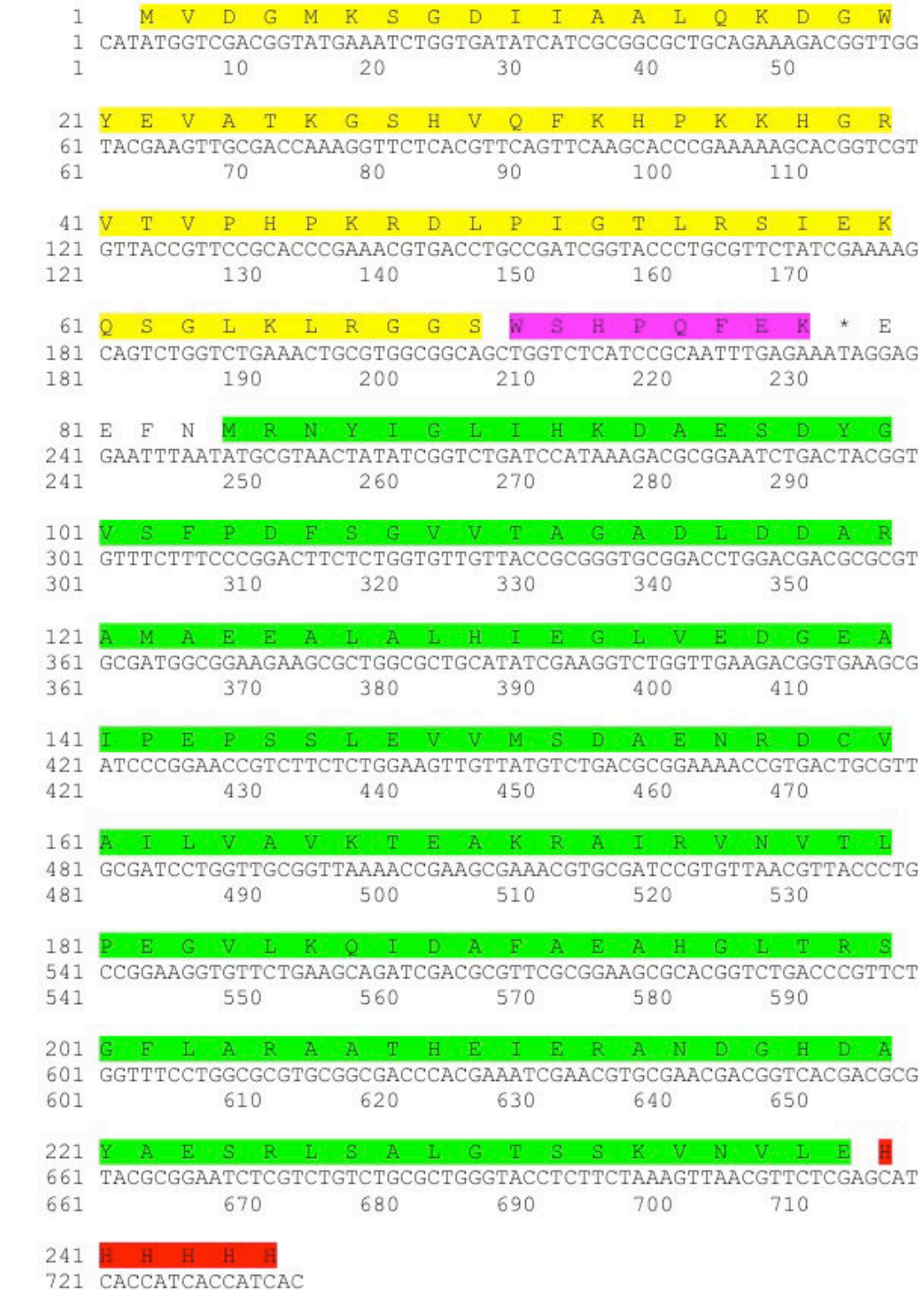
1 M V D G M K S G D I I A A L Q K D G W
1 CATATGGTCGACGGTATGAAATCTGGTGATATCATCGCGGCGCTGCAGAAAGACGGTTGG
1 10 20 30 40 50
21 Y E V A T K G S H V Q F K H P K K H G R
61 TACGAAGTTGCGACCAAAGGTTCTCACGTTCAGTTCAAGCACCCGAAAAAGCACGGTCGT
61 70 80 90 100 110
41 V T V P H P K R D L P I G T L R S I E K
121 GTTACCGTTCCGCACCCGAAACGTGACCTGCCGATCGGTACCCTGCGTTCTATCGAAAAG
121 130 140 150 160 170
61 Q S G L K L R G G S W S H P Q F E K * E
181 CAGTCTGGTCTGAAACTGCGTGGCGGCAGCTGGTCTCATCCGCAATTTGAGAAATAGGAG
181 190 200 210 220 230
81 E F N M R N Y I G L I H K D A E S D Y G
241 GAATTTAATATGCGTAACTATATCGGTCTGATCCATAAAGACGCGGAATCTGACTACGGT
241 250 260 270 280 290
101 V S F P D F S G V V T A G A D L D D A R
301 GTTTCTTTCCCGGACTTCTCTGGTGTTGTTACCGCGGGTGCGGACCTGGACGACGCGCGT
301 310 320 330 340 350
121 A M A E E A L A L H I E G L V E D G E A
361 GCGATGGCGGAAGAAGCGCTGGCGCTGCATATCGAAGGTCTGGTTGAAGACGGTGAAGCG
361 370 380 390 400 410
141 I P E P S S L E V V M S D A E N R D C V
421 ATCCCGGAACCGTCTTCTCTGGAAGTTGTTATGTCTGACGCGGAAAACCGTGACTGCGTT
421 430 440 450 460 470
161 A I L V A V K T E A K R A I R V N V T L
481 GCGATCCTGGTTGCGGTTAAAACCGAAGCGAAACGTGCGATCCGTGTTAACGTTACCCTG
481 490 500 510 520 530
181 P E G V L K Q I D A F A E A H G L T R S
541 CCGGAAGGTGTTCTGAAGCAGATCGACGCGTTCGCGGAAGCGCACGGTCTGACCCGTTCT
541 550 560 570 580 590
201 G F L A R A A T H E I E R A N D G H D A
601 GGTTTCCTGGCGCGTGCGGCGACCCACGAAATCGAACGTGCGAACGACGGTCACGACGCG
601 610 620 630 640 650
221 Y A E S R L S A L G T S S K V N V L E H
661 TACGCGGAATCTCGTCTGTCTGCGCTGGGTACCTCTTCTAAAGTTAACGTTCTCGAGCAT
661 670 680 690 700 710
241 H H H H H
721 CACCATCACCATCAC

Fig. S2

HicA

```
E. coli        ----------MKQSE------FRRWLESQGVDVANGSNHLKLRFHGRRS-VMPRHPCDEIKEPLRKAILKQLGLS--  58
S.pneumoniae   MVLSGGKSAIPMTQKEMVKLLTAHGWIKTRG---GKG-SHIKMEKQGERPITILH---GELNKYTERGIGKQAGL---  68
S. meliloti    ----------MKSGDIIAALQKDGWYEV----ATKG-SHVQFKHPKKHGRVTVPHPKRDLPIGTLRSIEKQSGLKLR  62
Y. pestis       ----------MESGELIKRLEDAGWQIRGGRKTNSG-SHVTLCKPGVRKIITLPYPRKDISKGLLRQAQKIAGIKLS 66
                          * . :         *         .* .*: :     :          ::     :   *  *:
```

HicB

```
S. pneumoniae    -----MLVTYPALFYYDDTDGTEATYFVHFPDFEYSATQGEGISEALAMGSEWLGITVAD    55
S. meliloti      -------MRNYIGLIH---KDAESDYGVSFPDFSGVVTAGADLDDARAMAEEALALHIEG    50
Y. pestis        ------MFSYPASYTV---DEASGEYHIHYRDFPELNSVTYSLEDVELEAQEGIKNGVAA    51
E. coli          MRETVEIMRYPVTLTP----APEGGYMVSFVDIPEALTQGETVAEAMEAAKDALLTAFDF    56
                        .              .. * : : *:    :    : :.   ..: :   .

S. pneumoniae    LIESDGELPQPSDINSLSLIDNDPFKDDEDFVSTYDLDKSFISMVSVDVSEYLGSQEPIK    115
S. meliloti      LVEDGEAIPEPSSLEVVMSDAENRDCVAILVAVKTEAKRAIRV--NVTL------PEGVL    102
Y. pestis        EMEERRLIPAPSALQPGDIA----VHVPILVRLKAELHNAMLA--SDTR------KADMA    99
E. coli          YFEDNELIPLPSPLNSHDHF----IEVPLSVASKVLLLNAFLQ--SEIT------QQELA    104
                  .*.   :* ** ::               .  .    .::    .           :

S. pneumoniae    KTLTIPKWADKLGREMGLNFSQTL--------------TDAIADKKVQA-----------    150
S. meliloti      K--QIDAFA----EAHGLTRSGFLARAATHEIERANDGHDAYAESRLSALGTSSKNV---    153
PCN63376.1       R--KL-----------SL---------NAAQMDRL---LDVYYASKVEALEQALYLLGFE    134
E. coli          R--RI-----------GK---------PKQEITRL---FNLHHATKIDAVQLAAKALGKE    139
                 :   :           .                      :    .::.*

S. pneumoniae    ---------  150
S. meliloti      ---------  153
Y. pestis        ADVTVRKIV  143
E. coli          LSLVMV---  145
```

Fig. S3

Additional file 4

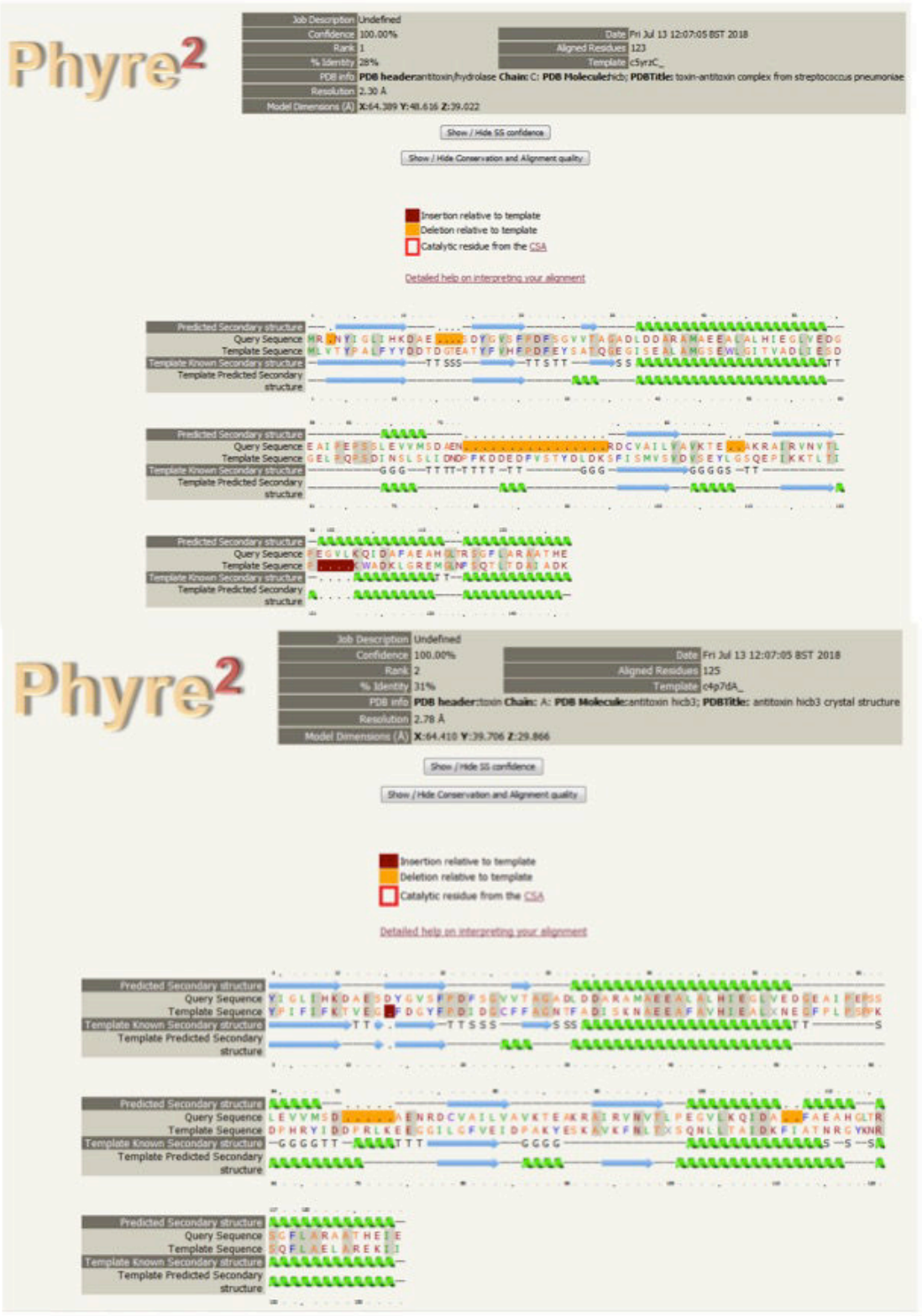

Fig. S4

Additional file 5

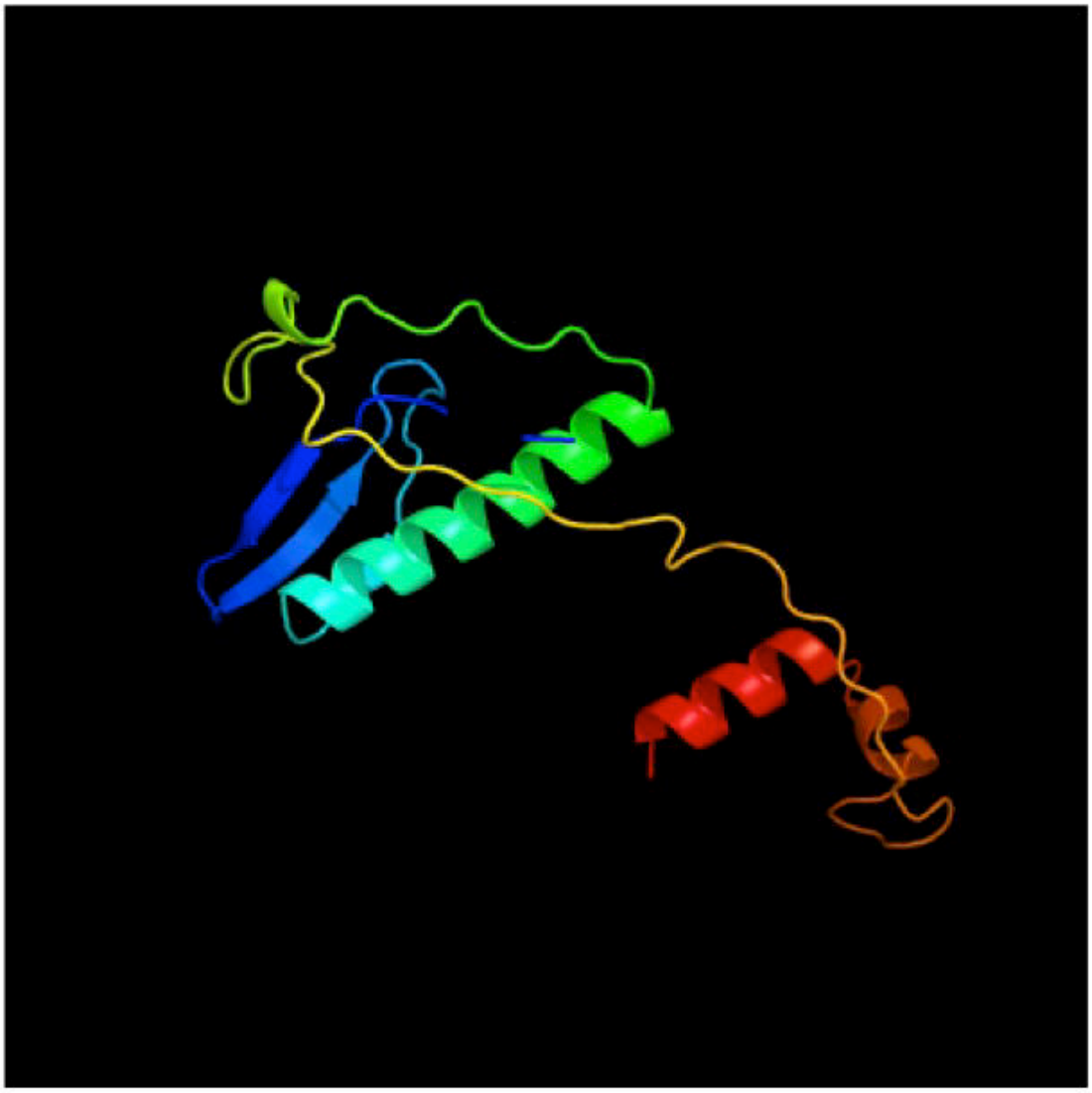

Fig. S5

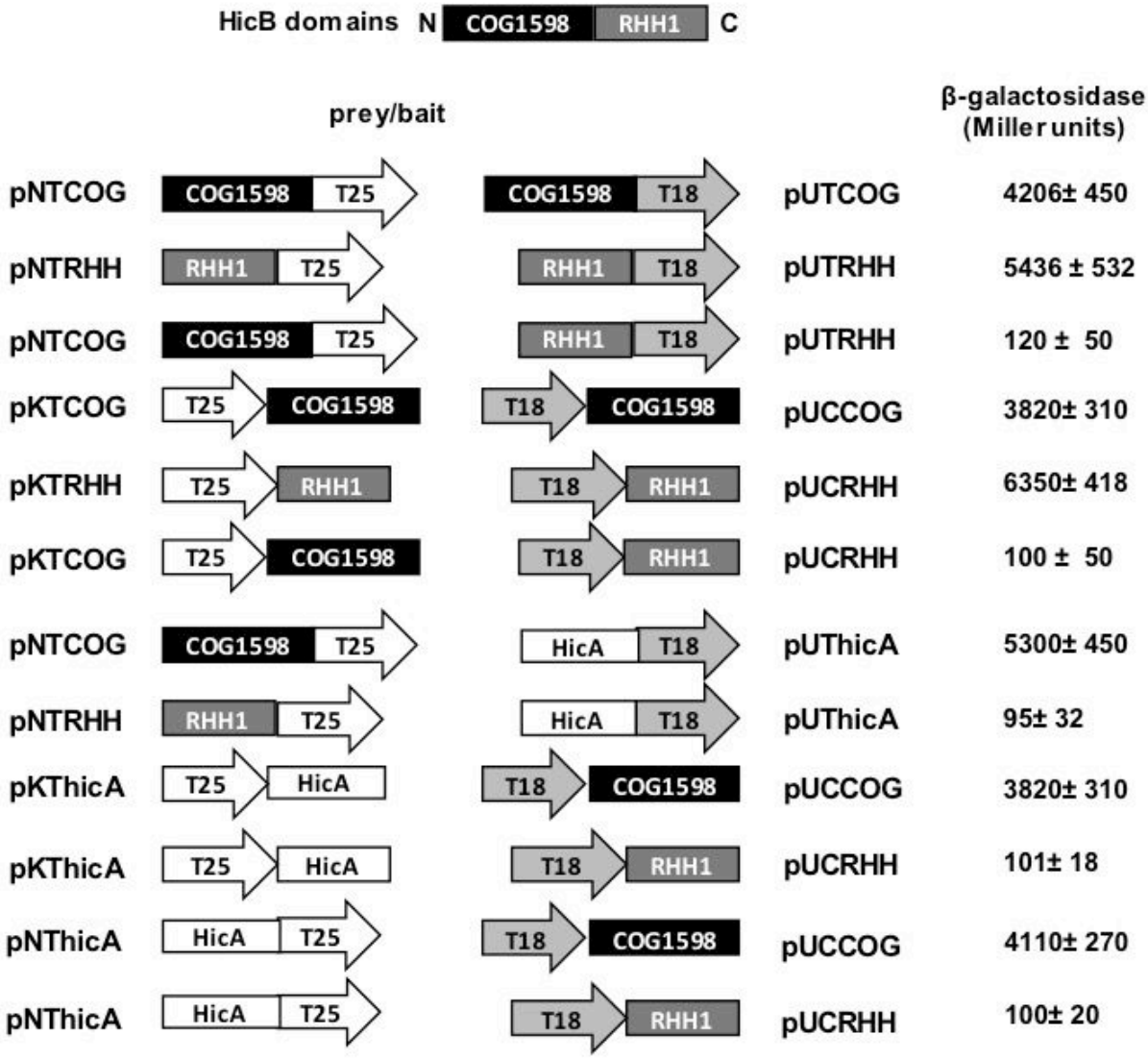
HicB domains N COG1598 RHH1 C
prey/bait
β-galactosidase (Miller units)
pNTCOG COG1598 T25 COG1598 T18 pUTCOG 4206± 450
pNTRHH RHH1 T25 RHH1 T18 pUTRHH 5436 ± 532
pNTCOG COG1598 T25 RHH1 T18 pUTRHH 120 ± 50
pKTCOG T25 COG1598 T18 COG1598 pUCCOG 3820± 310
pKTRHH T25 RHH1 T18 RHH1 pUCRHH 6350± 418
pKTCOG T25 COG1598 T18 RHH1 pUCRHH 100 ± 50
pNTCOG COG1598 T25 HicA T18 pUThicA 5300± 450
pNTRHH RHH1 T25 HicA T18 pUThicA 95± 32
pKThicA T25 HicA T18 COG1598 pUCCOG 3820± 310
pKThicA T25 HicA T18 RHH1 pUCRHH 101± 18
pNThicA HicA T25 T18 COG1598 pUCCOG 4110± 270
pNThicA HicA T25 T18 RHH1 pUCRHH 100± 20

Fig. S6

V. Conclusion and perspectives

To cope with environmental conditions, and particularly with stresses, bacteria have evolved many ways to adapt their physiology. Hence, stressful conditions influence transcription and translation to redirect bacterial metabolism quickly, for survival, and also for long-term adaptation.

Translation is regulated in different ways, and, what is described the most, are mechanisms impeding translation (regulatory RNAs, riboswitches, attenuation…). We aimed to consider the ribosome itself as a regulation factor. Indeed, the ribosome is not an invariable entity and may vary in terms of rRNAs (from different operons), associated ribosomal proteins, post-translational modifications of ribosomal proteins, rRNAs modifications, stress ribosomes produced by MazF. Those variations lead to the production of heterogeneous ribosomes within the cell, and as a consequence of the existence of different ribosomal subpopulations.

This work brings new insights since methylations affect ribosome efficiency and fidelity. Hence, it opens perspectives and new questions that must be solved in the future.

Lack of methylation impacts translation

We highlighted the impact of undermodified ribosomes, lacking methylations in the decoding centre, on translation during stress response. The main goals of this work were (i) to understand if those methylations could be involved in different translational aspects, such as translation of leaderless mRNAs (which could be generated by the stress-induced toxin MazF) or programmed and spontaneous frameshifting; and (ii) to evaluate the functional role of those methylations in physiological traits such as growth and fitness of the bacteria. To do so, our strategy was to examine these different aspects in deletion mutants of the methyltransferases RsmA, RsmB, RsmD, RsmE and RsmH catalysing base methylation in the decoding centre. Firstly, we had to develop genetic tools dedicated to evaluating canonical translation, leaderless mRNA translation and frameshifting.

Although those modifications of the decoding centre are highly conserved and implicated in key cellular processes, taken one by one, none of them are essential for growth and only one ($m^4Cm1402$) affects fitness. In addition, surprisingly, absence of

some methylations can significantly impact translation. Indeed, we showed that lack of RsmA, RsmB or RsmD increases translation under some stressful conditions. Otherwise, in controlled environments, only lack of RsmH impacted translation. Those methylations also impact accuracy of translation: some *rsm* mutants exhibited higher levels of ribosomal frameshifting. So, we could consider that the lack of some methylations is beneficial for translation while inducing more ribosomal frameshifting. However other types of errors can occur during translation such as stop codon read-through and missenses. We aimed to analyse these errors and to do so we generated genetic tools bearing a *lacZ* gene with single mutations in the coding sequence.

Do levels of methylations generate subpopulation of ribosomes?

A limitation in our study is the lack of data on quantification of each 16S rRNA methylation in the ribosomes. For instance, all studies consider that wild type ribosomes are fully and homogeneously methylated, so methylations levels are estimated relatively to wild type strain. It is important to estimate the absolute level of methylation. Our first results obtained using RT-PCR targeting the m^3U1498 added by RsmE in wild type strain MG1655 highlighted that about 20 % of the ribosome are unmethylated in exponential phase (data not shown). Unfortunately this method could not be applied to the other methylations. Other methods must be undertaken, like single cell *in situ* hybridization (Ranasinghe *et al.*, 2018). This method could be used with low amounts of bacteria in opposition to biochemical methods that need a high amount of cells and are not compatible with kinetic studies of various mutants under different growth conditions.

Other ribosome associated factors have to be considered in under methylated ribosomes.

Various proteins can affect ribosome activity under stress (RMF, Hpf, RaiA…) it is not known how they influence unmethylated ribosomes. This point must be studied in the future with purified ribosomes from *rsm* mutants. Other factors could affect ribosome biogenesis under stress, so the newly formed ribosomes begin to work after a lag time after stress. *In vivo* these ribosomes are in lower amount compared to pre-existing ribosomes so their influence is difficult to extract from a high

background of pre-existing ribosomes. In our *in vitro* study we used the total fraction of ribosomes, thus containing mainly ribosomes produced before stress. We plan to isolate ribosomes neo-synthesized after stress from the bulk and to analyse *in vitro* if they have a different behaviour compared to ribosomes produced before stress. The genetic tools have been constructed and tested: they use a plasmid bearing *rpsT* gene with a tag, able to repress the synthesis of chromosomal untagged *rpsT* gene. Its induction simultaneously to stresses allows isolation of neo-synthesized ribosomes which could be used for *in vitro* study.

Does the absence of methyltransferases impact maturation of the ribosome?

Some methylations of the 16S rRNA are added during its maturation, so it is important to determine if lacking methyltransferases could result in accumulation of 30S precursors. To do so, it would be possible to use MG1655 derivative strain 6006 and isogenic *rsm* mutants to purify heat-accumulated 21S particles produced during the lag phase of growth recovery after a heat stress. Accumulation of 21S particles is related to the mobilization of DnaK for folding heat induced mis-folded proteins (René and Alix, 2010). The strain 6006 leads to the production of two tagged ribosomal proteins that are assembled in the 16S rRNA in early steps during maturation for one and late steps for the second one. This system allows a differential purification of premature particles. The ribosome profiles from 6006 strain and isogenic *rsm* mutants would have to be examined to know if pre-particles accumulate or not. Then it would be possible to purify such premature particles and analyse them in terms of associated ribosomal proteins and 16S maturation.

Lack of methylation and *trans*-translation

Using a heterologous TA system, such as *S. meliloti* HicAB in *E. coli*, we could induce controlled mRNA cleavage under mild conditions more compatible with physiological studies. This cleavage induces stalling of the ribosomes on cleaved mRNAs and ribosomes must be rescued by *trans*-translation or by ArfA/ArfB. We plan to use *S. meliloti* HicAB to study the response of *rsm* mutants to mRNA cleavage. Moreover, their *trans*-translation activity also has to be evaluated. To do so, we already generated genetic tools with a modified tmRNA. Its messenger region,

coding for a proteolytic tag, was replaced by a hexamer of histidines to allow purification of *trans*-translated proteins.

The last (but not least) perspective of this work is the use of all the constructed genetic tools allowing the evaluation of leaderless mRNAs translation, frameshifting and *trans*-translation in other studies connected with the modulation or inhibition of translation, *e.g.* antimicrobial agents targeting translation and *trans*-translation.

VI. References

Aakre, C.D., Phung, T.N., Huang, D., and Laub, M.T. (2013). A bacterial toxin inhibits DNA replication elongation through a direct interaction with the β sliding clamp. Mol. Cell *52*, 617–628.

Adamski, F.M., Donly, B.C., and Tate, W.P. (1993). Competition between frameshifting, termination and suppression at the frameshift site in the Escherichia coli release factor-2 mRNA. Nucleic Acids Res. *21*, 5074–5078.

Aizenman, E., Engelberg-Kulka, H., and Glaser, G. (1996). An Escherichia coli chromosomal "addiction module" regulated by guanosine [corrected] 3',5'-bispyrophosphate: a model for programmed bacterial cell death. Proc. Natl. Acad. Sci. U. S. A. *93*, 6059–6063.

Al Refaii, A., and Alix, J.-H. (2009). Ribosome biogenesis is temperature-dependent and delayed in Escherichia coli lacking the chaperones DnaK or DnaJ. Mol. Microbiol. *71*, 748–762.

Amitai, S., Kolodkin-Gal, I., Hananya-Meltabashi, M., Sacher, A., and Engelberg-Kulka, H. (2009). Escherichia coli MazF leads to the simultaneous selective synthesis of both "death proteins" and "survival proteins." PLoS Genet. *5*, e1000390.

Arora, S., Bhamidimarri, S.P., Bhattacharyya, M., Govindan, A., Weber, M.H.W., Vishveshwara, S., and Varshney, U. (2013a). Distinctive contributions of the ribosomal P-site elements m 2 G966, m 5 C967 and the C-terminal tail of the S9 protein in the fidelity of initiation of translation in Escherichia coli. Nucleic Acids Res. *41*, 4963–4975.

Arora, S., Bhamidimarri, S.P., Weber, M.H.W., and Varshney, U. (2013b). Role of the Ribosomal P-Site Elements of m2G966, m5C967, and the S9 C-Terminal Tail in Maintenance of the Reading Frame during Translational Elongation in Escherichia coli. J. Bacteriol. *195*, 3524–3530.

Aspedon, A., Palmer, K., and Whiteley, M. (2006). Microarray Analysis of the Osmotic Stress Response in Pseudomonas aeruginosa. J. Bacteriol. *188*, 2721–2725.

Baba, T., Ara, T., Hasegawa, M., Takai, Y., Okumura, Y., Baba, M., Datsenko, K.A., Tomita, M., Wanner, B.L., and Mori, H. (2006). Construction of Escherichia coli K-12 in-frame, single-gene knockout mutants: the Keio collection. Mol. Syst. Biol. *2*, 2006.0008.

Balakin, A.G., Skripkin, E.A., Shatsky, I.N., Bogdanov, A.A., and Belozersky, A.N. (1992). Unusual ribosome binding properties of mRNA encoding bacteriophage λ repressor. Nucleic Acids Res. *20*, 563–571.

Bartholomäus, A., Fedyunin, I., Feist, P., Sin, C., Zhang, G., Valleriani, A., and Ignatova, Z. (2016). Bacteria differently regulate mRNA abundance to specifically respond to various stresses. Philos. Transact. A Math. Phys. Eng. Sci. *374*.

Basturea, G.N., and Deutscher, M.P. (2007). Substrate specificity and properties of the Escherichia coli 16S rRNA methyltransferase, RsmE. RNA *13*, 1969–1976.

Basturea, G.N., Rudd, K.E., and Deutscher, M.P. (2006). Identification and characterization of RsmE, the founding member of a new RNA base methyltransferase family. RNA *12*, 426–434.

Blattner, F.R., Plunkett, G., Bloch, C.A., Perna, N.T., Burland, V., Riley, M., Collado-Vides, J., Glasner, J.D., Rode, C.K., Mayhew, G.F., *et al.* (1997). The Complete Genome Sequence of Escherichia coli K-12. Science *277*, 1453–1462.

Blinkowa, A.L., and Walker, J.R. (1990). Programmed ribosomal frameshifting generates the Escherichia coli DNA polymerase III gamma subunit from within the tau subunit reading frame. Nucleic Acids Res. *18*, 1725–1729.

Boehringer, D., O'Farrell, H.C., Rife, J.P., and Ban, N. (2012). Structural Insights into Methyltransferase KsgA Function in 30S Ribosomal Subunit Biogenesis. J. Biol. Chem. *287*, 10453–10459.

Bojanovič, K., D'Arrigo, I., and Long, K.S. (2017). Global Transcriptional Responses to Osmotic, Oxidative, and Imipenem Stress Conditions in Pseudomonas putida. Appl. Environ. Microbiol. *83*.

Brigotti, M., Petronini, P.G., Carnicelli, D., Alfieri, R.R., Bonelli, M.A., Borghetti, A.F., and Wheeler, K.P. (2003). Effects of osmolarity, ions and compatible osmolytes on cell-free protein synthesis. Biochem. J. *369*, 369–374.

Brock, J.E., Pourshahian, S., Giliberti, J., Limbach, P.A., and Janssen, G.R. (2008). Ribosomes bind leaderless mRNA in Escherichia coli through recognition of their 5'-terminal AUG. RNA N. Y. N *14*, 2159–2169.

Bullwinkle, T.J., Reynolds, N.M., Raina, M., Moghal, A., Matsa, E., Rajkovic, A., Kayadibi, H., Fazlollahi, F., Ryan, C., Howitz, N., *et al.* (2014). Oxidation of cellular amino acid pools leads to cytotoxic mistranslation of the genetic code. ELife *3*, e02501.

Bunner, A.E., Nord, S., Wikström, P.M., and Williamson, J.R. (2010). The effect of ribosome assembly cofactors on *in vitro* 30S subunit reconstitution. J. Mol. Biol. *398*, 1–7.

Burakovsky, D.E., Prokhorova, I.V., Sergiev, P.V., Milón, P., Sergeeva, O.V., Bogdanov, A.A., Rodnina, M.V., and Dontsova, O.A. (2012). Impact of methylations of m2G966/m5C967 in 16S rRNA on bacterial fitness and translation initiation. Nucleic Acids Res. *40*, 7885–7895.

Buts, L., Lah, J., Dao-Thi, M.-H., Wyns, L., and Loris, R. (2005). Toxin-antitoxin modules as bacterial metabolic stress managers. Trends Biochem. Sci. *30*, 672–679.

van Buul, C.P., Visser, W., and van Knippenberg, P.H. (1984). Increased translational fidelity caused by the antibiotic kasugamycin and ribosomal ambiguity in mutants harbouring the ksgA gene. FEBS Lett. *177*, 119–124.

Byrgazov, K., Vesper, O., and Moll, I. (2013). Ribosome heterogeneity: another level of complexity in bacterial translation regulation. Curr. Opin. Microbiol. *16*, 133–139.

Caban, K., Pavlov, M., Ehrenberg, M., and Gonzalez, R.L. (2017). A conformational switch in initiation factor 2 controls the fidelity of translation initiation in bacteria. Nat. Commun. *8*, 1475.

Caliskan, N., Peske, F., and Rodnina, M.V. (2015). Changed in translation: mRNA recoding by -1 programmed ribosomal frameshifting. Trends Biochem. Sci. *40*, 265–274.

Chen, J., Petrov, A., Johansson, M., Tsai, A., O'Leary, S.E., and Puglisi, J.D. (2014). Dynamic pathways of −1 translational frameshifting. Nature *512*, 328–332.

Chen, Y.-T., Chang, K.-C., Hu, H.-T., Chen, Y.-L., Lin, Y.-H., Hsu, C.-F., Chang, C.-F., Chang, K.-Y., and Wen, J.-D. (2017). Coordination among tertiary base pairs results in an efficient frameshift-stimulating RNA pseudoknot. Nucleic Acids Res. *45*, 6011–6022.

Cherepanov, P.P., and Wackernagel, W. (1995). Gene disruption in Escherichia coli: TcR and KmR cassettes with the option of Flp-catalyzed excision of the antibiotic-resistance determinant. Gene *158*, 9–14.

Choudhury, P., and Flower, A.M. (2015). Efficient Assembly of Ribosomes Is Inhibited by Deletion of bipA in Escherichia coli. J. Bacteriol. *197*, 1819–1827.

Connolly, K., Rife, J.P., and Culver, G. (2008). Mechanistic insight into the ribosome biogenesis functions of the ancient protein KsgA. Mol. Microbiol. *70*, 1062–1075.

Culviner, P.H., and Laub, M.T. (2018). Global Analysis of the E. coli Toxin MazF Reveals Widespread Cleavage of mRNA and the Inhibition of rRNA Maturation and Ribosome Biogenesis. Mol. Cell *70*, 868-880.e10.

Dai, X., Zhu, M., Warren, M., Balakrishnan, R., Okano, H., Williamson, J.R., Fredrick, K., and Hwa, T. (2018). Slowdown of Translational Elongation in Escherichia coli under Hyperosmotic Stress. MBio *9*, e02375-17.

Darfeuille, F., Unoson, C., Vogel, J., and Wagner, E.G.H. (2007). An antisense RNA inhibits translation by competing with standby ribosomes. Mol. Cell *26*, 381–392.

Das, G., Thotala, D.K., Kapoor, S., Karunanithi, S., Thakur, S.S., Singh, N.S., and Varshney, U. (2008). Role of 16S ribosomal RNA methylations in translation initiation in Escherichia coli. EMBO J. *27*, 840–851.

Datsenko, K.A., and Wanner, B.L. (2000). One-step inactivation of chromosomal genes in Escherichia coli K-12 using PCR products. Proc. Natl. Acad. Sci. U. S. A. *97*, 6640–6645.

Davis, J.H., and Williamson, J.R. (2017). Structure and dynamics of bacterial ribosome biogenesis. Phil Trans R Soc B *372*, 20160181.

Decatur, W.A., and Fournier, M.J. (2002). rRNA modifications and ribosome function. Trends Biochem. Sci. *27*, 344–351.

deLivron, M.A., and Robinson, V.L. (2008). Salmonella enterica Serovar Typhimurium BipA Exhibits Two Distinct Ribosome Binding Modes. J. Bacteriol. *190*, 5944–5952.

Demeshkina, N., Jenner, L., Westhof, E., Yusupov, M., and Yusupova, G. (2012). A new understanding of the decoding principle on the ribosome. Nature *484*, 256–259.

Demirci, H., Murphy, F., Belardinelli, R., Kelley, A.C., Ramakrishnan, V., Gregory, S.T., Dahlberg, A.E., and Jogl, G. (2010). Modification of 16S ribosomal RNA by the KsgA methyltransferase restructures the 30S subunit to optimize ribosome function. RNA *16*, 2319–2324.

Desai, P.M., and Rife, J.P. (2006). The adenosine dimethyltransferase KsgA recognizes a specific conformational state of the 30S ribosomal subunit. Arch. Biochem. Biophys. *449*, 57–63.

Deutscher, M.P. (2009). Chapter 9 Maturation and Degradation of Ribosomal RNA in Bacteria. In Progress in Molecular Biology and Translational Science, (Academic Press), pp. 369–391.

Dinman, J.D. (2012). Mechanisms and implications of programmed translational frameshifting. Wiley Interdiscip. Rev. RNA *3*, 661–673.

Donly, B.C., Edgar, C.D., Adamski, F.M., and Tate, W.P. (1990). Frameshift autoregulation in the gene for Escherichia coli release factor 2: partly functional mutants result in frameshift enhancement. Nucleic Acids Res. *18*, 6517–6522.

Dukan, S., and Nyström, T. (1999). Oxidative stress defense and deterioration of growth-arrested Escherichia coli cells. J. Biol. Chem. *274*, 26027–26032.

Dunkle, J.A., and Dunham, C.M. (2015). Mechanisms of mRNA frame maintenance and its subversion during translation of the genetic code. Biochimie *114*, 90–96.

El Hage, A., and Alix, J.-H. (2004). Authentic precursors to ribosomal subunits accumulate in Escherichia coli in the absence of functional DnaK chaperone. Mol. Microbiol. *51*, 189–201.

Ernst, F.G.M., Erber, L., Sammler, J., Jühling, F., Betat, H., and Mörl, M. (2018). Cold adaptation of tRNA nucleotidyltransferases: A tradeoff in activity, stability and fidelity. RNA Biol. *15*, 144–155.

Evans, C.R., Fan, Y., Weiss, K., and Ling, J. (2018). Errors during Gene Expression: Single-Cell Heterogeneity, Stress Resistance, and Microbe-Host Interactions. MBio *9*.

Fan, Y., Wu, J., Ung, M.H., De Lay, N., Cheng, C., and Ling, J. (2015). Protein mistranslation protects bacteria against oxidative stress. Nucleic Acids Res. *43*, 1740–1748.

Farabaugh, P.J. (1996). Programmed translational frameshifting. Annu. Rev. Genet. *30*, 507–528.

Fischer, N., Neumann, P., Konevega, A.L., Bock, L.V., Ficner, R., Rodnina, M.V., and Stark, H. (2015). Structure of the *E. coli* ribosome–EF-Tu complex at <3 Å resolution by C_s-corrected cryo-EM. Nature *520*, 567–570.

Flower, A.M., and McHenry, C.S. (1990). The gamma subunit of DNA polymerase III holoenzyme of Escherichia coli is produced by ribosomal frameshifting. Proc. Natl. Acad. Sci. U. S. A. *87*, 3713–3717.

Fritz, B.R., Jamil, O.K., and Jewett, M.C. (2015). Implications of macromolecular crowding and reducing conditions for *in vitro* ribosome construction. Nucleic Acids Res. *43*, 4774–4784.

Gao, H., Zhou, Z., Rawat, U., Huang, C., Bouakaz, L., Wang, C., Cheng, Z., Liu, Y., Zavialov, A., Gursky, R., *et al.* (2007). RF3 Induces Ribosomal Conformational Changes Responsible for Dissociation of Class I Release Factors. Cell *129*, 929–941.

Genuth, N.R., and Barna, M. (2018). The Discovery of Ribosome Heterogeneity and Its Implications for Gene Regulation and Organismal Life. Mol. Cell *71*, 364–374.

Giliberti, J., O'Donnell, S., Van Etten, W.J., and Janssen, G.R. (2012). A 5′-terminal phosphate is required for stable ternary complex formation and translation of leaderless mRNA in Escherichia coli. RNA *18*, 508–518.

Giudice, E., and Gillet, R. (2013). The task force that rescues stalled ribosomes in bacteria. Trends Biochem. Sci. *38*, 403–411.

Grigoriadou, C., Marzi, S., Pan, D., Gualerzi, C.O., and Cooperman, B.S. (2007). The Translational Fidelity Function of IF3 During Transition from the 30 S Initiation Complex to the 70 S Initiation Complex. J. Mol. Biol. *373*, 551–561.

Grill, S., Moll, I., Hasenöhrl, D., Gualerzi, C.O., and Bläsi, U. (2001). Modulation of ribosomal recruitment to 5′-terminal start codons by translation initiation factors IF2 and IF3. FEBS Lett. *495*, 167–171.

Gu, X.R., Gustafsson, C., Ku, J., Yu, M., and Santi, D.V. (1999). Identification of the 16S rRNA m5C967 Methyltransferase from Escherichia coli. Biochemistry *38*, 4053–4057.

Gualerzi, C.O., and Pon, C.L. (2015). Initiation of mRNA translation in bacteria: structural and dynamic aspects. Cell. Mol. Life Sci. *72*, 4341–4367.

Gualerzi, C.O., Giuliodori, A.M., Brandi, A., Di Pietro, F., Piersimoni, L., Fabbretti, A., and Pon, C.L. (2011). Translation initiation at the root of the cold-shock translational bias. In Ribosomes: Structure, Function, and Dynamics, M.V. Rodnina, W. Wintermeyer, and R. Green, eds. (Vienna: Springer Vienna), pp. 143–154.

Guimaraes, J.C., Rocha, M., and Arkin, A.P. (2014). Transcript level and sequence determinants of protein abundance and noise in Escherichia coli. Nucleic Acids Res. *42*, 4791–4799.

Gunasekera, T.S., Csonka, L.N., and Paliy, O. (2008). Genome-Wide Transcriptional Responses of Escherichia coli K-12 to Continuous Osmotic and Heat Stresses. J. Bacteriol. *190*, 3712–3720.

Guzman, L.M., Belin, D., Carson, M.J., and Beckwith, J. (1995). Tight regulation, modulation, and high-level expression by vectors containing the arabinose PBAD promoter. J. Bacteriol. *177*, 4121–4130.

Hamma, T., and Ferré-D'Amaré, A.R. (2006). Pseudouridine Synthases. Chem. Biol. *13*, 1125–1135.

Hanahan, D. (1983). Studies on transformation of Escherichia coli with plasmids. J. Mol. Biol. *166*, 557–580.

Harcum, S.W., and Bentley, W.E. (1999). Heat-shock and stringent responses have overlapping protease activity in Escherichia coli. Implications for heterologous protein yield. Appl. Biochem. Biotechnol. *80*, 23–37.

Harms, A., Brodersen, D.E., Mitarai, N., and Gerdes, K. (2018). Toxins, Targets, and Triggers: An Overview of Toxin-Antitoxin Biology. Mol. Cell *70*, 768–784.

Hase, Y., Yokoyama, S., Muto, A., and Himeno, H. (2009). Removal of a ribosome small subunit-dependent GTPase confers salt resistance on Escherichia coli cells. RNA *15*, 1766–1774.

Hase, Y., Tarusawa, T., Muto, A., and Himeno, H. (2013). Impairment of Ribosome Maturation or Function Confers Salt Resistance on Escherichia coli Cells. PLOS ONE *8*, e65747.

Hecht, A., Glasgow, J., Jaschke, P.R., Bawazer, L.A., Munson, M.S., Cochran, J.R., Endy, D., and Salit, M. (2017). Measurements of translation initiation from all 64 codons in E. coli. Nucleic Acids Res. *45*, 3615–3626.

Helm, M. (2006). Post-transcriptional nucleotide modification and alternative folding of RNA. Nucleic Acids Res. *34*, 721–733.

Helser, T.L., Davies, J.E., and Dahlberg, J.E. (1972). Mechanism of Kasugamycin Resistance in *Escherichia coli*. Nature. New Biol. *235*, 6–9.

Ito, K., Uno, M., and Nakamura, Y. (2000). A tripeptide 'anticodon' deciphers stop codons in messenger RNA. Nature *403*, 680–684.

Jewett, M.C., Fritz, B.R., Timmerman, L.E., and Church, G.M. (2013). In vitro integration of ribosomal RNA synthesis, ribosome assembly, and translation. Mol. Syst. Biol. *9*, 678.

Jiang, L., Schaffitzel, C., Bingel-Erlenmeyer, R., Ban, N., Korber, P., Koning, R.I., de Geus, D.C., Plaisier, J.R., and Abrahams, J.P. (2009). Recycling of aborted

ribosomal 50S subunit-nascent chain-tRNA complexes by the heat shock protein Hsp15. J. Mol. Biol. *386*, 1357–1367.

Jin, H., Kelley, A.C., Loakes, D., and Ramakrishnan, V. (2010). Structure of the 70S ribosome bound to release factor 2 and a substrate analog provides insights into catalysis of peptide release. Proc. Natl. Acad. Sci. U. S. A. *107*, 8593–8598.

Jones, P.G., VanBogelen, R.A., and Neidhardt, F.C. (1987). Induction of proteins in response to low temperature in Escherichia coli. J. Bacteriol. *169*, 2092–2095.

Jørgensen, M.G., Pandey, D.P., Jaskolska, M., and Gerdes, K. (2009). HicA of Escherichia coli defines a novel family of translation-independent mRNA interferases in bacteria and archaea. J. Bacteriol. *191*, 1191–1199.

Jozefczuk, S., Klie, S., Catchpole, G., Szymanski, J., Cuadros-Inostroza, A., Steinhauser, D., Selbig, J., and Willmitzer, L. (2010). Metabolomic and transcriptomic stress response of Escherichia coli. Mol. Syst. Biol. *6*, 364.

Kimura, S., and Suzuki, T. (2010). Fine-tuning of the ribosomal decoding center by conserved methyl-modifications in the Escherichia coli 16S rRNA. Nucleic Acids Res. *38*, 1341–1352.

Koutmou, K.S., McDonald, M.E., Brunelle, J.L., and Green, R. (2014). RF3:GTP promotes rapid dissociation of the class 1 termination factor. RNA.

Krzyzosiak, W., Denman, R., Nurse, K., Hellmann, W., Boublik, M., Gehrke, C.W., Agris, P.F., and Ofengand, J. (1987). In vitro synthesis of 16S ribosomal RNA containing single base changes and assembly into a functional 30S ribosome. Biochemistry *26*, 2353–2364.

Kurland, C.G. (1992). Translational accuracy and the fitness of bacteria. Annu. Rev. Genet. *26*, 29–50.

Lafontaine, D., Delcour, J., Glasser, A.L., Desgrès, J., and Vandenhaute, J. (1994). The DIM1 gene responsible for the conserved m6(2)Am6(2)A dimethylation in the 3'-terminal loop of 18 S rRNA is essential in yeast. J. Mol. Biol. *241*, 492–497.

Lang, K., Erlacher, M., Wilson, D.N., Micura, R., and Polacek, N. (2008). The Role of 23S Ribosomal RNA Residue A2451 in Peptide Bond Synthesis Revealed by Atomic Mutagenesis. Chem. Biol. *15*, 485–492.

Larsen, B., Wills, N.M., Gesteland, R.F., and Atkins, J.F. (1994). rRNA-mRNA base pairing stimulates a programmed -1 ribosomal frameshift. J. Bacteriol. *176*, 6842–6851.

Larsen, B., Gesteland, R.F., and Atkins, J.F. (1997). Structural probing and mutagenic analysis of the stem-loop required for Escherichia coli dnaX ribosomal frameshifting: programmed efficiency of 50%. J. Mol. Biol. *271*, 47–60.

Laurberg, M., Asahara, H., Korostelev, A., Zhu, J., Trakhanov, S., and Noller, H.F. (2008). Structural basis for translation termination on the 70S ribosome. Nature *454*, 852–857.

Lesnyak, D.V., Osipiuk, J., Skarina, T., Sergiev, P.V., Bogdanov, A.A., Edwards, A., Savchenko, A., Joachimiak, A., and Dontsova, O.A. (2007). Methyltransferase That Modifies Guanine 966 of the 16 S rRNA FUNCTIONAL IDENTIFICATION AND TERTIARY STRUCTURE. J. Biol. Chem. *282*, 5880–5887.

Liao, P.-Y., Gupta, P., Petrov, A.N., Dinman, J.D., and Lee, K.H. (2008). A new kinetic model reveals the synergistic effect of E-, P- and A-sites on +1 ribosomal frameshifting. Nucleic Acids Res. *36*, 2619–2629.

Ling, J., and Söll, D. (2010). Severe oxidative stress induces protein mistranslation through impairment of an aminoacyl-tRNA synthetase editing site. Proc. Natl. Acad. Sci. U. S. A. *107*, 4028–4033.

Lopez, P.J., Iost, I., and Dreyfus, M. (1994). The use of a tRNA as a transcriptional reporter: the T7 late promoter is extremely efficient in Escherichia coli but its transcripts are poorly expressed. Nucleic Acids Res. *22*, 1186–1193.

Lu, P., Vogel, C., Wang, R., Yao, X., and Marcotte, E.M. (2007). Absolute protein expression profiling estimates the relative contributions of transcriptional and translational regulation. Nat. Biotechnol. *25*, 117–124.

Marianovsky, I., Aizenman, E., Engelberg-Kulka, H., and Glaser, G. (2001). The regulation of the Escherichia coli mazEF promoter involves an unusual alternating palindrome. J. Biol. Chem. *276*, 5975–5984.

Miller, J.H. (1972). Experiments in molecular genetics ([Cold Spring Harbor, N.Y.]: Cold Spring Harbor Laboratory).

Moll, I., and Engelberg-Kulka, H. (2012). Selective translation during stress in Escherichia coli. Trends Biochem. Sci. *37*, 493–498.

Moll, I., Hirokawa, G., Kiel, M.C., Kaji, A., and Bläsi, U. (2004). Translation initiation with 70S ribosomes: an alternative pathway for leaderless mRNAs. Nucleic Acids Res. *32*, 3354–3363.

Motorin, Y., and Helm, M. (2011). RNA nucleotide methylation. Wiley Interdiscip. Rev. RNA *2*, 611–631.

Muthuramalingam, M., White, J.C., and Bourne, C.R. (2016). Toxin-Antitoxin Modules Are Pliable Switches Activated by Multiple Protease Pathways. Toxins *8*.

Nagano, T., Kojima, K., Hisabori, T., Hayashi, H., Morita, E.H., Kanamori, T., Miyagi, T., Ueda, T., and Nishiyama, Y. (2012). Elongation Factor G Is a Critical Target during Oxidative Damage to the Translation System of Escherichia coli. J. Biol. Chem. *287*, 28697–28704.

Nagano, T., Yutthanasirikul, R., Hihara, Y., Hisabori, T., Kanamori, T., Takeuchi, N., Ueda, T., and Nishiyama, Y. (2015). Oxidation of translation factor EF-G transiently retards the translational elongation cycle in Escherichia coli. J. Biochem. (Tokyo) *158*, 165–172.

Netzer, N., Goodenbour, J.M., David, A., Dittmar, K.A., Jones, R.B., Schneider, J.R., Boone, D., Eves, E.M., Rosner, M.R., Gibbs, J.S., *et al.* (2009). Innate immune and chemically triggered oxidative stress modifies translational fidelity. Nature *462*, 522–526.

O'Connor, M., Thomas, C.L., Zimmermann, R.A., and Dahlberg, A.E. (1997). Decoding Fidelity at the Ribosomal A and P Sites: Influence of Mutations in three Different Regions of the Decoding Domain in 16S rRNA. Nucleic Acids Res. *25*, 1185–1193.

O'Donnell, S.M., and Janssen, G.R. (2002). Leaderless mRNAs Bind 70S Ribosomes More Strongly than 30S Ribosomal Subunits in Escherichia coli. J. Bacteriol. *184*, 6730–6733.

O'Farrell, H.C., Pulicherla, N., Desai, P.M., and Rife, J.P. (2006). Recognition of a complex substrate by the KsgA/Dim1 family of enzymes has been conserved throughout evolution. RNA *12*, 725–733.

Ogle, J.M., Brodersen, D.E., Clemons, W.M., Tarry, M.J., Carter, A.P., and Ramakrishnan, V. (2001). Recognition of cognate transfer RNA by the 30S ribosomal subunit. Science *292*, 897–902.

Orelle, C., Carlson, E.D., Szal, T., Florin, T., Jewett, M.C., and Mankin, A.S. (2015). Protein synthesis by ribosomes with tethered subunits. Nature *524*, 119–124.

Page, R., and Peti, W. (2016). Toxin-antitoxin systems in bacterial growth arrest and persistence. Nat. Chem. Biol. *12*, 208–214.

Poldermans, B., Roza, L., and Van Knippenberg, P.H. (1979). Studies on the function of two adjacent N6,N6-dimethyladenosines near the 3' end of 16 S ribosomal RNA of Escherichia coli. III. Purification and properties of the methylating enzyme and methylase-30 S interactions. J. Biol. Chem. *254*, 9094–9100.

Polikanov, Y.S., Melnikov, S.V., Söll, D., and Steitz, T.A. (2015). Structural insights into the role of rRNA modifications in protein synthesis and ribosome assembly. Nat. Struct. Mol. Biol. *22*, 342–344.

Qin, B., Yamamoto, H., Ueda, T., Varshney, U., and Nierhaus, K.H. (2016). The Termination Phase in Protein Synthesis is not Obligatorily Followed by the RRF/EF-G-Dependent Recycling Phase. J. Mol. Biol. *428*, 3577–3587.

Ranasinghe, R.T., Challand, M.R., Ganzinger, K.A., Lewis, B.W., Softley, C., Schmied, W.H., Horrocks, M.H., Shivji, N., Chin, J.W., Spencer, J., *et al.* (2018). Detecting RNA base methylations in single cells by in situ hybridization. Nat. Commun. *9*, 655.

René, O., and Alix, J.-H. (2011). Late steps of ribosome assembly in E. coli are sensitive to a severe heat stress but are assisted by the HSP70 chaperone machine. Nucleic Acids Res. *39*, 1855–1867.

Reynolds, N.M., Lazazzera, B.A., and Ibba, M. (2010). Cellular mechanisms that control mistranslation. Nat. Rev. Microbiol. *8*, 849–856.

Ringquist, S., Shinedling, S., Barrick, D., Green, L., Binkley, J., Stormo, G.D., and Gold, L. (1992). Translation initiation in Escherichia coli: sequences within the ribosome-binding site. Mol. Microbiol. *6*, 1219–1229.

Rodnina, M.V., Fricke, R., Kuhn, L., and Wintermeyer, W. (1995). Codon-dependent conformational change of elongation factor Tu preceding GTP hydrolysis on the ribosome. EMBO J. *14*, 2613–2619.

Rodnina, M.V., Savelsbergh, A., Katunin, V.I., and Wintermeyer, W. (1997). Hydrolysis of GTP by elongation factor G drives tRNA movement on the ribosome. Nature *385*, 37–41.

Saraiya, A.A., Lamichhane, T.N., Chow, C.S., SantaLucia, J., and Cunningham, P.R. (2008). Identification and role of functionally important motifs in the 970 loop of Escherichia coli 16S ribosomal RNA. J. Mol. Biol. *376*, 645–657.

Sauert, M., Temmel, H., and Moll, I. (2015). Heterogeneity of the translational machinery: Variations on a common theme. Biochimie *114*, 39–47.

Schmeing, T.M., and Ramakrishnan, V. (2009). What recent ribosome structures have revealed about the mechanism of translation. Nature *461*, 1234–1242.

Scolnick, E., Tompkins, R., Caskey, T., and Nirenberg, M. (1968). Release factors differing in specificity for terminator codons. Proc. Natl. Acad. Sci. U. S. A. *61*, 768–774.

Seier, T., Padgett, D.R., Zilberberg, G., Sutera, V.A., Toha, N., and Lovett, S.T. (2011). Insights into Mutagenesis Using Escherichia coli Chromosomal lacZ Strains that Enable Detection of a Wide Spectrum of Mutational Events. Genetics genetics.111.127746.

Sergeeva, O.V., Prokhorova, I.V., Ordabaev, Y., Tsvetkov, P.O., Sergiev, P.V., Bogdanov, A.A., Makarov, A.A., and Dontsova, O.A. (2012). Properties of small rRNA methyltransferase RsmD: Mutational and kinetic study. RNA *18*, 1178–1185.

Sergiev, P.V., Golovina, A.Y., Prokhorova, I.V., Sergeeva, O.V., Osterman, I.A., Nesterchuk, M.V., Burakovsky, D.E., Bogdanov, A.A., and Dontsova, O.A. (2011). Modifications of ribosomal RNA: From enzymes to function. In Ribosomes, (Springer, Vienna), pp. 97–110.

Sergiev, P.V., Aleksashin, N.A., Chugunova, A.A., Polikanov, Y.S., and Dontsova, O.A. (2018). Structural and evolutionary insights into ribosomal RNA methylation. Nat. Chem. Biol. *14*, 226–235.

Shabala, L., Bowman, J., Brown, J., Ross, T., McMeekin, T., and Shabala, S. (2009). Ion transport and osmotic adjustment in Escherichia coli in response to ionic and non-ionic osmotica. Environ. Microbiol. *11*, 137–148.

Shajani, Z., Sykes, M.T., and Williamson, J.R. (2011). Assembly of Bacterial Ribosomes. Annu. Rev. Biochem. *80*, 501–526.

Shine, J., and Dalgarno, L. (1974). The 3′-Terminal Sequence of Escherichia coli 16S Ribosomal RNA: Complementarity to Nonsense Triplets and Ribosome Binding Sites. Proc. Natl. Acad. Sci. *71*, 1342–1346.

Srivastava, A., Gogoi, P., Deka, B., Goswami, S., and Kanaujia, S.P. (2016). In silico analysis of 5'-UTRs highlights the prevalence of Shine-Dalgarno and leaderless-dependent mechanisms of translation initiation in bacteria and archaea, respectively. J. Theor. Biol. *402*, 54–61.

Tamarit, J., Cabiscol, E., and Ros, J. (1998). Identification of the major oxidatively damaged proteins in Escherichia coli cells exposed to oxidative stress. J. Biol. Chem. *273*, 3027–3032.

Tedin, K., Moll, I., Grill, S., Resch, A., Graschopf, A., Gualerzi, C.O., and Bläsi, U. (1999). Translation initiation factor 3 antagonizes authentic start codon selection on leaderless mRNAs. Mol. Microbiol. *31*, 67–77.

Thammana, P., and Held, W.A. (1974). Methylation of 16S RNA during ribosome assembly *in vitro*. Nature *251*, 682–686.

Tscherne, J.S., Nurse, K., Popienick, P., Michel, H., Sochacki, M., and Ofengand, J. (1999). Purification, Cloning, and Characterization of the 16S RNA m5C967 Methyltransferase from Escherichia coli. Biochemistry *38*, 1884–1892.

Tsuchihashi, Z., and Brown, P.O. (1992). Sequence requirements for efficient translational frameshifting in the Escherichia coli dnaX gene and the role of an unstable interaction between tRNA(Lys) and an AAG lysine codon. Genes Dev. *6*, 511–519.

Tsuchihashi, Z., and Kornberg, A. (1990). Translational frameshifting generates the gamma subunit of DNA polymerase III holoenzyme. Proc. Natl. Acad. Sci. U. S. A. *87*, 2516–2520.

Turnbull, K.J., and Gerdes, K. (2017). HicA toxin of Escherichia coli derepresses hicAB transcription to selectively produce HicB antitoxin. Mol. Microbiol. *104*, 781–792.

Udagawa, T., Shimizu, Y., and Ueda, T. (2004). Evidence for the Translation Initiation of Leaderless mRNAs by the Intact 70 S Ribosome without Its Dissociation into Subunits in Eubacteria. J. Biol. Chem. *279*, 8539–8546.

Valle, M., Zavialov, A., Li, W., Stagg, S.M., Sengupta, J., Nielsen, R.C., Nissen, P., Harvey, S.C., Ehrenberg, M., and Frank, J. (2003). Incorporation of aminoacyl-tRNA into the ribosome as seen by cryo-electron microscopy. Nat. Struct. Biol. *10*, 899–906.

Vesper, O., Amitai, S., Belitsky, M., Byrgazov, K., Kaberdina, A.C., Engelberg-Kulka, H., and Moll, I. (2011). Selective translation of leaderless mRNAs by specialized ribosomes generated by MazF in Escherichia coli. Cell *147*, 147–157.

Villa, E., Sengupta, J., Trabuco, L.G., LeBarron, J., Baxter, W.T., Shaikh, T.R., Grassucci, R.A., Nissen, P., Ehrenberg, M., Schulten, K., *et al.* (2009). Ribosome-induced changes in elongation factor Tu conformation control GTP hydrolysis. Proc. Natl. Acad. Sci. U. S. A. *106*, 1063–1068.

Wang, X., Lord, D.M., Cheng, H.-Y., Osbourne, D.O., Hong, S.H., Sanchez-Torres, V., Quiroga, C., Zheng, K., Herrmann, T., Peti, W., *et al.* (2012). A new type V toxin-antitoxin system where mRNA for toxin GhoT is cleaved by antitoxin GhoS. Nat. Chem. Biol. *8*, 855–861.

Weber, A., Kögl, S.A., and Jung, K. (2006). Time-dependent proteome alterations under osmotic stress during aerobic and anaerobic growth in Escherichia coli. J. Bacteriol. *188*, 7165–7175.

Weitzmann, C., Tumminia, S.J., Boublik, M., and Ofengand, J. (1991). A paradigm for local conformational control of fucntion in the ribosome: binding of ribosomal protein S19 to Escherichia coli 16S rRNA in the presence of S7 is required for methylation of m 2 G966 and blocks methylation of m 5 C967 by their respective methyltransferases. Nucleic Acids Res. *19*, 7089–7095.

Weixlbaumer, A., Jin, H., Neubauer, C., Voorhees, R.M., Petry, S., Kelley, A.C., and Ramakrishnan, V. (2008). Insights into Translational Termination from the Structure of RF2 Bound to the Ribosome. Science *322*, 953–956.

Winter, A.J., Williams, C., Isupov, M.N., Crocker, H., Gromova, M., Marsh, P., Wilkinson, O.J., Dillingham, M.S., Harmer, N.J., Titball, R.W., *et al.* (2018). The molecular basis of protein toxin HicA-dependent binding of the protein antitoxin HicB to DNA. J. Biol. Chem.

Withman, B., Gunasekera, T.S., Beesetty, P., Agans, R., and Paliy, O. (2013). Transcriptional Responses of Uropathogenic Escherichia coli to Increased Environmental Osmolality Caused by Salt or Urea. Infect. Immun. *81*, 80–89.

Wood, J.M., Bremer, E., Csonka, L.N., Kraemer, R., Poolman, B., van der Heide, T., and Smith, L.T. (2001). Osmosensing and osmoregulatory compatible solute accumulation by bacteria. Comp. Biochem. Physiol. A. Mol. Integr. Physiol. *130*, 437–460.

Yamamoto, H., Wittek, D., Gupta, R., Qin, B., Ueda, T., Krause, R., Yamamoto, K., Albrecht, R., Pech, M., and Nierhaus, K.H. (2016). 70S-scanning initiation is a novel and frequent initiation mode of ribosomal translation in bacteria. Proc. Natl. Acad. Sci. 201524554.

Zhang, D., Yan, K., Zhang, Y., Liu, G., Cao, X., Song, G., Xie, Q., Gao, N., and Qin, Y. (2015). New insights into the enzymatic role of EF-G in ribosome recycling. Nucleic Acids Res. *43*, 10525–10533.

Zhang, H., Wan, H., Gao, Z.-Q., Wei, Y., Wang, W.-J., Liu, G.-F., Shtykova, E.V., Xu, J.-H., and Dong, Y.-H. (2012). Insights into the Catalytic Mechanism of 16S rRNA Methyltransferase RsmE (m3U1498) from Crystal and Solution Structures. J. Mol. Biol. *423*, 576–589.

Zhang, Y., Zhang, J., Hoeflich, K.P., Ikura, M., Qing, G., and Inouye, M. (2003). MazF cleaves cellular mRNAs specifically at ACA to block protein synthesis in Escherichia coli. Mol. Cell *12*, 913–923.

Zhang, Y., Xiao, Z., Zou, Q., Fang, J., Wang, Q., Yang, X., and Gao, N. (2017). Ribosome Profiling Reveals Genome-wide Cellular Translational Regulation upon Heat Stress in Escherichia coli. Genomics Proteomics Bioinformatics *15*, 324–330.

Zhang, Y., Burkhardt, D.H., Rouskin, S., Li, G.-W., Weissman, J.S., and Gross, C.A. (2018). A Stress Response that Monitors and Regulates mRNA Structure Is Central to Cold Shock Adaptation. Mol. Cell *70*, 274-286.e7.

Zhao, K., Liu, M., and Burgess, R.R. (2005). The global transcriptional response of Escherichia coli to induced sigma 32 protein involves sigma 32 regulon activation followed by inactivation and degradation of sigma 32 *in vivo*. J. Biol. Chem. *280*, 17758–17768.

Zheng, X., Hu, G.-Q., She, Z.-S., and Zhu, H. (2011). Leaderless genes in bacteria: clue to the evolution of translation initiation mechanisms in prokaryotes. BMC Genomics *12*, 361.

LIST OF FIGURES

LIST OF TABLES

Résumé étendu

L'expression génétique peut être décrite comme l'ensemble des processus menant à la production des supports fonctionnels des gènes (qui peuvent être des protéines ou de l'ARN non codant). Elle se compose de la transcription d'un gène en un ARN messager (ARNm) qui est ensuite traduit en une protéine. Le processus de traduction est réalisé par une machinerie cellulaire complexe appelée ribosome. Le ribosome bactérien est un complexe ribonucléoprotéique asymétrique. Il se compose d'environ un tiers de protéines ribosomales (r-protéines) et de deux tiers d'ARN ribosomaux (ARNr). Le ribosome contient deux sous-unités un petite de 30S et une grande de 50S qui forment ensemble le complexe 70S. L'activité catalytique du ribosome est due aux composants de l'ARN, le ribosome est donc un ribozyme. En outre, les deux sous-unités ont des activités différentes. La petite sous-unité est responsable de la liaison de l'ARNm et du décodage du code génétique tandis que la sous-unité 50S est capable de former une liaison peptidique entre le peptide naissant et l'acide aminé entrant. Ces deux réactions sont effectuées par le ribosome avec l'aide des ARN de transfert (ARNt). Les ARNt sont chargés avec l'acide aminé correspondant et peuvent être considérés comme les substrats du ribosome qui fournissent les acides aminés. Il existe trois sites de liaison de l'ARNt sur le ribosome : le site A où l'ARNt chargé se lie et est décodé dans le centre de décodage, le site P qui contient l'ARNt portant la chaîne polypeptidique et le site E pour la sortie de l'ARNt non chargé.

Même s'il a longtemps été considéré comme une particule invariable du fait de son rôle central, il est désormais admis que la composition du ribosome peut changer. En effet, des variations peuvent exister au niveau des ARNr utilisés (il existe différents opérons codants les ARNr chez *Escherichia coli),* de la composition en protéines ribosomales et des facteurs associés mais aussi au niveau des modifications de tous ces composants. Les ARNr contiennent différents types de modifications par exemple des pseudouridylations et des méthylations.

Dans ce travail, nous avons étudié les six méthylations situées dans le centre de décodage du ribosome d'*Escherichia coli*, qui sont catalysées par les méthyltransférases RsmA, RsmB, RsmD, RsmE et RsmH. Ces méthylations semblent moduler la structure de cette région fonctionnelle du ribosome en créant un encombrement stérique et des interactions hydrophobes. Il est donc probable que le réseau formé par les méthylations influence les interactions entre l'ARNm et l'ARNr 16S, l'ARNt et l'ARNr 16S et les interactions avec les facteurs d'initiation et d'élongation de la traduction. Par conséquent, ces modifications pourraient influencer l'ancrage de l'ARNm, la liaison de l'ARNt ou les interactions codon-anticodon et donc le décodage. Cela pourrait également affecter les activités fonctionnelles du ribosome telles que l'initiation, la fidélité et l'efficacité de la traduction. De plus, la plupart des modifications du centre de décodage sont conservées chez les bactéries (et même chez les Archaea et les eucaryotes pour certaines). Cette conservation évolutive tend à mettre en évidence un rôle important de ces méthylations. Cependant, à ce jour, peu de choses sont connues sur leur fonction physiologique et sur leur potentiel rôle dans la réponse des bactéries à des conditions environnementales en constante évolution. Les données montrant certaines variations de l'expression et de l'abondance protéique de ces méthyltransférases dans des conditions de stress sont rares. Mais de telles variations, ainsi que les changements potentiels dans le niveau global des modifications au sein du ribosome, pourraient impliquer les modifications ribosomiques dans la régulation traductionnelle de la réponse au stress. Ainsi, nous nous sommes concentrés sur les méthylations du centre de décodage et avons cherché à évaluer différents aspects liés à la sensibilité au stress et à l'activité ribosomique.

Nous avons étudié le phénotype de souches mutantes arborant un gène de méthyltransférase délété : Δ*rsmA,* Δ*rsmB,* Δ*rsmD,* Δ*rsmE* et Δ*rsmH*. Nous avons ainsi pu établir que l'absence de ces modifications n'est pas essentielle aussi bien pour la croissance, la survie ou la compétition avec la souche sauvage, excepté pour la souche Δ*rsmH* qui montre un défaut de compétition.

Par la suite, la traduction de ces souches mutantes a été étudiée en conditions stressantes ou non. Pour cela, différents rapporteurs ont été utilisés : un rapporteur *lacZ* canonique, inductible à l'arabinose, ainsi qu'un rapporteur

fluorescent arborant les gènes de la *gfp* et de la *mcherry* exprimés de manière constitutive. Nous avons ainsi démontré que l'absence de certaines modifications (celles catalysées par RsmA, RsmB, RsmD) augmente le taux de traduction en condition non stressante, tandis que les souches délétées de RsmE et RsmH ont un taux similaire à celui de la souche sauvage. De plus, l'application de stress a différents effets en fonction des souches et des conditions : la traduction de la souche Δ*rsmA* n'est pas affectée par un stress oxydant tandis qu'elle diminue fortement dans la souche sauvage (et dans les autres souches mutantes), en condition de stress chaud, les souches Δ*rsmB* et Δ*rsmD* montrent une forte diminution de la traduction alors que ce n'est pas le cas dans les autres souches. On peut donc supposer que des ribosomes différemment modifiés peuvent jouer un rôle bénéfique lors de la réponse au stress.

Par ailleurs, afin de mieux caractériser l'impact de l'absence de méthylations sur la traduction, nous avons également étudié les erreurs traductionnelles (décalage du cadre de lecture) dans les souches mutantes. Pour se faire, nous avons utilisé le double rapporteur fluorescent permettant la traduction canonique de la Mcherry alors que la traduction de la GFP dépend d'un événement de décalage du cadre de lecture. Ceci a permis de montrer que certaines souches, Δ*rsmA,* Δ*rsmB* et Δ*rsmH,* ont tendance à faire plus d'erreur que la souche sauvage tandis que Δ*rsmD* et Δ*rsmE* ont un taux d'erreur identique ou inférieur. Ainsi les méthylations ont un impact sur la traduction et les effets observés en condition de stress ou sur le taux d'erreur sont spécifiques à chaque méthylation.

Dans une deuxième partie, le travail de caractérisation du système toxine-antitoxine HicAB de *Sinorhizobium meliloti* est présenté. Les systèmes toxine-antitoxine sont de petites unités génétiques généralement composées de deux gènes codant l'antitoxine et la toxine. Ces systèmes sont impliqués dans de nombreuses fonctions qui peuvent entraîner l'arrêt de la croissance et la mort cellulaire. Parmi les différents types de systèmes toxine-antitoxine, le type II regroupe les systèmes où l'antitoxine se lie directement à l'antitoxine et inhibe son action. Parmi ces systèmes de type II, le module HicAB est largement distribué chez les bactéries et les Archaea. La toxine HicA fonctionne en se liant à l'ARN et en le

clivant. Le génome de la bactérie symbiotique *Sinorhizobium meliloti* code de nombreux systèmes toxine-antitoxine et seuls quelques-uns d'entre eux sont fonctionnels. Dans cette étude, nous avons caractérisé le module toxine-antitoxine HicAB de *S. meliloti*. La production de HicA de *S. meliloti* dans les cellules d'*Escherichia coli* inhibe la croissance et diminue la viabilité cellulaire. Nous avons montré que l'expression de HicB de *S. meliloti* neutralise la toxicité de HicA. Les résultats d'expériences de dosages doubles hybrides et de co-purification ont permis de démontrer l'interaction de HicB avec la toxine HicA. De plus, HicA est capable de dégrader l'ARN ribosomal *in vitro*, mais pas le complexe HicAB. L'analyse des domaines séparés de la protéine HicB a permis de définir l'activité antitoxine et le domaine de liaison à l'opérateur. Ceci a mis en évidence la première caractérisation du système HicAB de *S. meliloti* avec HicA, une toxine à activité ribonucléase et HicB une antitoxine comprenant deux domaines : le COOH-terminal qui lie l'opérateur et le NH2-terminal qui inhibe la toxine.

Titre : Stress et traduction : implication des méthylations de l'ARNr 16S chez *Escherichia coli* et caractérisation d'un système toxine-antitoxine de *Sinorhizobium meliloti*

Mots clés : stress, traduction, ribosome, méthylation

Résumé : Les bactéries sont capables de vivre dans une grande variété d'environnements différents et sont confrontées à des conditions en constante évolution. Par conséquent, elles doivent rapidement adapter leur métabolisme en utilisant différentes régulations aux niveaux transcriptionnel et traductionnel. Ces régulations sont largement étudiées et bien caractérisées. Cependant, les implications du ribosome sur la modulation de la traduction au cours de la réponse aux stress commencent à être explorées. Dans ce contexte de régulation ribosomique, l'hétérogénéité de la machinerie pourrait jouer un rôle important. En effet, le ribosome n'est pas une particule invariable et ses composants (ARNr, protéines ribosomiques) et leurs modifications peuvent varier. Les modifications des ARNr sont situées dans les sites fonctionnels du ribosome et sont particulièrement conservées, ce qui sous-entend leur potentielle importance. Cependant, leur rôle physiologique n'est pas toujours bien défini. Nous nous sommes intéressés aux méthylations de l'ARNr 16S et avons étudié leur rôle dans la traduction, dans des conditions favorables et stressantes. Nous avons démontré que l'absence de certaines méthylations augmente la traduction dans des conditions stressantes et non stressantes. Ainsi, les ribosomes modifiés peuvent jouer un rôle bénéfique lors de la réponse au stress. Une autre façon d'agir sur la traduction dans des conditions stressantes consiste à cibler les ARNm. C'est notamment le cas des toxines endoribonucléases qui sont spécifiquement produites lors de conditions stressantes. Ainsi, nous avons caractérisé le système toxine-antitoxine HicAB de *Sinorhizobium meliloti*. Nous prévoyons d'utiliser la toxine HicA afin d'étudier la réponse à son activité endoribonucléase chez les mutants ne possédant pas certaines modifications ribosomiques.

Title: Stress and translation: implication of 16S rRNA methylations in *Escherichia coli* and characterization of a toxin-antitoxin system of *Sinorhizobium meliloti*

Keywords: stress, translation, ribosome, methylation

Abstract:

Bacteria are able to live in a large variety of environments and they face constantly changing conditions. Therefore they have to adapt quickly to their metabolism using different regulations at the transcriptional and translational levels. Those types of regulation are extensively studied and well characterized. However, the implications of the ribosome in modulation of translation during stress response remains poorly understood. In this context of ribosomal regulation, the heterogeneity of the machinery could play a relevant role. Indeed, the ribosome is not an invariable particle and its components (rRNAs, r-proteins) and their modifications may vary. Modifications of ribosomal RNAs are clustered in the functional sites of the ribosome and are particularly conserved, underlying their potential importance. However their physiological role is still unclear. We focused on methylations of the 16S rRNA and investigated their role in translation under favourable and stressful conditions. We successfully demonstrated that lack of some methylations increases translation under stressful and non stressful conditions. So, lack of methylation may give an advantage to ribosomes during stress response. Another way to act on translation under stressful conditions resides in targeting mRNAs. This is particularly the case for endoribonuclease toxins that are specifically produced during detrimental conditions. Thus, we characterized *S. meliloti* toxin-antitoxin system HicAB. We plan to use it in order to study the response to HicA toxin of mutants lacking some ribosomal modifications.